UNIVERSITY OF CALIFORNIA, SAN DIEGO

SAN DIEGO STATE UNIVERSITY

Functional and Structural Investigation of *Drosophila* UNC–45, a Chaperone for Myosin

A dissertation submitted in partial satisfaction of the requirements

for the degree of Doctor of Philosophy

in

Biology

by

Chi F. Lee

Committee in charge:

University of California, San Diego

Professor Randolph Hampton
Professor William McGinnis

San Diego State University

Professor Sanford I. Bernstein, Chair
Professor Christopher Glembotski
Professor Greg L. Harris

2010

The Dissertation of Chi F. Lee is approved, and it is acceptable in quality and form for publication on microfilm:

_____

_____

_____

_____

_____
Chair

University of California, San Diego

San Diego State University

2010

For my mother, my sister, and the people who believe in me

Table of Contents

List of Figures

List of Tables

Acknowledgements

I would like to thank Dr. Bernstein for his mentoring, patience, and support throughout this journey. I hid under his wings for many years and was allowed to fully experience the joy science has to offer. I wish to express my appreciation to the dissertation committee members, Dr. Randy Hampton, Dr. Greg Harris, Dr. Bill McGinnis, and Dr. Chris Glembotski for always being flexible and supportive. Special thanks to Dr. Chris Glembotski for allowing me the use of his laboratory to explore the feasibility of an idea.

I wish to thank Dr. Steve Barlow who trained me on confocal microscopy techniques which generated data that are crucial for this project and Dr. Tom Huxford without whom the structure of UNC–45 would still be three ellipses that do not correspond to the actual sizes of the protein domains. I would like to thank Dr. Aileen Knowles for her words of support and encouragement. For allowing me the chance to work in their laboratories, Dr. Judith Zyskind, Dr. Jacques Perrault, and Dr. Constantine D. Tsoukas passed on to me valuable knowledge that continuously help me becoming a better scientist.

I wish to thank members of the Bernstein lab, past and present, who made this experience fun and enjoyable with special acknowledgement to Qin Yu who paved the road for the final fruition of my project. I also wish to thank the members of the Huxford lab, past and present, who shared their lab space, equipment, and their personalities.

In chapter one, the collective efforts from Dr. Girish Melkani, Jennifer Suggs, William Kronert, and Yoko Suzuki contributed to the completion of the project and made the work less daunting. In chapter two, Dr. Girish Melkani, Dr. Anthony Cammarato, and Anju Melkani were instrumental in gathering the data needed for the completion of the chapter. Chapter two also included data published in BBRC.

> Melkani, G. C., Lee, C. F., Cammarato, A. and Bernstein, S. I. (2010). *Drosophila* UNC-45 prevents heat-induced aggregation of skeletal muscle myosin and facilitates refolding of citrate synthase. *Biochem Biophys Res Commun* 396, 317-322.

In chapter three, Dr. Tom Huxford, Arthur Hauenstein, Jonathan Fleming, Clarke Gasper, and Valerie Engelke contributed a tremendous amount of time and energy in piecing the puzzles together. Special thanks to Dr. Tom Huxford who oversaw the entire crystallography project and gave me permission to run his four thousand dollar computer into the ground, which freed me from the fear of making mistakes and gave me the courage to keep clicking away.

Vita

Education/Employment:

Dec. 1999 - May 2002	Research Associate San Diego State University Department of Biology
June 2002	Bachelor of Science in Biology San Diego State University
Aug. 2002 - May 2004	Graduate TA San Diego State University Department of Biology
June 2008	Master in Business Administration San Diego State University
Sept. 2010	Doctor of Philosophy in Biology SDSU-UCSD Joint Ph.D. Program

Honors and Awards:

Aug. 1993 - May 1997	Clemens Foundation Scholarship
May 2007	Invitrogen Distinguished Scientist Fellowship

Peer-Reviewed Publications:

Wilkinson, T.G. II, Kedar, G.C., **Lee, C.F.**, Guzman, E.C., Smith, D.W. and Zyskind, J.W. (2006). The synchrony phenotype persists after elimination of multiple GATC sites from the *dnaA* promoter of *Escherichia coli*. *J. Bacteriol.* 188, 4573-4573.

Melkani, G.C., **Lee, C.F.**, Cammarato, A., and Bernstein, S.I. (2010). *Drosophila* UNC–45 prevents heat-induced aggregation of skeletal muscle myosin and facilitates refolding of citrate synthase. *BBRC* 396, 317-322.

Lee, C.F., Melkani, G.C., Yu, Q., Suggs, J.A., Kronert, W.A., Suzuki, Y., Hipolito, L., Price, M.G., Epstein, H.F., and Bernstein, S.I. *Drosophila* UNC–45 accumulates in embryonic blastoderm and in muscles and is essential for muscle myosin stability. Submitted to *J. Cell. Sci*.

Lee, C.F., Hauenstein, A.V., Fleming, J.K., Gasper, W.C., Engelke, V., Sankaran, B., Bernstein, S.I., and Huxford, T. X-ray crystal structure of the UCS domain-containing UNC–45 protein from *Drosophila melanogaster*. Submitted to *Structure*.

Abstracts:

Yu, Q., Hipolito, L., Kronert, W., **Lee, C.**, Liu, H., Price, M., Epstein, H., and Bernstein, S.I. (2005). Characterization and functional analysis of the *Drosophila melanogaster unc–45* (d*unc–45*) gene. In 46th Annual *Drosophila* Research Conference. San Diego, CA.

Melkani, G., **Lee, C.**, Cammarato, A., and Bernstein, S.I. (2005). Nucleotide-mediated chaperonin function of *Drosophila* UNC–45 (DUNC–45). In 50th Biophysical Society Annual Meeting. Salt Lake City, UT. *Biophys. J.*

Lee, C., Cammarato, A., Melkani, G., and Bernstein, S.I. (2006). Characterization and functional analysis of the *Drosophila* UNC–45 chaperone *in vitro* and *in vivo*. In American Society for Cell Biology 46th Annual Meeting. San Diego, CA.

Melkani, G., Cammarato, A., **Lee, C.**, and Bernstein, S.I. (2007). DUNC–45 maintains the structural integrity of skeletal muscle myosin during *in vitro* stress. In 51st Biophysical Society Annual Meeting. Baltimore, MD. *Biophys. J.*

Lee, C., Melkani, G.C., Suggs, J.A., Melkani, A., Cammarato, A., and Bernstein, S.I. (2007) Absence of the *Drosophila* UNC–45 results in depressed myosin accumulation and loss of thick filaments. In American Society for Cell Biology 47th Annual Meeting. Washington, DC.

Cammarato, A., Li, X., Suggs, J., Yu, Q., **Lee, C.**, Li, P., Lehman, W., and Bernstein, S.I. (2009) Residues in the hydrophobic seam of the myosin S2/LMM hinge impart myosin rod- and muscle-specific properties. In American Society for Cell Biology 49th Annual Meeting. San Diego, CA.

Lee, C., Hauenstein, A.V., Gasper, W.C., Sankaran, B., Bernstein, S.I., and Huxford, T. (2009) Structure of the putative myosin chaperone, UNC–45. In American Society for Cell Biology 49th Annual Meeting. San Diego, CA.

Cammarato, A., Li, X, Reedy, M.C., **Lee, C.**, Li, P., Lehman, W., and Bernstein, S.I. (2010) Transgenic replacement of the myosin S2/HMM hinge alters the rod's nano-mechanical properties and affects sarcomeric organization. In 54th Biophysical Society Annual Meeting. San Francisco, CA. *Biophys. J.*

Lee, C., Hauenstein, A.V., Gasper, W.C., Sankaran, B., Bernstein, S.I., and Huxford, T. (2009) Crystal structure of *Drosophila* UNC–45, a putative myosin chaperone. In 54th Biophysical Society Annual Meeting. San Francisco, CA. *Biophys. J.*

ABSTRACT OF THE DISSERTATION

Functional and Structural Investigation of *Drosophila* UNC–45, a Chaperone for Myosin

by

Chi F. Lee

Doctor of Philosophy in Biology

University of California, San Diego, 2010

San Diego State University, 2010

Professor Sanford I. Bernstein, Chair

The UCS family of proteins is important for myosin folding, stability, and maintenance. To understand the expression pattern, function, and structure of a UCS protein, the *Drosophila* UNC–45 (dUNC–45) was investigated.

In chapter one, Western blot analysis indicates that dUNC–45 is expressed throughout development. Immunofluorescence confocal microscopy shows strong dUNC–45 expression in the body-wall muscles of 14 hour wild-type embryos. Examination of third instar wild-type larvae body-wall muscles using the same approach localized dUNC–45 to the Z discs of sarcomeres. In the dUNC–45 knock

out line (*T–33*), the strong dUNC–45 skeletal muscle expression is lost in the 14 hour old embryos and the embryos do not hatch. Electron microscopy assessment of 22 hour *T–33* embryos showed poor myofibril organization and a loss of thick filaments, which is reflected by a loss of myosin on the Western blot analysis. Results in the wild-type and the *T–33* embryos suggest a post-translational association between myosin and dUNC–45.

In chapter two, the chaperone function of bacterially expressed dUNC–45 was analyzed using *in vitro* chaperone assays. The results demonstrate that dUNC–45 is capable of refolding chemically denatured citrate synthase (CS) and suppressing heat-induced aggregation of CS, α-lactalbumin, and myosin. The addition of ATP or AMP-PNP enhanced dUNC–45 chaperone function, but no ATP hydrolysis was detected. *In vivo*, immunofluorescence confocal microscopy of third instar wild-type larvae body-wall muscle suggest that heat stress induces translocation of dUNC–45 from the Z disc to the A band and possibly up-regulates protein level as shown in Western analysis.

Chapter three focuses on the derivation and analysis of dUNC–45 x-ray crystal structure using bacterially expressed dUNC–45. Our 3.0 Å resolution model shows the Central and the UCS domains of dUNC–45 are composed of armadillo repeat protein motifs, but that the TPR domain is not resolved. Inspection of the surface hydrophobicity unveiled a groove in the UCS domain as the possible active site for myosin interaction. Future studies will involve defining the structure-function relationship between particular domains of UNC–45 and its chaperone activity.

Introduction

Chaperones help proteins fold into their proper three-dimensional structures in order to perform their physiological functions. When cells are under stress (i.e. heat shock, oxidative stress, etc), the expression level of certain chaperones are up-regulated to ensure the integrity of the cell by stabilizing and preventing protein denaturation and by refolding denatured proteins. Due to their participation in the stress response, some chaperones are also referred to as heat shock proteins (Hsp) [Gething and Sambrook, 1992].

Chaperones can be roughly grouped into six classes based on their molecular weight: small heat shock proteins (sHsp), Hsp40, Hsp60 (chaperonins), Hsp70, Hsp90, and high molecular weight chaperones [Macario *et al.*, 2005]. Each class of chaperone has its own unique mechanism of function but they all essentially act to inhibit the off-pathway folding of proteins [Ellis, 1993]. Beyond the generally accepted role of chaperones in preventing protein aggregation and refolding denatured protein, chaperones may be involved in facilitating protein degradation when the substrate can no longer be recovered [McClellan and Frydman, 2001]. As an active participant in cell protection, the potential of chaperones in the therapeutic treatment of diseases is starting to be recognized [Calderwood, 2005; Soti *et al.*, 2005; Sun and MacRae, 2005].

In order to further understand the functional mechanisms of chaperones, we are studying a newly characterized protein called UNC–45, which is hypothesized to be a chaperone or a co-chaperone necessary for myosin maturation.

Background on myosin folding

Myosin is one of the molecular motors of the cell. It is involved in cellular processes from cytokinesis and vesicle transport to cell motility. It is a major component of the muscle thick filaments and is indispensable in muscle contraction. Currently, there are at least 24 classes of myosin [Foth *et al.*, 2006], each with its own unique characteristics. Even though the different types of myosin are involved in different cellular functions, they all have similar overall structural configuration. Each myosin molecule has a globular head and a tail. The globular head is the catalytic unit, which contains the ATPase domain and the actin binding domain. Different tails can form coiled-coil dimers or form attachments to substrates. Similar to all other proteins, myosin function is dependent on the correct folding of the molecule.

To facilitate the investigation of myosin function, researchers have tried to synthesize myosins *in vitro*. Functional cardiac [Sweeney *et al.*, 1994] and smooth muscle [Trybus, 1994] myosin isoforms have been synthesized successfully using insect cells, but *in vitro* expression of functional skeletal muscle isoforms cannot be done without using a myogenic cell line or its lysate [Srikakulam and Winkelmann, 1999; Chow *et al.*, 2002]. However, functional α-helical tails of rabbit skeletal muscle myosin that forms coiled-coil can be synthesized in *E. coli* [Atkinson and Stewart, 1991], suggesting the existence of some factor(s) in the myogenic cell line that facilitates the folding of skeletal muscle globular head into the correct conformation. UNC–45 is thought to be one of these factors.

Background on UNC–45

UNC–45 was first identified through the phenotypic effect of a temperature-sensitive *Caenorhabditis elegans* (*C. elegans*) mutation [Epstein and Thomson, 1974]. When grown at the permissive temperature of 20°C, the mutant worm appeared as wild-type. When grown at the non-permissive temperature of 25°C, the mutant worm became uncoordinated (UNC) in movement and showed signs of paralysis. In addition, mutants grown at the non-permissive temperature showed disrupted myofilament organization under electron microscopy, correlating the UNC phenotype to muscle dysfunction. The uncoordinated movement phenotype, however, is reversible during larval development. Mutant worms hatched at 25°C and then shifted to 20°C during larval stage developed into adult worms with wild-type movement, even when later incubated at 25°C again. Close examination of the muscle structure by electron microscopy showed UNC–45 mutant worms grown at the restrictive temperature had decreased thick filament accumulation and disrupted distribution of myosin heavy chain isoforms along the thick filament [Barral *et al.*, 1998]. The above observations suggest that *C. elegans* UNC–45 (cUNC–45) is essential for muscle development, but only transiently, and that it does not play a structural role. Once the muscle is fully formed, cUNC–45 is no longer necessary.

A conflicting result, however, was presented when a GFP::cUNC–45 fusion protein was found to localize in the A bands of sarcomeres in adult *C. elegans* body wall muscle [Ao and Pilgrim, 2000]. Furthermore, antibodies raised against an N–terminal peptide of cUNC–45 also showed localization to the thick filaments of body

wall muscle. The above observations led the authors to believe that UNC–45 is a component of thick filaments and functions in stabilizing the myosin isoform (Mhc B) at both ends of the thick filaments. However, the conclusion that UNC–45 is a component of thick filaments awaits further evidence to be persuasive—especially needed is proof of a direct interaction between UNC–45 and components of the thick filament. Such proof is described below.

Sequence comparison between various organisms suggests that the UNC–45 protein contains two functional domains [Barral *et al.*, 1998; Venolia *et al.*, 1999]. At its N–terminus is a tetratricopeptide repeat (TPR) domain that was found by comparing amino acid sequence of unrelated proteins such as human Tom34, yeast protein phosphatase T, and bovine cyclophilin–40. The TPR domain is a co-chaperone domain motif that participates in protein-protein interaction especially with Hsp70 and Hsp90 [Scheufler *et al.*, 2000]. The C–terminus was labeled the UCS domain (UNC–45, CRO1, She4p) by the Epstein group for its homology to the fungal CRO1 protein and the yeast She4p protein. The region connecting the two terminal domains does not contain a recognizable motif, but DNA alignment between *Caenorhabditis briggsae* and *C. elegans* suggests sequence conservation and therefore that it could serve as a functional domain [Venolia *et al.*, 1999]. It is now being called the central domain (Figure 1).

Evidence for direct interaction between UNC–45 and skeletal muscle myosin was obtained using an *in vitro* pull-down assay [Barral *et al.*, 2002]. By expressing

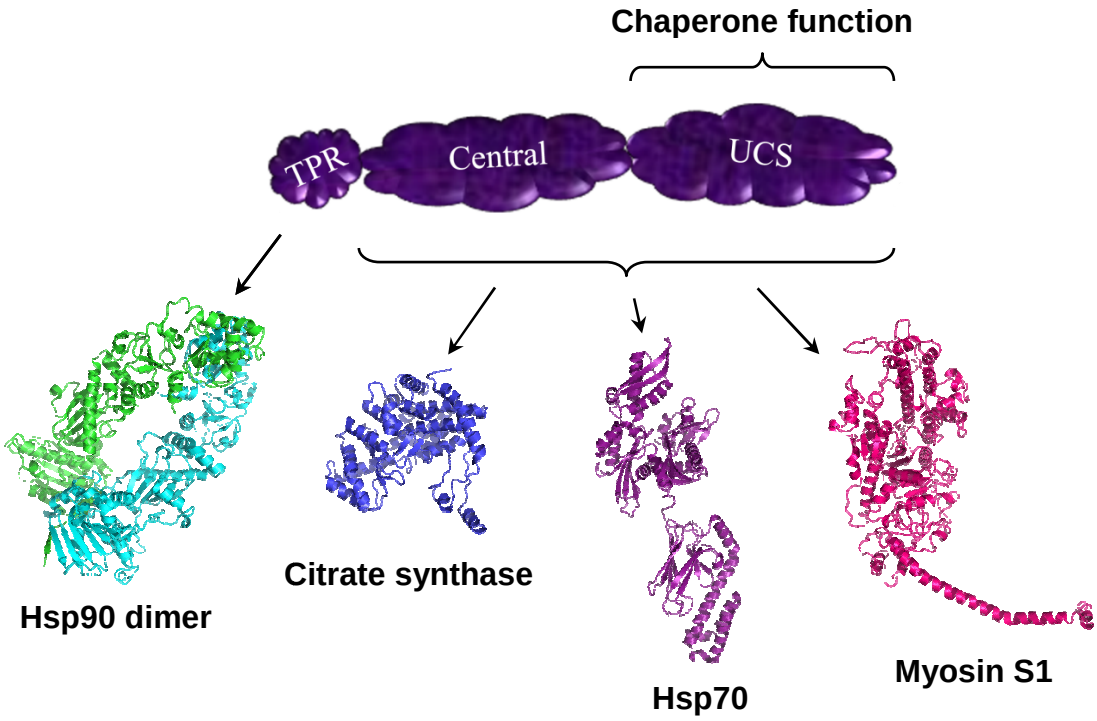

Figure 1. Schematic showing UNC–45 structural domains and their interacting proteins. Myosin S1 (chicken skeletal muscle myosin, PDBID 2MYS with light chains excluded). Hsp70 (*E. coli* DnaK, PDBID 2KHO). Citrate synthase (porcine heart CS, PDBID 3ENJ). Hsp90 (*S. cerevisiae* Hsp90 dimer in the ATP bound closed conformation, PDBID 2CG9).

recombinant cUNC–45 (His::cUNC–45::Flag) protein in Sf9 insect cells using engineered baculovirus, the authors were able to purify the protein for *in vitro* assays. Through various pull-down combinations and co-immunoprecipitations, they found direct interaction of cUNC–45 with myosin, and also with insect Hsp90 and Hsp70. The interaction with Hsp90 was further validated with *Escherichia coli* (*E. coli*) expressed *C. elegans* Hsp90. The recombinant cUNC–45 protected citrate synthase and myosin sub-fragment 1 (S1) from heat induced aggregation. Taken together, the results support the hypothesis that UNC–45 is a component of the thick filament and functions as a chaperone or co-chaperone for myosin folding. In addition, using truncated versions of cUNC–45, Barral *et al*. showed that the cUNC–45 TPR domain interacts with the C-terminal peptide of Hsp90, and they demonstrated that the UCS domain is the functional chaperone domain that interacts with myosin S1 (Figure 1). Further, the yeast two-hybrid screening method confirmed that the UCS domain of She4p is indeed necessary for interaction with type V unconventional myosin [Toi *et al.*, 2003].

More recently, cUNC–45 was found to be ubiquitylated by the proteins CHN–1 and UFD–2 [Hoppe *et al.*, 2004]. Both CHN–1 and UFD–2 contain a C-terminal U Box and function as E3/E4 ubiquitin ligases. Either one alone can add one to three ubiquitin monomers to cUNC–45. For cUNC–45 to be multi-ubiquitylated for degradation, however, both enzymes need to be present at the same time. The authors propose that the E3/E4 ubiquitin ligases precisely control UNC–45 level in the cells, and dis-regulation of UNC–45 levels attests to its importance in

muscle function. This notion is echoed by subsequent research papers and review articles [Janiesch *et al.*, 2007; Landsverk *et al.*, 2007; Hoppe, 2008; Kachur and Pilgrim, 2008; Kim *et al.*, 2008; Willis *et al.*, 2009].

Thus far, UNC–45 homologues have been identified in worms, flies, fish, mice, and humans [Etheridge *et al.*, 2002; Price *et al.*, 2002; Yu and Bernstein, 2003]. All of them have the three domain configuration, including the UCS domain that appears to interact with myosin. The presence of UNC–45 proteins in a multitude of organisms affirms the importance of its function. In worms and flies, there is one UNC–45 protein. In vertebrates, there are two UNC–45 isoforms [Price *et al.*, 2002], one that is expressed in all general cell (gc) types (gcUNC–45/UNC–45A/SMAP–1) and another that is striated muscle (sm) specific (smUNC–45/UNC–45B/CMYA4 in mice/Steif in zebrafish). When knocked-down in mouse skeletal myogenic C2C12 cells using antisense experiments, the general cell type UNC–45 was shown to be important for cell proliferation and fusion; while the striated muscle UNC–45 was shown to be essential for myoblast fusion and sarcomere organization [Price *et al.*, 2002]. The striated muscle specific isoform seems to highlight the necessity of UNC–45 function during muscle development, but its mechanism of function still needs further investigation.

In yeast and other fungi, there is no UNC–45 protein *per se*. Instead, they have proteins containing only the UCS domain. Rng3 (*S. pombe*) [Wesche *et al.*, 2003; Wohlgemuth *et al.*, 2007], She4p (*S. cerevisiae*) [Swank *et al.*, 2000], and CRO1 (*P. anserine*) [Wohlgemuth *et al.*, 2007] are all UCS proteins that, when disrupted, cause

defects in actin cytoskeleton organization, cytokinesis, and other cellular processes associated with myosins such as myosin I, V, and non-muscle myosin II.

As UNC–45 becomes more widely accepted as important for myosin function, the need for investigation in other model organisms becomes apparent. In addition to the pioneering studies in *C. elegans*, UNC–45 has more recently been studied in other model organisms such as the zebrafish. While the study of UNC–45 using the zebrafish started relatively recently [Swank *et al.*, 2000], the contributions from these experiments have been tremendous. The zebrafish model was used to track localization of UNC–45 *in vivo* during myofibrillogenesis which resulted in better understanding of UNC–45 function. Moreover, zebrafish has facilitated the discovery that UNC–45 is also important for cardiac muscle function [Wohlgemuth *et al.*, 2007]. To further understand the mechanism of UNC–45 function in myosin maturation and muscle development, and to gain insight on the relationship between its structure and function at the atomic level, I employed the model system *Drosophila melanogaster*.

Drosophila melanogaster

Drosophila has been an excellent model organism for muscle research due to its well-developed genetics as well as the availability of techniques to study its muscle structure and physiology [Swank *et al.*, 2000]. Its genome is composed of four chromosomes, which were completely sequenced in 2000 [Adams *et al.*, 2000]. In addition to its small genome, it has only one skeletal muscle myosin heavy chain gene [Bernstein *et al.*, 1983; Rozek and Davidson, 1983]. Genetic and transgenic analyses have provided insights into the mechanisms of muscle development, myofibril

assembly, and muscle contraction. Information gained from *Drosophila* on UNC–45 function can be used to complement previous findings and provide further insights into its mechanism of action.

This study

Here, results of UNC–45 studies using *Drosophila melanogaster* are presented. Chapter 1 explores dUNC–45 characteristics *in vivo* by examining body wall muscles of embryos and larvae in both the wild-type and a d*unc–45* mutant. Chapter 2 focuses more on *in vitro* demonstration of dUNC–45's chaperone function. Furthermore, one of its possible modes of function as a chaperone *in vivo* is also presented. Chapter 3 details the process and outcomes of solving the *Drosophila* UNC–45 x-ray crystal structure, with an eventual goal of understanding its interaction with myosin on the molecular level. The concluding chapter summarizes and discusses all the results of this study and provides directions for future experiments.

References

Adams, M. D., Celniker, S. E., Holt, R. A., Evans, C. A., Gocayne, J. D., Amanatides, P. G., Scherer, S. E., Li, P. W., Hoskins, R. A., Galle, R. F. *et al.* (2000). The genome sequence of *Drosophila melanogaster*. Science *287*, 2185-2195.

Ao, W. and Pilgrim, D. (2000). *Caenorhabditis elegans* UNC–45 is a component of muscle thick filaments and colocalizes with myosin heavy chain B, but not myosin heavy chain A. J Cell Biol *148*, 375-384.

Atkinson, S. J. and Stewart, M. (1991). Expression in *Escherichia coli* of fragments of the coiled-coil rod domain of rabbit myosin: influence of different regions of the molecule on aggregation and paracrystal formation. J Cell Sci *99 (Pt 4)*, 823-836.

Barral, J. M., Bauer, C. C., Ortiz, I. and Epstein, H. F. (1998). Unc–45 mutations in *Caenorhabditis elegans* implicate a CRO1/She4p-like domain in myosin assembly. J Cell Biol *143*, 1215-1225.

Barral, J. M., Hutagalung, A. H., Brinker, A., Hartl, F. U. and Epstein, H. F. (2002). Role of the myosin assembly protein UNC–45 as a molecular chaperone for myosin. Science *295*, 669-671.

Bernstein, S. I., Mogami, K., Donady, J. J. and Emerson, C. P., Jr. (1983). *Drosophila* muscle myosin heavy chain encoded by a single gene in a cluster of muscle mutations. Nature *302*, 393-397.

Calderwood, S. K. (2005). Chaperones and slow death--a recipe for tumor immunotherapy. Trends Biotechnol *23*, 57-59.

Chow, D., Srikakulam, R., Chen, Y. and Winkelmann, D. A. (2002). Folding of the striated muscle myosin motor domain. J Biol Chem *277*, 36799-36807.

Ellis, R. J. (1993). The general concept of molecular chaperones. Philos Trans R Soc Lond B Biol Sci *339*, 257-261.

Epstein, H. F. and Thomson, J. N. (1974). Temperature-sensitive mutation affecting myofilament assembly in *Caenorhabditis elegans*. Nature *250*, 579-580.

Etheridge, L., Diiorio, P. and Sagerstrom, C. G. (2002). A zebrafish *unc–45*-related gene expressed during muscle development. Dev Dyn *224*, 457-460.

Foth, B. J., Goedecke, M. C. and Soldati, D. (2006). New insights into myosin evolution and classification. Proc Natl Acad Sci U S A *103*, 3681-3686.

Gething, M. J. and Sambrook, J. (1992). Protein folding in the cell. Nature *355*, 33-45.

Hoppe, T. (2008). Less is more: how protein degradation regulates muscle development. Ernst Schering Found Symp Proc, 67-73.

Hoppe, T., Cassata, G., Barral, J. M., Springer, W., Hutagalung, A. H., Epstein, H. F. and Baumeister, R. (2004). Regulation of the myosin-directed chaperone UNC–45 by a novel E3/E4-multiubiquitylation complex in *C. elegans*. Cell *118*, 337-349.

Janiesch, P. C., Kim, J., Mouysset, J., Barikbin, R., Lochmuller, H., Cassata, G., Krause, S. and Hoppe, T. (2007). The ubiquitin-selective chaperone CDC–48/p97 links myosin assembly to human myopathy. Nat Cell Biol *9*, 379-390.

Kachur, T. M. and Pilgrim, D. B. (2008). Myosin assembly, maintenance and degradation in muscle: role of the chaperone UNC–45 in myosin thick filament dynamics. Int J Mol Sci *9*, 1863-1875.

Kim, J., Lowe, T. and Hoppe, T. (2008). Protein quality control gets muscle into shape. Trends Cell Biol *18*, 264-272.

Landsverk, M. L., Li, S., Hutagalung, A. H., Najafov, A., Hoppe, T., Barral, J. M. and Epstein, H. F. (2007). The UNC–45 chaperone mediates sarcomere assembly through myosin degradation in *Caenorhabditis elegans*. J Cell Biol *177*, 205-210.

Macario, A. J., Grippo, T. M. and de Macario, E. C. (2005). Genetic disorders involving molecular-chaperone genes: A perspective. Genet Med *7*, 3-12.

McClellan, A. J. and Frydman, J. (2001). Molecular chaperones and the art of recognizing a lost cause. Nat Cell Biol *3*, E51-53.

Price, M. G., Landsverk, M. L., Barral, J. M. and Epstein, H. F. (2002). Two mammalian UNC–45 isoforms are related to distinct cytoskeletal and muscle-specific functions. J Cell Sci *115*, 4013-4023.

Rozek, C. E. and Davidson, N. (1983). *Drosophila* has one myosin heavy-chain gene with three developmentally regulated transcripts. Cell *32*, 23-34.

Scheufler, C., Brinker, A., Bourenkov, G., Pegoraro, S., Moroder, L., Bartunik, H., Hartl, F. U. and Moarefi, I. (2000). Structure of TPR domain-peptide complexes: critical elements in the assembly of the Hsp70-Hsp90 multichaperone machine. Cell *101*, 199-210.

Soti, C., Nagy, E., Giricz, Z., Vigh, L., Csermely, P. and Ferdinandy, P. (2005). Heat shock proteins as emerging therapeutic targets. Br J Pharmacol *146*, 769-780.

Srikakulam, R. and Winkelmann, D. A. (1999). Myosin II folding is mediated by a molecular chaperonin. J Biol Chem *274*, 27265-27273.

Sun, Y. and MacRae, T. H. (2005). The small heat shock proteins and their role in human disease. Febs J *272*, 2613-2627.

Swank, D. M., Wells, L., Kronert, W. A., Morrill, G. E. and Bernstein, S. I. (2000). Determining structure/function relationships for sarcomeric myosin heavy chain by genetic and transgenic manipulation of *Drosophila*. Microsc Res Tech *50*, 430-442.

Sweeney, H. L., Straceski, A. J., Leinwand, L. A., Tikunov, B. A. and Faust, L. (1994). Heterologous expression of a cardiomyopathic myosin that is defective in its actin interaction. J Biol Chem *269*, 1603-1605.

Toi, H., Fujimura-Kamada, K., Irie, K., Takai, Y., Todo, S. and Tanaka, K. (2003). She4p/Dim1p interacts with the motor domain of unconventional myosins in the budding yeast, *Saccharomyces cerevisiae*. Mol Biol Cell *14*, 2237-2249.

Trybus, K. M. (1994). Regulation of expressed truncated smooth muscle myosins. Role of the essential light chain and tail length. J Biol Chem *269*, 20819-20822.

Venolia, L., Ao, W., Kim, S., Kim, C. and Pilgrim, D. (1999). *unc–45* gene of *Caenorhabditis elegans* encodes a muscle-specific tetratricopeptide repeat-containing protein. Cell Motil Cytoskeleton *42*, 163-177.

Wesche, S., Arnold, M. and Jansen, R. P. (2003). The UCS domain protein She4p binds to myosin motor domains and is essential for class I and class V myosin function. Curr Biol *13*, 715-724.

Willis, M. S., Schisler, J. C., Portbury, A. L. and Patterson, C. (2009). Build it up--tear it down: protein quality control in the cardiac sarcomere. Cardiovasc Res *81*, 439-448.

Wohlgemuth, S. L., Crawford, B. D. and Pilgrim, D. B. (2007). The myosin co-chaperone UNC-45 is required for skeletal and cardiac muscle function in zebrafish. Dev Biol *303*, 483-492.

Yu, Q. and Bernstein, S. I. (2003). UCS proteins: managing the myosin motor. Curr Biol *13*, R525-527.

Chapter 1: *in vivo* characterization of *Drosophila* UNC–45

Introduction

Myosins are molecular motors that function in cellular processes from cytokinesis and vesicle transport to cell motility. Currently, there are at least 24 classes of myosin [Foth *et al.*, 2006], each with its own unique characteristics. Structurally, myosin molecule has a globular head and a tail. The globular head is the catalytic motor unit, which contains the ATPase domain and the actin binding site. The tail can be used to form coiled-coil dimers or attachments to substrates. Even though the different types of myosin are involved in different cellular functions, they have similar overall structure in the globular head.

Myosin II is a major component of muscle thick filaments and is indispensable in muscle contraction. To facilitate the investigation of its function, researchers have attempted to synthesize muscle myosin *in vitro*. Functional cardiac [Sweeney *et al.*, 1994] and smooth muscle [Trybus, 1994] myosin isoforms have been produced using insect cells, but *in vitro* expression of skeletal muscle isoforms has not been routinely performed without using a myogenic cell line [Chow *et al.*, 2002] or its lysate [Srikakulam and Winkelmann, 1999]. Since functional α-helical tails of rabbit skeletal muscle myosin can be synthesized in *E. coli* [Atkinson and Stewart, 1991], it appears that some factor(s) in the myogenic cell line facilitates the folding of skeletal muscle myosin globular heads into the correct conformation. To gain an

understanding of myosin folding, we are investigating the function of a recently characterized myosin chaperone UNC–45.

From its first description in a temperature-sensitive *C. elegans* mutant [Epstein and Thomson, 1974], to recent data supporting its role in facilitating myosin degradation [Landsverk *et al.*, 2007], UNC–45 has been shown to be important for myosin maturation, thick filament assembly, and muscle function. The discovery of a muscle-specific isoform of UNC–45 in vertebrates [Price *et al.*, 2002] further underscores the importance of UNC–45 in muscle. UNC–45 is critical for muscle function. *C. elegans* mutants of UNC–45 showed movement defects and decreased thick filament formation [Barral *et al.*, 1998], while morpholino knock-down of UNC–45 in zebrafish resulted in paralysis and cardiac dysfunction [Wohlgemuth *et al.*, 2007]. RNAi knock-down of UNC–45 in *Drosophila* embryos showed wild-type body-wall muscle patterning, yet these muscles did not contract [Estrada *et al.*, 2006].

UNC–45 is composed of three domains: an N-terminal tetratricopeptide repeat (TPR) motif, a central domain, and a C-terminal UCS domain (Figure 2A). The TPR domain has been found to interact with heat shock protein 90 [Mishra *et al.*, 2005; Etard *et al.*, 2007; Liu *et al.*, 2008], which led to the notion that UNC–45 is a co-chaperone for heat shock protein 90. The UCS domain is named after the three proteins (UNC–45, Cro1, and She4p) discovered to contain the homologous domain, which was subsequently found to interact with myosin [Barral *et al.*, 2002; Toi *et al.*, 2003]. The central domain of UNC–45 has an unknown function and its sequence is

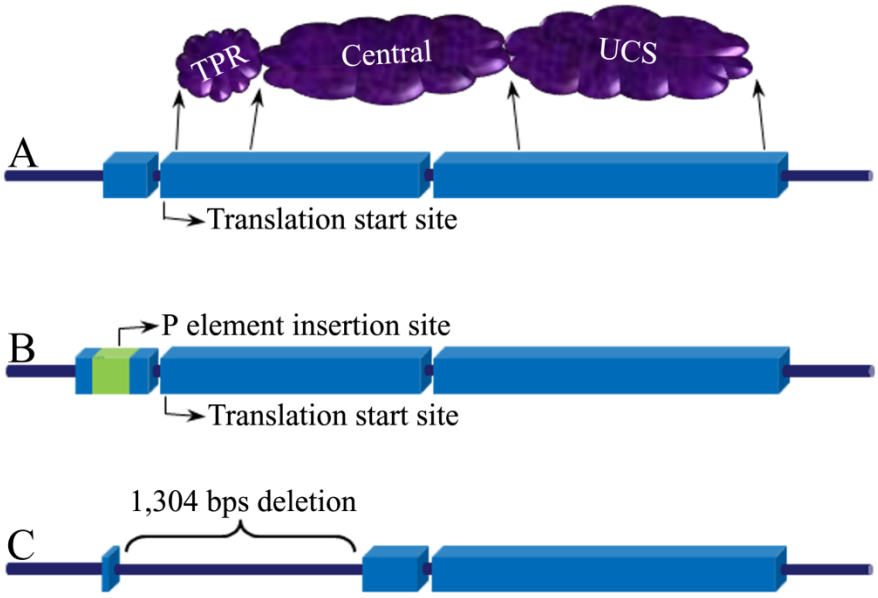

Figure 2. Schematic of *Drosophila unc–45* genomic region in three fly lines. (A) The normal/wild-type gene consists of three exons and two introns, with the translation start site located 14 base pairs downstream from the beginning of the second exon. The gene encodes a three-domain protein of approximately 105 kDa with an N-terminal TPR domain, a central domain, and a C-terminal UCS domain. (B) The *Drosophila unc–45* mutant *Tom34*^{EY03034} contains a *P* element insertion in the first exon, upstream of the translation start site. (C) The *T–33* dUNC–45 knockout mutant contains a 1,304 bp deletion that removes the majority of both the first and second exons.

not well conserved between species. In-depth reviews of UNC–45 function have been published recently [Young *et al.*, 2003; Yu and Bernstein, 2003; Kim *et al.*, 2008; Willis *et al.*, 2009].

Drosophila is an excellent model organism for muscle research due to its well-developed genetics and the availability of techniques to study its muscle structure and physiology [Bernstein *et al.*, 1993; Maughan and Vigoreaux, 1999; Vigoreaux, 2006]. Its genome is composed of four chromosomes, which have been completely sequenced [Adams *et al.*, 2000]. Genetic and transgenic analyses have provided insights into the mechanisms of muscle development, myofibril assembly, and muscle contraction. Here, we present cell biological and genetic analyses of UNC–45 function in *Drosophila*. Our data show that *Drosophila* UNC–45 is expressed during the entire life cycle, that it is enriched in muscle as embryogenesis proceeds, and that it is essential for thick filament accumulation and embryo viability.

Materials & Methods

Fly lines. *Yellow white* (*yw*) flies were used as a wild-type control line. The *Tom34*^{EY03034}/*TM3*(*Sb*) UNC–45 mutant was obtained from the Bloomington Stock Center. It was crossed to a balancer line containing *MKRS*(*Sb*)/*TM3*(y^+, *Ser*) to take advantage of the y^+ and the *Serrate* markers, which resulted in the generation of *Tom34*^{EY03034}/*TM3*(y^+, *Ser*). This line was used to create the dUNC–45 knockout *T–33* /*TM3*(y^+, *Ser*) line through *P* element mobilization by selecting for imperfect excision mutants with deletions in the genomic DNA regions of d*unc –45* (Robertson *et al.*, 1988). Briefly, virgin females of *Tom34*^{EY03034}/*TM3*(y^+, *Ser*) were crossed with males

of the balancer line w^{*}; *CyO*/*Sp*; *TM2*(*Ubx*)/(*Δ2–3, Sb*) containing the *Δ2–3* transposase. The F1 male individuals with blotchy eye color, stubble bristles, and curly wings (*yw*; *CyO*/+; $Tom34^{EY03034}$/(*Δ2–3, Sb*)) were selected and crossed with the *yw*; +; *MKRS*(*Sb*)/*TM3*(y^{+}, *Ser*) balancer line to remove the transposase. The F2 male individuals with white eyes, wild-type cuticle coloration, and serrated wings (*yw*; +; $Tom34^{EY03034}$*Δ*/*TM3*(y^{+}, *Ser*)) were selected and crossed with the *MKRS*(*Sb*)/*TM3*(y^{+}, *Ser*) balancer line again to stabilize the line. A total of 23 potential hypomorphic d*unc–45* jump-out lines were created and each was assessed by Western blot analysis for dUNC–45 expression. Each line was placed in a Plexiglas box containing apple agar plates at 25°C to obtain fertilized eggs that produced homozygous 22 h old embryos, identified by yellow mouth hooks (*yw*; +; $Tom34^{EY03034}$*Δ*/$Tom34^{EY03034}$*Δ*). Western blotting analysis identified the *T–33* line as a dUNC–45 knockout line. PCR and DNA sequencing of *T–33* genomic DNA showed a 1,304 bps deletion starting from 5'-CTTCTCAATTTTTATTTATA-3' to 5'-ACGAGAGTGCAATGG ATATC-3'. Furthermore, a piece of the *P* element (5'-CATGATGAAATAACATC ATGTTAGCCACAG-3') was left behind.

To identify homozygous 14 h old *T–33* embryos, the *T–33*/*TM3*(y^{+}, *Ser*) line was crossed with the *TM3*(*lacZ-hg*, *Sb*) balancer [Gorman and Kaufman, 1995]. The resulting line, *T–33*/*TM3*(*lacZ-hg*, *Sb*), with stubble bristles and normal wings was used to obtain fertilized eggs for immunofluorescence confocal microscopy. Homozygous *T–33* embryos showed an absence of lacZ staining in the hind-gut.

Antibodies, sera, and fluorescent probes. Polyclonal dUNC–45 antibody was obtained through Sigma-Genosys (St. Louis, MO) using the standard antibody service. Bacterially-expressed recombinant His-tagged full-length dUNC–45 [Melkani *et al.*, 2010] was used as the immunizing agent in two New Zealand white rabbits (GN–15577 and GN–15578). The pre-immune serum and third bleed serum from rabbit GN–15578 was used in this study. Rabbit anti-non-muscle myosin and rabbit anti-muscle myosin antibodies were provided by Dan Kiehart, Duke University [Kiehart and Feghali, 1986]. Mouse anti-*Drosophila*-α-actinin antibody was a generous gift from Judith Saide, Boston University School of Medicine. Other antibodies, sera, and fluorescent probe were purchased from commercial sources: goat-anti-rabbit-HRP (BioRad, Hercules, CA), goat-anti-rabbit-Cy5 (Chemicon, Temecula, CA), goat-anti-mouse-FITC (Sigma, St. Louis, MO), mouse-anti-LacZ (Promega, Madison, WI), normal goat serum (Thermo Fisher, Waltham, MA), phalloidin-TRITC (Sigma, St. Louis, MO).

Protein electrophoresis and Western blot analysis. Protein electrophoresis of *Drosophila* lysates and Western blotting were performed as described [Laemmli, 1970; Sambrook and Russell, 2001] using a Bio-Rad Mini-Protean II minigel apparatus and precast 4% stacking, 10% separating acrylamide gels. For detection of dUNC–45 and/or skeletal muscle myosin in the various developmental stages and fly lines, specimens were collected and protein was extracted with Laemmli sample buffer (Bio-Rad, Hercules, CA). Insoluble debris was removed by centrifugation. Protein

quantification was done using advanced protein assay reagent (Cytoskeleton Inc, Denver, CO). 10 µg of protein were loaded for each sample. dUNC–45 antibody was diluted 1:1000 and myosin antibody was diluted 1:20,000. Each primary antibody was incubated with the membrane for at least 4 h to overnight at 4°C. Secondary goat-anti-rabbit-HRP antibody was diluted 1:2000 and incubated with the membrane for 2 h at room temperature.

Wild-type d*unc–45* transgene construction and rescue. The wild-type genomic DNA sequence of d*unc–45* was cloned into the *P* element vector *pCaSpeR4* [Thummel and Pirrotta, 1992]. It contains the mini-white gene, w^+, as a selectable eye color marker to identify transformants. The d*unc–45* transgene contains sequence from 5'-CGTTATATCACATGAAAATT-3' to 5'-AGAAACTTTCGGTTTCGGTT-3', which includes 654 bps upstream of the transcription initiation site and 1,154 bps downstream of the translation stop codon. The final plasmid construct *pW-UNC* was verified by restriction enzymes digest and DNA sequencing. DNA for injection was purified using a QIAfilter Plasmid Maxi Kit (Qiagen, Valencia, CA) according to the manufacturer's instructions. The *pW-UNC* construct was inserted into the *yw Drosophila* background via *P* element-mediated germline transformation using previously established method [Rubin and Spradling, 1982], which was described in detail by Cripps and Bernstein [Cripps *et al.*, 1994]. Red eye color was used as an indication of the presence of the w^+ marker gene and the *P[*w^+, d*unc–45]* transgene in the G1 generation.

To determine the chromosomal location of the inserted transgene, transformants were crossed with w^{1118}; *CyO/Bl*^{1}; *TM2*(*Ubx*)/*TM6B*(*Tb*) flies. We obtained five transgenic lines. Two transgenes were inserted into the 2nd chromosome, two in the third chromosome and one in the 4th chromosome. Transgenic lines on the 2nd and 4th chromosomes were used to rescue the d*unc–45* mutant.

For rescue, adults heterozygous for the *T–33* allele (balanced with *TM3*) were crossed with flies homozygous for each d*unc–45* transgene. Offspring heterozygous for their respective mutant d*unc–45* allele and the transgene were self-crossed. Adult offspring from this second cross were screened for the presence of two copies of the mutant d*unc–45* allele (absence of balancer chromosome) in the presence of one or two copies of the d*unc–45* transgene.

Immunofluorescence confocal microscopy. Whole mount embryo immunofluorescence confocal microscopy was carried out using the fixation protocol previously described [Kosman *et al.*, 2004], but with 4% paraformaldehyde. After fixation, embryos were rehydrated using a series of brief methanol/PBST washes with increasing PBST concentration (5%, 15%, 25%, 50%, 70%) until 100% PBST was reached. The subsequent washes and incubations were all performed using PBST. Blocking of embryos was done using 5% normal goat serum in PBST at room temperature for 30 minutes. Primary antibodies were used at the dilutions indicated: anti-dUNC–45 1:500, anti-skeletal muscle myosin 1:1000, anti-non-muscle myosin 1:1000, anti-LacZ 1:200. Each primary antibody was incubated with the embryos for

at least 4 h to overnight at 4°C. Secondary goat-anti-rabbit-Cy5 antibody was diluted 1:500 and goat-anti-mouse-FITC 1:500, and incubated with the embryos for 2 h at room temperature. Stained embryos were stored in PBS with 50% glycerol. Vectorshield (Vector laboratories, Inc., Burlingame, CA) was added before imaging using a Leica DM IRBE confocal microscope. Phalloidin-TRITC was added with the secondary antibodies at 1:500 dilution to stain filamentous actin.

yw third instar larvae were dissected on Sylgard 184 Silicone elastomer (K.R. Anderson, Morgan Hill, CA). Fixation and staining were performed as previously described [Molina and Cripps, 2001]. Primary antibodies were used at the following dilutions: anti-dUNC–45 1:500, anti-skeletal muscle myosin 1:1000, anti-α-actinin 1:500. Each primary antibody was incubated with the larvae for at least 4 h to overnight at 4°C. Secondary goat-anti-rabbit-Cy5 or goat-anti-mouse-FITC antibodies were diluted 1:500 and incubated with the larvae for 2 h at room temperature. Stained larvae were then visualized as with embryos.

Electron microscopy. 22 h old embryos of *yw*, *T–33* mutant, and *T–33* mutant rescued with an d*unc–45* transgene were isolated and prepared for transmission electron microscopy as described [Cripps *et al.*, 1999]. Fixatives and Embed812 resin were from Electron Microscopy Sciences (Fort Washington, PA); other reagents were from Sigma (St. Louis, MO). Samples were examined with a FEI Tecnai 12 transmission electron microscope operating at 80 kV. Digital images were taken with a TVIPS (Tietz) TemCam-F214 high-resolution digital camera.

Results

Developmental expression of UNC–45 in *Drosophila.* We determined dUNC–45 expression in the *yw* wild-type background using Western blotting analysis for developmental expression and immunofluorescence confocal microscopy for localization. A polyclonal antibody was generated in rabbits using bacterially expressed full-length, His-tagged dUNC–45 as the immunizing agent. The antibodies were highly specific on Western blots (Figure 3A) when probed against whole fly lysates, recognizing a single band of 105 kD. The Western blot analyses show that dUNC–45 is expressed at all developmental stages (Figure 3B-D). To determine the correlation between dUNC–45 localization and myosin accumulation, we used immunofluorescence confocal microscopy to visualize *yw* embryos labeled with antibodies to dUNC–45, muscle myosin, or non-muscle myosin II. At 2 h after egg laying (AEL, Stage 5) (Figure 4A-C), dUNC–45 localized to the embryonic blastoderm and co-localized with non-muscle myosin II. Muscle myosin is not expressed at this time. At 14 h AEL (stage 12) (Figure 4D-G), dUNC–45 localization was similar to that of muscle myosin, which is expressed strongly in the skeletal muscles such as body-wall muscle and pharyngeal muscle. Non-muscle myosin localized to non-muscle tissues, as did some dUNC–45. However, dUNC–45 staining intensity is much brighter in the skeletal muscles. Lateral views of 14 h old embryos show intense dUNC–45 fluorescence in the body-wall muscle similar to skeletal muscle myosin (Figure 4G). Furthermore, dUNC–45 localized to other skeletal

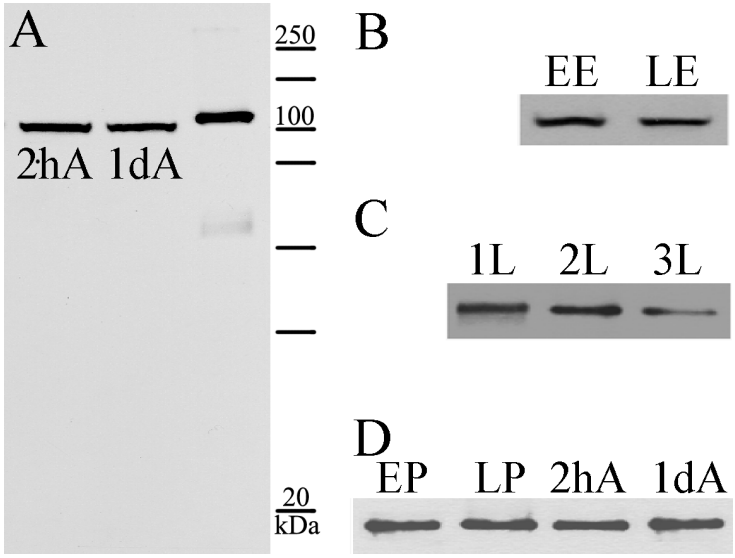

Figure 3. Western blot analysis showing dUNC–45 antibody specificity and dUNC–45 expression at all stages of development in wild-type *Drosophila*. (A) Western blot of 2 h old adult (2hA) and 1 day old adult (1dA) whole fly lysates. The third lane is bacterially-expressed recombinant dUNC–45. It contains a His tag, which accounts for its slightly larger size. The protein size ladder is indicated to the right. (B-D) Developmental expression of dUNC–45. (B) Early (EE) and late stage embryos (LE). (C) First instar (1L), second instar (2L), and third instar larvae (3L). (D) Early pupae (EP), late pupae (LP), 2 h old adult (2hA), and 1 day old adult (1dA). Equivalent amounts of protein were loaded in each lane.

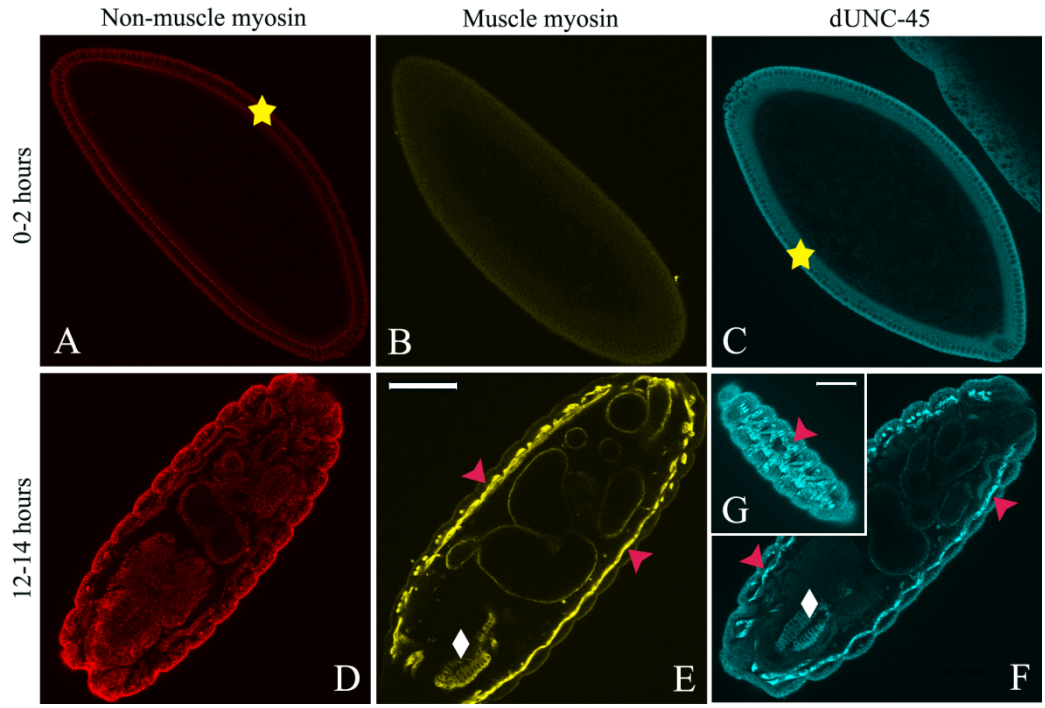

Figure 4. Immunofluorescence confocal micrographs showing protein localization in wild-type, *yw* embryos. The embryos were probed with non-muscle myosin (A, D), muscle myosin (B, E), and dUNC–45 (C, F, G) antibodies. (A-C) 2 h old embryos. At this stage, both non-muscle myosin and dUNC-45 localized to the embryonic blastoderm (yellow stars); muscle myosin is not expressed. (D-F) Ventral views of 14 h old embryos. At 14 h, dUNC–45 localization is more similar to muscle myosin, which can be found in the body-wall (pink arrowheads) and the pharyngeal muscles (white diamonds). Panel G is a lateral view of an embryo confirming dUNC–45 localization in the body wall muscle. Scale bars = 75 µm.

muscle examined including: embryonic dorsal tube, larval body wall muscle, adult body wall muscle, adult dorsal tube, and adult indirect flight muscle (data not shown).

dUNC–45 subcellular localization was also investigated using immunofluorescence confocal microscopy. Third instar larval body wall muscle was used to examine dUNC–45 sarcomeric localization since embryonic body-wall muscles do not show a distinct sarcomeric structure at 14 h of age, and antibodies do not penetrate older embryos due to cuticle formation. Both skeletal muscle myosin and dUNC–45 antibodies were generated using rabbits as host species, co-staining was non-feasible. Instead, dissected third instar *yw* larvae were co-stained with dUNC–45 antibodies, α-actinin antibodies (Z-disc specific), and phalloidin (for actin/I band visualization). The result of the triple staining indicates that dUNC–45 is localized to the Z-discs (Figure 5). It co-localized with α-actinin staining and bisected phalloidin staining.

Mutant analysis. To discern the effects of mutating *unc–45* in *Drosophila*, a mutant line (*Tom34*^{EY03034}) from the Bloomington fly stock center was examined. *Tom34*^{EY03034} is an *unc–45* allele created by insertion of a *P* element in the promoter region, upstream of the translation start site (Figure 2B). *Tom34*^{EY03034} allele homozygotes display third larval instar lethality. Since the coding region of d*unc–45* is not disrupted, it is conceivable that functional protein could still be synthesized, albeit in lower amounts than normal, which could impede our mutant phenotype analysis. Western blotting of 22 h old homozygous *Tom34*^{EY03034} embryos confirmed the presence of the full-length protein (Figure 6A lane 2).

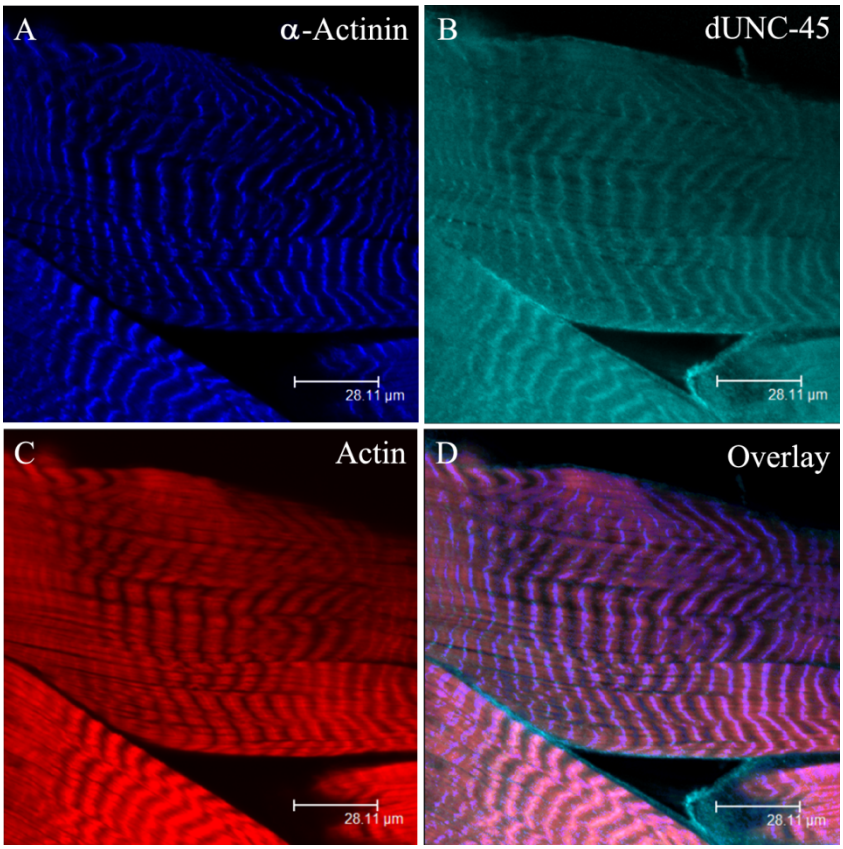

Figure 5. Immunofluorescence confocal micrographs showing subcellular dUNC–45 localization in the body wall muscle of third instar wild-type larvae. (A) α-Actinin staining highlights the location of the Z discs and (C) actin staining with phalloidin shows the location of the I bands in the sarcomeres. (B) dUNC–45 is discretely localized in the sarcomere. (D) dUNC–45 co-localizes with α-actinin (bright pink in the overlay panel) and bisects the actin-containing I bands, which supports dUNC–45 location in the Z discs of the sarcomeres.

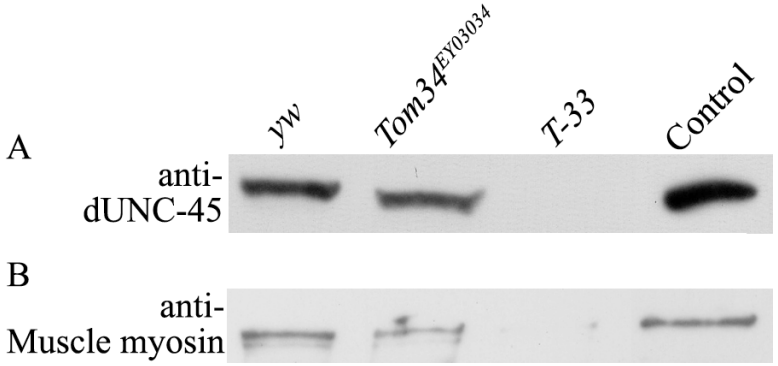

Figure 6. Western blot analysis of dUNC–45 (panel A) and myosin (panel B) expression in wild-type (*yw*), *Tom34*^{EY03034}, and *T–33* embryos. Control in panel A is bacterially-expressed recombinant dUNC–45 while the control in panel B is indirect flight muscle lysate. Results of the analysis show that dUNC–45 can still be detected in the *Tom34*^{EY03034} line but not in the *T–33* line. Muscle myosin heavy chain is somewhat reduced in *Tom34*^{EY03034} homozygotes, but is nearly absent from *T–33* embryos.

To create an *unc–45* null allele, which might have a more severe phenotype, a *P* element mobilization procedure was performed. Potential dUNC–45 null lines were identified by the absence of specific genetic marker phenotypes (see Materials and Methods) and confirmed by Western blotting and DNA sequencing. Analysis of 22 h old homozygous embryos showed that line 33 (*Tom34*$^{EY03043–33}$ or *T–33*) is dUNC–45 null (Figure 6A, lane 3).

T–33 homozygotes display embryonic lethality, which can be rescued by a wild-type d*unc–45* transgene but not by the *Tom34*^{EY03034} allele in the heterozygous complementation test (data not shown). Together, the data comfirm that the lethal phenotype is specifically due to the d*unc–45* knockout. DNA sequencing shows that *T–33* contains a 1,304 bp deletion of the d*unc–45* DNA from the promoter to the second exon (Figure 2C), which includes the translation start site; therefore, subsequent mutant characterization was carried out using this line.

To determine whether the *T–33* allele disrupts dUNC–45 localization, we performed immunofluorescence microscopy of 14 h old embryos. Figures 7A-C show that embryos carrying at least one wild-type d*unc–45* allele, identified by *lacZ* expression in the hindgut, had intense UNC–45 expression in the body-wall muscles, similar to *yw* wild-type. Homozygous *T–33* embryos show barely detectable dUNC–45 staining in the body-wall muscles (Figure 7F). Interestingly, the lack of dUNC–45 did not affect skeletal muscle myosin translation (Figure 7E). However, myosin did not remain stable during the normal period of myofibril assembly, in that

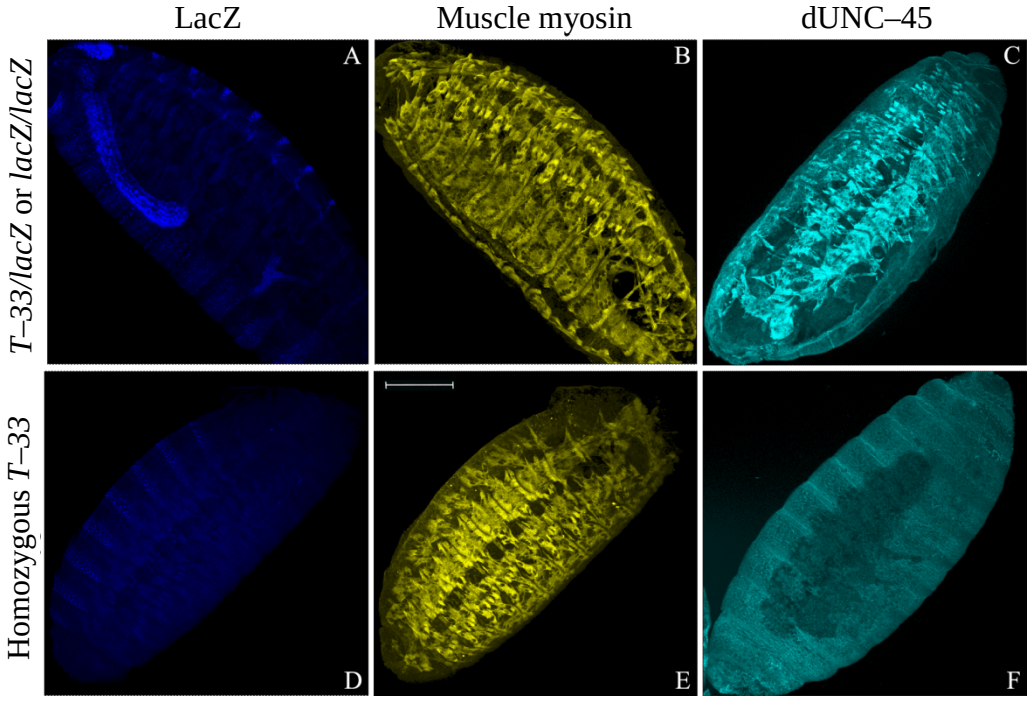

Figure 7. Immunofluorescence confocal micrographs of 14 h *T–33*/*lacZ* or *lacZ*/*lacZ* embryos (panels A-C) and homozygous *T–33* embryos (panels D-F). Embryos were probed with antibodies to lacZ (A, D), muscle myosin (B, E), and dUNC–45 (C, F). *T–33*/*lacZ* or *lacZ*/*lacZ* embryos were identified by the LacZ expression in the hind gut (A), while homozygous *T–33* embryos do not show a detectable expression of LacZ (D). dUNC–45 cannot be detected in the body-wall muscle of the homozygous *T–33* embryos (F). Muscle patterning and muscle myosin expression are not affected in the absence of dUNC–45 at this stage of embryogenesis (E). Scale bar = 75 µm.

myosin levels are greatly reduced in 22 h old homozygous *T–33* embryos (Figure 6B, lane 2). We examined the body wall muscle ultrastructure of such embryos using transmission electron microscopy. Figure 8 shows that 22 h old *yw* wild-type embryos exhibit regular thick and thin filament packing in transverse section (Figure 8A) and regularly spaced thick filaments in longitudinal section (Figure 8B). Homozygous *T–33* embryos of the same age showed disrupted filament packing and a near absence of thick filament accumulation (Figure 8C, D). The muscle defects in the *T–33* homozygous embryos were rescued by a wild-type d*unc–45* transgene (Figure 8E, F).

Discussion

Using *Drosophila melanogaster* wild-type and the mutant flies, we examined UNC–45 localization and function. We find that dUNC–45 is expressed throughout development and its expression is maintained in adulthood (Figure 3 B-D), suggesting that it functions not only in myosin assembly/folding but possibly in muscle maintenance and/or repair.

dUNC–45 co-localizes with non-muscle myosin in 2 h old embryos, prior to the expression of skeletal muscle myosin (Figure 4 upper panels). At this cellularization stage, non-muscle myosin displays a cytosolic/peri-nuclear localization pattern [Young *et al.*, 1991], which co-localizes with dUNC–45. It is likely that dUNC–45 is interacting with non-muscle myosins, as there is evidence that UNC–45 does so during cytokinesis in early *C. elegans* embryos [Kachur and Pilgrim, 2008]. Similarly, other UNC–45-like proteins such as She4p and Rng3 interact with myosin V and non-muscle myosin II respectively [Wong *et al.*, 2000; Wesche *et al.*, 2003].

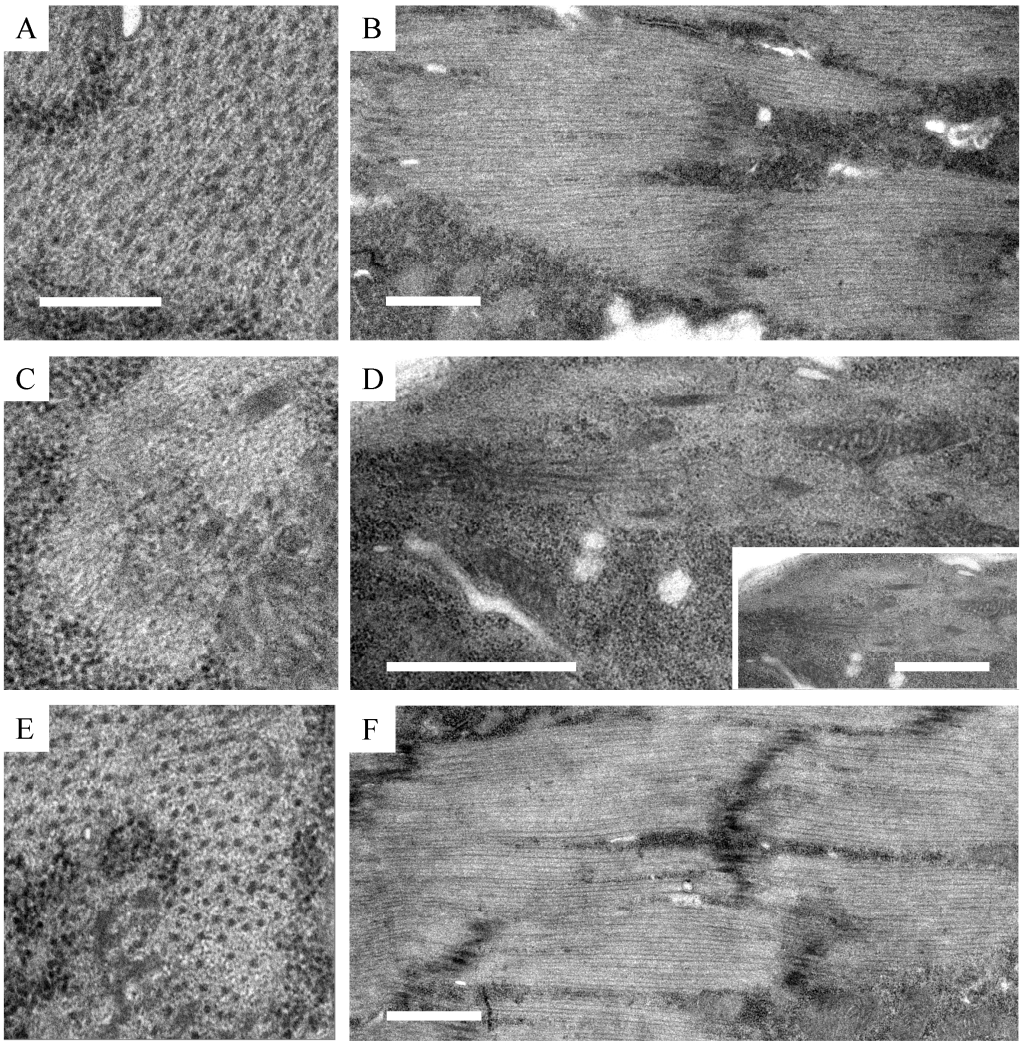

Figure 8. Electron micrographs of 22 h old embryos examining body wall muscle ultrastructure in transverse (A, C, and E) and longitudinal orientations (B, D, and F). *yw* control line (A, B), *T–33* dUNC–45 knockout (C, D), and *T–33* rescued with a wild-type transgene (E, F). Electron micrographs show that *T–33* embryos exhibit a reduced level of thick filaments and a loss of the thick/thin filament lattice spacing (C, D). This phenotype can be rescued with a wild-type d*unc–45* transgene, which confirms the effects of dUNC–45 knockout in the muscles. Scale bar for A = 0.25 µm (applies to C and E). Bar for B, D inset, and F = 1.0 µm. D = 1.0 µm.

Furthermore, UNC–45 is maternally inherited in *C. elegans* [Venolia and Waterston, 1990]. It is plausible that the *Drosophila* UNC–45 present at the blastoderm stage is maternally inherited as well.

In 14 h old embryos, dUNC–45 co-localizes with skeletal muscle myosin (Figure 4 lower panels). Skeletal muscle myosin expression starts at approximately 10 h AEL, correlating with the onset of muscle bundle formation and patterning (data not shown). Since skeletal muscle myosin and dUNC–45 showed intense staining in the embryonic body wall muscle, it appears that the major zygotic expression of dUNC–45 coincides with muscle myosin expression both spatially and temporally. Subcellularly, dUNC–45 localizes to the Z-discs of the sarcomeres in the body wall muscle of wild-type *yw* third instar larvae (Figure 5). This result agrees with the observations of Etard, *et al*. (2007), who localized UNC–45 at the Z-discs of zebrafish under normal developmental conditions. We used a polyclonal antibody against wild-type dUNC–45, whereas an UNC–45-GFP chimera was used in the zebrafish study. It is possible that our polyclonal dUNC–45 antibodies recognize targets other than UNC–45. However, since immunofluorescence confocal microscopy staining using pre-immunized rabbit serum did not yield specific staining pattern above background (data not shown) and Western blot analysis showed a single band of the correct protein size when using total adult fly lysate (Figure 3A), this is unlikely.
It may be important to regulate UNC–45 localization, since UNC–45 contributes to myosin degradation when over-expressed in *C. elegans* [Landsverk *et al.*, 2007]. Consequently, Z-disc localization may be required to prevent the degradation of

functional myosin to prevent the degradation of normal, functional myosin. The Z-disc could store UNC–45, which is released in response to muscle stress/damage, as has been shown to occur in zebrafish [Etard *et al.*, 2008].

Analysis of *T–33* dUNC–45 mutant flies provided important insights into the function of UNC–45 during muscle formation. Western blot analysis showed a drastic decrease of dUNC–45 in the 22 h old homozygous embryos compared to wild-type *yw* embryos (Figure 6A). Occasionally, a small amount of dUNC–45 could be seen in the *T–33* line, which is likely the remnant of maternally inherited protein. Immunofluorescence confocal microscopy showed that 14 h old *T–33* homozygous embryos barely stain for dUNC–45 in their body wall muscles (Figure 7), which contrasts with intense staining in the heterozygous *T–33* and the wild type. This confirms the zygotic expression of dUNC–45 at this stage, which coincides with skeletal muscle myosin expression. Interestingly, in the absence of zygotically expressed dUNC–45, skeletal muscle myosin is still expressed in abundance and the muscle patterning appears normal (Figure 7E). The skeletal muscle myosin produced at this time may be folded by the remnants of maternally inherited dUNC–45 or not folded appropriately. In contrast, Western blot analysis of 22 h homozygous *T–33* embryos showed a drastic decrease in skeletal muscle myosin (Figure 6B). Together, the data support the idea that the lack of dUNC–45 does not affect skeletal muscle myosin translation, but results in the accumulation of non-functional myosin that is later degraded. The body wall muscles of homozygous null 22 h embryos showed a

lack of sarcomeric structure, with few visible thick filaments (Figure 8C, D), resulting in embryonic lethality.

If dUNC–45 is not needed during myosin translation, then it must be needed post-translationally for proper myosin folding and/or stabilization. *In vitro* translation of chicken smooth muscle myosin in the presence of mouse UNC–45 also supports a post-translational association of the two proteins [Liu *et al.*, 2008]. However, a yeast UCS protein, Rng3, associates with myosin mRNA in polysomes in ribonucleoprotein immunoprecipitation-microarray experiments, which implies a co-translational involvement [Amorim and Mata, 2009].

Overall we demonstrated that dUNC–45 is essential for *Drosophila* skeletal muscle myosin stability, muscle function, and viability during myosin production. However, as a chaperone, UNC–45 could also functions in muscle maintenance and protection during stress. Structural information will advance our knowledge about this protein greatly by facilitating *in vivo* studies of specific UNC–45 site-directed mutants in *Drosophila* and other model organisms. Once UNC–45's mechanism of action is unraveled, it could serve as a therapeutic target for muscle/heart disease.

References

Adams, M. D. Celniker, S. E. Holt, R. A. Evans, C. A. Gocayne, J. D. Amanatides, P. G. Scherer, S. E. Li, P. W. Hoskins, R. A. Galle, R. F. *et al.* (2000). The genome sequence of *Drosophila melanogaster*. Science *287*, 2185-2195.

Amorim, M. J. and Mata, J. (2009). Rng3, a member of the UCS family of myosin co-chaperones, associates with myosin heavy chains cotranslationally. EMBO Rep *10*, 186-191.

Atkinson, S. J. and Stewart, M. (1991). Expression in *Escherichia coli* of fragments of the coiled-coil rod domain of rabbit myosin: influence of different regions of the molecule on aggregation and paracrystal formation. J Cell Sci *99 (Pt 4)*, 823-836.

Barral, J. M., Bauer, C. C., Ortiz, I. and Epstein, H. F. (1998). Unc–45 mutations in *Caenorhabditis elegans* implicate a CRO1/She4p-like domain in myosin assembly. J Cell Biol *143*, 1215-1225.

Barral, J. M., Hutagalung, A. H., Brinker, A., Hartl, F. U. and Epstein, H. F. (2002). Role of the myosin assembly protein UNC–45 as a molecular chaperone for myosin. Science *295*, 669-671.

Bernstein, S. I., O'Donnell, P. T. and Cripps, R. M. (1993). Molecular genetic analysis of muscle development, structure, and function in *Drosophila*. Int Rev Cytol *143*, 63-152.

Chow, D., Srikakulam, R., Chen, Y. and Winkelmann, D. A. (2002). Folding of the striated muscle myosin motor domain. J Biol Chem *277*, 36799-36807.

Cripps, R. M., Becker, K. D., Mardahl, M., Kronert, W. A., Hodges, D. and Bernstein, S. I. (1994). Transformation of *Drosophila melanogaster* with the wild-type myosin heavy-chain gene: rescue of mutant phenotypes and analysis of defects caused by overexpression. J Cell Biol *126*, 689-699.

Cripps, R. M., Suggs, J. A. and Bernstein, S. I. (1999). Assembly of thick filaments and myofibrils occurs in the absence of the myosin head. EMBO J *18*, 1793-1804.

Epstein, H. F. and Thomson, J. N. (1974). Temperature-sensitive mutation affecting myofilament assembly in *Caenorhabditis elegans*. Nature *250*, 579-580.

Estrada, B., Choe, S. E., Gisselbrecht, S. S., Michaud, S., Raj, L., Busser, B. W., Halfon, M. S., Church, G. M. and Michelson, A. M. (2006). An Integrated Strategy for Analyzing the Unique Developmental Programs of Different Myoblast Subtypes. PLoS Genet *2*, e16.

Etard, C., Behra, M., Fischer, N., Hutcheson, D., Geisler, R. and Strahle, U. (2007). The UCS factor Steif/Unc–45b interacts with the heat shock protein Hsp90a during myofibrillogenesis. Dev Biol *308*, 133-143.

Etard, C., Roostalu, U. and Strahle, U. (2008). Shuttling of the chaperones Unc45b and Hsp90a between the A band and the Z line of the myofibril. J Cell Biol *180*, 1163-1175.

Foth, B. J., Goedecke, M. C. and Soldati, D. (2006). New insights into myosin evolution and classification. Proc Natl Acad Sci U S A *103*, 3681-3686.

Gorman, M. J. and Kaufman, T. C. (1995). Genetic analysis of embryonic cis-acting regulatory elements of the *Drosophila* homeotic gene sex combs reduced. Genetics *140*, 557-572.

Kachur, T. M. and Pilgrim, D. B. (2008). Myosin Assembly, Maintenance and Degradation in Muscle: Role of the Chaperone UNC–45 in Myosin Thick Filament Dynamics. Int J Mol Sci *9*, 1863-1875.

Kiehart, D. P. and Feghali, R. (1986). Cytoplasmic myosin from *Drosophila melanogaster*. J Cell Biol *103*, 1517-1525.

Kim, J., Lowe, T. and Hoppe, T. (2008). Protein quality control gets muscle into shape. Trends Cell Biol *18*, 264-272.

Kosman, D., Mizutani, C. M., Lemons, D., Cox, W. G., McGinnis, W. and Bier, E. (2004). Multiplex detection of RNA expression in *Drosophila* embryos. Science *305*, 846.

Laemmli, U. K. (1970). Cleavage of structural proteins during the assembly of the head of bacteriophage T4. Nature *227*, 680-685.

Landsverk, M. L., Li, S., Hutagalung, A. H., Najafov, A., Hoppe, T., Barral, J. M. and Epstein, H. F. (2007). The UNC–45 chaperone mediates sarcomere assembly through myosin degradation in *Caenorhabditis elegans*. J Cell Biol *177*, 205-210.

Liu, L., Srikakulam, R. and Winkelmann, D. A. (2008). Unc45 activates Hsp90-dependent folding of the myosin motor domain. J Biol Chem *283*, 13185-13193.

Maughan, D. W. and Vigoreaux, J. O. (1999). An Integrated View of Insect Flight Muscle: Genes, Motor Molecules, and Motion. News Physiol Sci *14*, 87-92.

Melkani, G. C., Lee, C. F., Cammarato, A. and Bernstein, S. I. (2010). *Drosophila* UNC–45 prevents heat-induced aggregation of skeletal muscle myosin and facilitates refolding of citrate synthase. Biochem Biophys Res Commun *396*, 317-322.

Mishra, M., D'Souza V, M., Chang, K. C., Huang, Y. and Balasubramanian, M. K. (2005). Hsp90 protein in fission yeast Swo1p and UCS protein Rng3p facilitate myosin II assembly and function. Eukaryot Cell *4*, 567-576.

Molina, M. R. and Cripps, R. M. (2001). Ostia, the inflow tracts of the *Drosophila* heart, develop from a genetically distinct subset of cardial cells. Mech Dev *109*, 51-59.

Price, M. G., Landsverk, M. L., Barral, J. M. and Epstein, H. F. (2002). Two mammalian UNC–45 isoforms are related to distinct cytoskeletal and muscle-specific functions. J Cell Sci *115*, 4013-4023.

Rubin, G. M. and Spradling, A. C. (1982). Genetic transformation of *Drosophila* with transposable element vectors. Science *218*, 348-353.

Sambrook, J. and Russell, D. W. (2001). Molecular cloning: a laboratory manual, 3rd edn (Cold Spring Harbor, N.Y., Cold Spring Harbor Laboratory Press).

Srikakulam, R. and Winkelmann, D. A. (1999). Myosin II folding is mediated by a molecular chaperonin. J Biol Chem *274*, 27265-27273.

Sweeney, H. L., Straceski, A. J., Leinwand, L. A., Tikunov, B. A. and Faust, L. (1994). Heterologous expression of a cardiomyopathic myosin that is defective in its actin interaction. J Biol Chem *269*, 1603-1605.

Thummel, C.S., Pirrotta, V. (1992). Technical notes: new pCasper P-element vectors. Dros. Inf. Serv. *71* (1992), p. 150.

Toi, H., Fujimura-Kamada, K., Irie, K., Takai, Y., Todo, S. and Tanaka, K. (2003). She4p/Dim1p interacts with the motor domain of unconventional myosins in the budding yeast, *Saccharomyces cerevisiae*. Mol Biol Cell *14*, 2237-2249.

Trybus, K. M. (1994). Regulation of expressed truncated smooth muscle myosins. Role of the essential light chain and tail length. J Biol Chem *269*, 20819-20822.

Venolia, L. and Waterston, R. H. (1990). The unc–45 gene of *Caenorhabditis elegans* is an essential muscle-affecting gene with maternal expression. Genetics *126*, 345-353.

Vigoreaux, J. O. (2006). Nature's versatile engine insect flight muscle inside and out. in Molecular biology intelligence unit (Georgetown, Tex. New York, N.Y., Landes Bioscience/Eurekah.com; Springer Science Business Media), pp. 288.

Wesche, S., Arnold, M. and Jansen, R. P. (2003). The UCS domain protein She4p binds to myosin motor domains and is essential for class I and class V myosin function. Curr Biol *13*, 715-724.

Willis, M. S., Schisler, J. C., Portbury, A. L. and Patterson, C. (2009). Build it up--tear it down: protein quality control in the cardiac sarcomere. Cardiovasc Res *81*, 439-448.

Wohlgemuth, S. L., Crawford, B. D. and Pilgrim, D. B. (2007). The myosin co-chaperone UNC–45 is required for skeletal and cardiac muscle function in zebrafish. Dev Biol *303*, 483-492.

Wong, K. C., Naqvi, N. I., Iino, Y., Yamamoto, M. and Balasubramanian, M. K. (2000). Fission yeast Rng3p: an UCS-domain protein that mediates myosin II assembly during cytokinesis. J Cell Sci *113 (Pt 13)*, 2421-2432.

Young, J. C., Barral, J. M. and Ulrich Hartl, F. (2003). More than folding: localized functions of cytosolic chaperones. Trends Biochem Sci *28*, 541-547.

Young, P. E., Pesacreta, T. C. and Kiehart, D. P. (1991). Dynamic changes in the distribution of cytoplasmic myosin during *Drosophila* embryogenesis. Development *111*, 1-14.

Yu, Q. and Bernstein, S. I. (2003). UCS proteins: managing the myosin motor. Curr Biol *13*, R525-527.

Acknowledgements

This chapter is a manuscript draft. The experiments performed by Chi Lee include: 1) Prepared the dUNC–45 protein as an immunizing agent for antibody production in rabbits. 2) Evaluated the specificity of dUNC–45 antibodies using Western blot analysis. 3) Performed *P* element mobilization on *Tom34*^{EY03034} flies to obtain the dUNC–45 null line *T–33*. 4) Prepared the samples and imaged all the immunofluorescence confocal microscopy to characterize dUNC–45 localization in the embryos and larvae.

Dr. Melkani performed mutant complementation rescues and the Western blot analysis of dUNC–45 expression in figures 3B-D, and all of figure 6. Jennifer Suggs carried out the sample preparation and imaging of embryos using electron microscopy. William Kronert constructed the d*unc–45* transgene. Finally, Yoko Suzuki characterized the *T–33* DNA lesion in the d*unc–45* gene through sequencing analysis.

Chapter 2: *in vitro* characterization of *Drosophila* UNC–45 chaperone function

Introduction

Since the first description of a *C. elegans* mutant in 1974, much has been studied about UNC–45. It is now well established that UNC–45 interacts with heat shock protein 90 (Hsp90) [Etard *et al.*, 2007; Srikakulam *et al.*, 2008] during myosin production and muscle development. This interaction involves the N-terminal tetratricopeptide repeat (TPR) domain of UNC–45 and the MEEVD peptide on the C-terminus of Hsp90 [Barral *et al.*, 2002]. Due to its association with the well known Hsp90 chaperone and the fact that it contains the TPR co-chaperone domain motif, UNC–45 is being referred to as a co-chaperone that serves to activate Hsp90 function during myosin maturation [Liu *et al.*, 2008]. Some of the Hsp90 co-chaperones, such as p23 and FKBP52, however, demonstrated intrinsic chaperone functions by suppressing heat induced aggregation of various *in vitro* chaperone assay substrates [Bose *et al.*, 1996; Picard, 2002]. UNC–45 has also exhibited intrinsic chaperone functions.

The first characterization of UNC–45 chaperone function was performed using recombinant *C. elegans* UNC–45 with a histidine-tag at the N-terminus and a FLAG tag at the C-terminus, which was expressed in Sf9 insect cells [Barral *et al.*, 2002]. The expressed protein interacted with purified *C. elegans* myosin in pull-down assays and prevented the myosin motor domain (S1) of scallop from undergoing heat induced aggregation in a concentration dependent manner. In addition, the authors used citrate

synthase (CS), a well-known *in vitro* chaperone assay substrate, to show that cUNC–45 suppressed heat induced CS aggregation to a similar level as Hsp90. Besides this characterization of UNC–45 chaperone function, no other UNC–45 protein has been purified to homogeneity and used in *in vitro* chaperone assays. However, as discussed below, efforts were made to synthesize functional skeletal muscle myosin *in vitro* by adding exogenous expressed UNC–45.

As mentioned in the introduction, skeletal muscle myosin cannot be synthesized *in vitro* without addition of a myogenic cell lysate. For these types of assays, skeletal muscle myosin is synthesized in an *in vitro* coupled transcription and translation reticulocyte synthesis system supplemented with cell lysate derived from the mouse C2C12 myogenic cell line [Srikakulam and Winkelmann, 1999]. These myosin molecules bound and released actin in an ATP dependent manner, suggesting a native myosin conformation. By replacing the C2C12 cell lysate with UNC–45, Winkelmann *et al*. demonstrated that both vertebrate isoforms of UNC–45, UNC–45A and UNC–45B, dramatically enhance myosin folding, but not to the final native conformation [Liu *et al.*, 2008]. In addition, both UNC–45A and UNC–45B fold myosin in an Hsp90 dependent manner. By inhibiting Hsp90 function using geldanamycin (inhibits Hsp90 ATPase activity), the enhanced myosin folding afforded by UNC–45 was abrogated. The authors concluded that UNC–45 is a co-chaperone and placed it upstream of Hsp90 in the myosin maturation pathway.

Whether UNC–45 functions as a chaperone independently of Hsp90 or it only functions as a co-chaperone for Hsp90 is currently unclear. To further characterize

UNC–45's intrinsic chaperone function and capability, bacterially expressed *Drosophila* UNC–45 (dUNC–45) is used here to facilitate UNC–45 analysis *in vitro*. Moreover, the possible *in vivo* mechanism of dUNC–45 function is also explored.

Materials & Methods

Cloning, expression, and purification of dUNC–45. *Drosophila unc–45* cDNA was reverse transcribed from total mRNA of 50 wild-type (*yw*) pupae and PCR amplified using forward primer 5'-ATTCAGTACATATGACAAACACC ATCAACA-3' and reverse primer 5'-ACGTTCTCGAGTTAATCATCGATAA TCTCA-3'. d*unc–45* cDNA was cloned into the pET–16b vector (Novagen) between the Nde I and Xho I sites and the resulting plasmid was sequenced to insure fidelity. The pET–16b vector incorporates a ten-histidine tag at the N-terminus of d*unc–45*, and the resulting construct was expressed in the Rosetta (DE3)pLysS strain of bacteria (Novagen). After addition of IPTG (final concentration 0.5 mM) to induce protein production, cells were lysed by freezing and thawing. Sonication was used to further ensure cell lysis. The cell lysate was then centrifuged to separate soluble and insoluble protein fractions; UNC–45 is found in the soluble fraction. The his-tagged dUNC–45 protein was affinity purified from the soluble protein fraction using a HisTrap HP column (GE Healthcare). Protein was eluted from the HisTrap column with 20 mM Tris, 500 mM NaCl, 500 mM imidazole, pH 7.4. dUNC–45 was further purified through size exclusion chromatography using a Superdex 200 16/60 column (GE Healthcare) and exchanged into 20 mM Tris, 500 mM NaCl, 1 mM DTT, pH 7.5.

The homogeneity of the purified protein was verified by Coomassie blue staining of samples separated by SDS-PAGE.

dUNC–45 chaperone function assay using citrate synthase and α-lactalbumin. DTT-induced aggregation of α-lactalbumin was carried out at 37°C as previously reported [Reddy *et al.*, 2002] in the presence or absence of dUNC–45. In brief, 0.5 µM α-lactalbumin was incubated with 20 mM DTT with or without 1.0 µM dUNC–45 in 100 mM NaCl, 20 mM Tris-HCl, pH 7.5. Heat-induced aggregation of citrate synthase (0.25 µM) was performed as previously described [Buchner *et al.*, 1991] in 100 mM NaCl, 20 mM Tris-HCl, pH 7.5 in the absence or presence of dUNC–45 (0.5 µM) and measured at 45°C. Protein aggregation was detected by light scattering (LS) using a PTI spectrofluorometer equipped with a temperature-controlled cell holder. The excitation and emission wavelengths were set to 360 nm and output was monitored in arbitrary units (AU). Urea-induced unfolding of citrate synthase was performed using 8M urea for 30 min as described previously [Buchner *et al.*, 1991; Muchowski and Clark, 1998]. Refolding of CS was carried out in the presence or absence of dUNC–45 at 25°C after 100 fold dilutions. CS activity was monitored at various time points at 412 nm and GroEL or α-crystallin was used as a control as described previously [Buchner *et al.*, 1991; Muchowski and Clark, 1998].

Binding of dUNC–45 with ATP. The binding of dUNC–45 with ATP was assessed using fluorescence spectroscopy. Intrinsic tryptophan fluorescence of dUNC–45 (1 µM) was recorded at 25ºC in the presence or absence of ATP in 20 mM Tris-HCl, pH 7.5, containing 100 mM NaCl. The pH of ATP was adjusted to pH 7.5

prior to use. The excitation wavelength for tryptophan fluorescence was 295 nm and fluorescence emission was recorded between 310-400 nm, using a PTI spectrofluorometer (Photon Technology International). Trp fluorescence of BSA was used as a negative control for it does not bind ATP (not shown). All spectra and intensity measurement were corrected for buffer, protein and nucleotide absorbance. Quenching of dUNC–45 tryptophan was also confirmed in the presence of the neutral quencher acrylamide (not shown). To see the effect of salt, control titrations were performed with 20 mM Tris-HCl, pH 7.5, containing 100 mM NaCl (not shown).

Purification of chicken muscle myosin and preparation of S–1. The skeletal muscle myosin from frozen chicken pectoralis muscle (obtained from Pel-Freeze, Rogers, AK) was prepared according to the method of Margossian and Lowey [Margossian and Lowey, 1982]. Isolated chicken myosin was stored at -20ºC in 0.6 M KCl, 20 mM sodium phosphate, pH 7.0, 1 mM DTT, 3 mM NaN3 and 50% glycerol. S–1 fragment from chicken skeletal muscle myosin was prepared by chymotrypsin proteolysis as described previously [Miller *et al.*, 2003].

dUNC–45 chaperone assay using full-length myosin and S–1. The ability of dUNC–45 to prevent protein aggregation at heat shock temperature was previously described for chicken myosin using light scattering [Melkani *et al.*, 2006]. In brief, light scattering of chicken skeletal muscle myosin (0.25 µM) or S–1 (0.5 µM) in the presence or absence of dUNC–45 (0.25-8 µM) was measured at 43ºC using the same instrument. For monitoring chaperone function of dUNC–45 in the presence of AMP-PNP, dUNC–45 was incubated with 1.0-3.5 mM AMP-PNP for 15 min at 25ºC

prior to its incubation with myosin or S–1 at 25ºC, 37ºC, or 43ºC. Furthermore, for monitoring the influence of AMP-PNP on myosin and S-1 aggregation kinetics, myosin or S–1 was incubated with 1~3.5 mM AMP-PNP prior to incubation at 43ºC.

Electron microscopy of myosin and dUNC–45. Electron microscopy of full-length chicken skeletal muscle myosin, in the absence and in the presence of dUNC–45 and at different temperatures, was carried out by modifying established methods [Craig *et al.*, 1983] as previously described in detail [Melkani *et al.*, 2006]. Structural analysis consisted of counting particles that resembled the normal two-headed myosin structure at room temperature and at elevated temperatures. The number of molecules that showed inter- or intra-molecular associations at room temperature and upon heating and incubation with or without ATP-UNC–45 were distinguished from those molecules that did not show such associations.

Western blot analysis of dUNC–45 expression. One-day-old adult *yw* flies were separated to individual food vials and allowed to recover from CO_2 treatment overnight at 25°C. Flies marked for starvation stress were transferred to fly vials without food and allowed to recover from CO_2. The next day, individual vials were subjected to various stresses as indicated. Heat shock was achieved by incubating flies at 37°C for one hour while cold shock was done at 4°C for one hour. CO_2 treatment was performed by leaving the flies on the CO_2 stage for half an hour un-covered. Hydrogen peroxide treatment was carried out by transferring flies to a new food vial with hydrogen peroxide dripped into the food and incubated at 25°C for one hour. Control flies and flies marked for starvation stress were left in 25°C for one

hour while stress treatment was in progress for other flies. All flies were stored at -80°C right after stress treatment. Protein samples were prepared by homogenizing ten flies into 100 µl Laemmli buffer and 10 µl of each sample were loaded onto an SDS polyacrylamide gel. SDS-PAGE and Western blot analysis were carried out as in chapter one.

Confocal microscopy of dUNC–45 localization. Confocal microscopy and embryo collection were performed as in chapter one. Upon hatching, first instar larvae were transferred to a new apple agar plate containing yeast paste, and allowed to mature at 25°C until of correct age. Third instar larvae marked for heat shock were incubated at 37°C for two hours while control larvae were left at 25°C for the duration of the heat shock treatment. Larvae dissection, fixation, and antibody staining were carried out as in chapter one.

Results

To begin investigating the intrinsic chaperone function of dUNC–45 *in vitro*, a recombinant dUNC–45 with an N-terminal 10 histidine-tag was expressed in *E. coli*. The his-tag could be cleaved by using the factor Xa protease, but it was left intact. The recombinant dUNC–45 was purified using a nickel column followed by size exclusion chromatography. The nickel column purified protein appeared greater than 95% pure on Coomassie blue stained protein gels (Figure 9A) and eluted from the size-exclusion column as a single peak (Figure 9B), indicating a single, homogeneous species of dUNC–45 protein suitable for *in vitro* assays. Upon successfully purifying

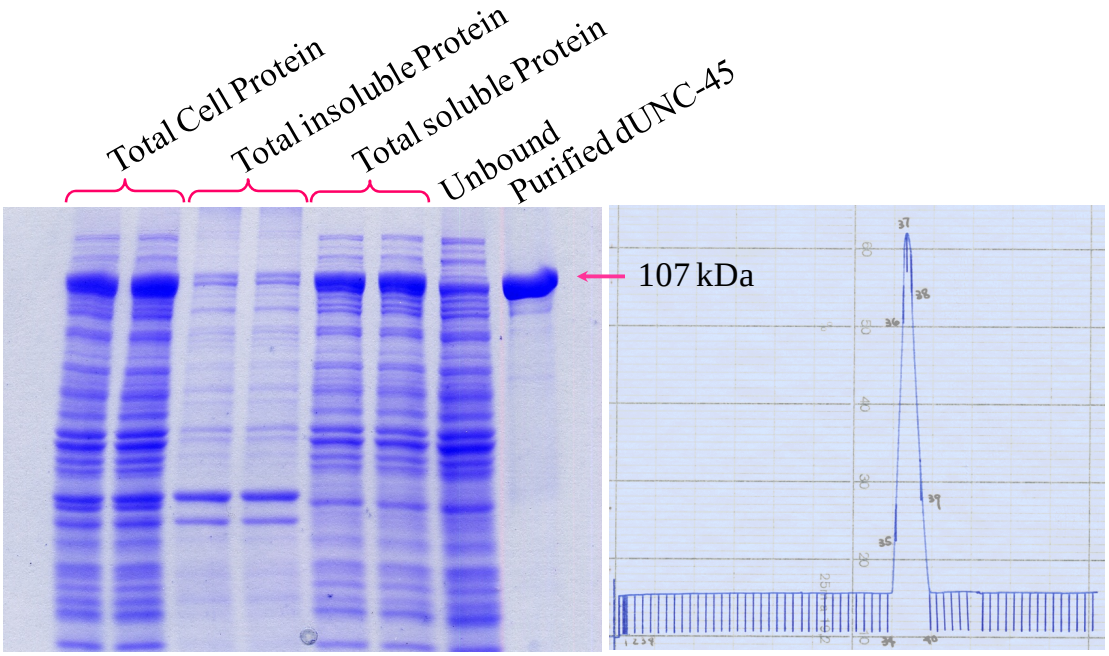

Figure 9. Recombinant dUNC–45 can be purified to homogeneity. (Left panel) Coomassie stained SDS-PAGE of the various fractions from cell fractionation and immobilized metal affinity chromatography. (Right panel) dUNC–45 eluted from the size-exclusion column (Superdex 200 16/60 column) in a single symmetrical peak indicating a pure, homogeneous population of protein suitable for *in vitro* assays.

the recombinant dUNC–45 from bacteria, testing of dUNC–45 chaperone function was performed by Dr. Girish Melkani who is a postdoctoral chemist in the laboratory.

We tested whether *Drosophila* UNC–45 could function as a chaperone similarly to the purified *C. elegans* UNC–45, by examining its ability to protect CS from heat induced protein aggregation. Protein aggregation was detected by increased light scattering. Figure 10 shows the light scattering profile of CS incubated at 45°C over time in the presence and absence of dUNC–45. In the presence of dUNC–45, CS aggregation was suppressed approximately 25%. Testing using α–lactalbumin (not shown), which is another routinely used substrate for testing chaperone functions confirmed our CS results.

Since the protection capabilities of many chaperones, such as Hsp90, Hsp70, and αB-crystalin [Muchowski and Clark, 1998] are enhanced by ATP, we tested dUNC–45 chaperone function in the presence of ATP. In the presence of ATP, dUNC–45 suppressed heat induced CS aggregation approximately 60%, nearly double the amount obtained when no nucleotide is present (Figure 10). This ATP enhanced chaperone function of UNC–45 is preserved when using UNC–45's native substrate myosin (Figure 11). Myosin is an ATPase that uses the energy from ATP hydrolysis to move alone the filament. To avoid confounding our result, a non-hydrolysable ATP analogue, AMP-PNP, was used for *in vitro* myosin protection assays. In the absence of dUNC–45, chicken skeletal myosin motor domain (S1) forms protein aggregates when incubated at 43°C. Such aggregation is suppressed approximately 56% in the presence of dUNC–45. Inclusion of AMP-PNP afforded an additional 38% protection

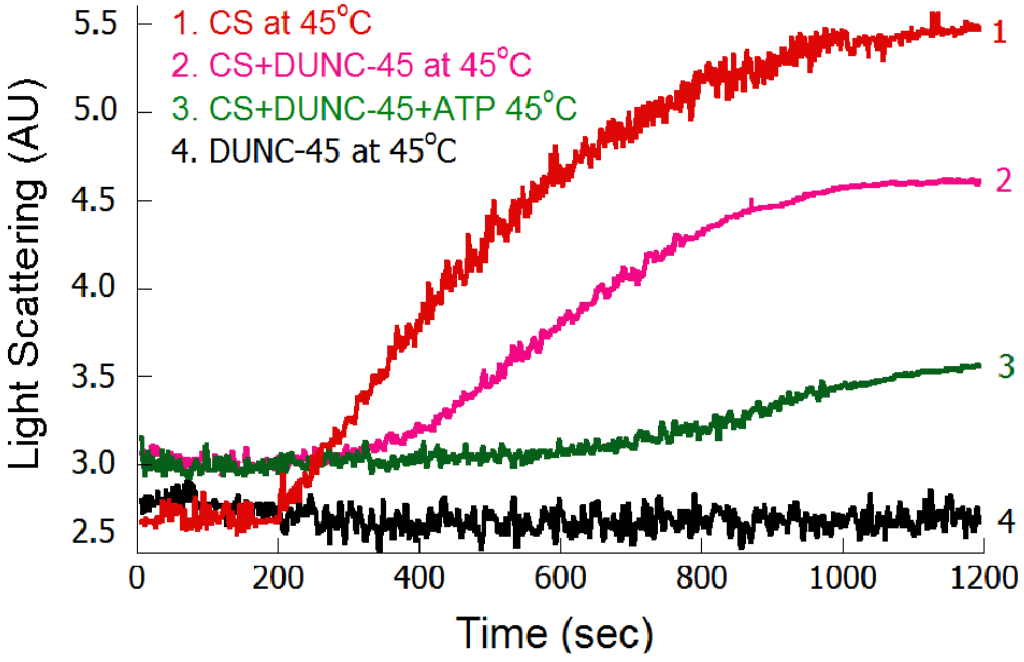

Figure 10. dUNC–45 protects citrate synthase (CS) from heat induced protein aggregation. Light scattering is used to reflect protein aggregation. CS alone forms protein aggregates when incubated at 45°C (curve 1). In the presence of dUNC–45, CS aggregation is decreased (curve 2). ATP enhances dUNC–45 conferred heat protection (curve 3). dUNC–45 is stable by itself during the experiment (curve 4).

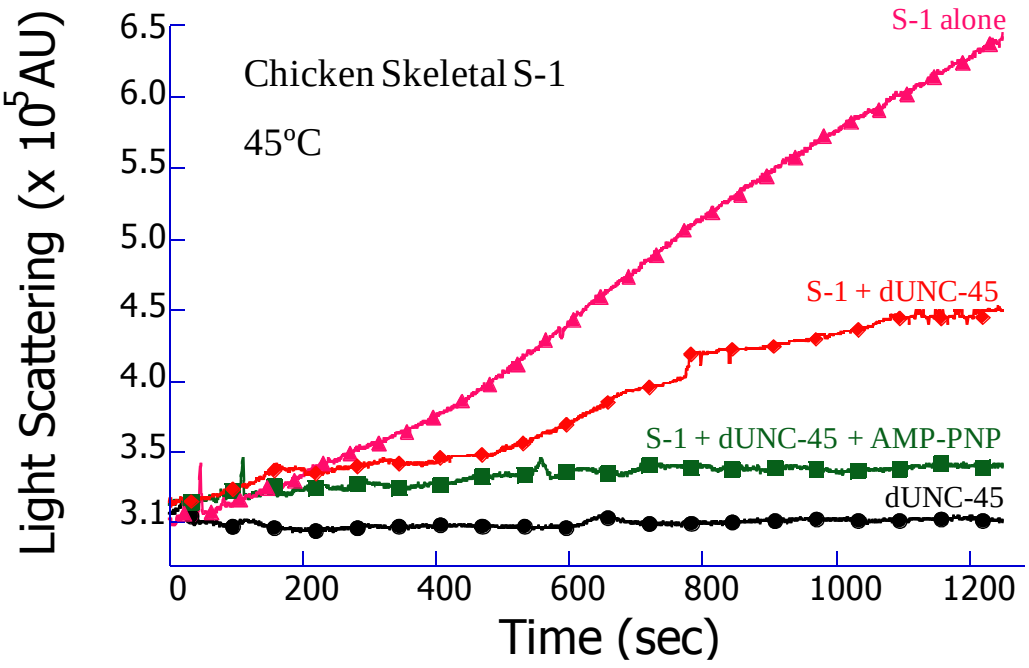

Figure 11. dUNC–45 protects chicken skeletal muscle motor domain (S1) from heat induced protein aggregation. Light scattering is used to reflect protein aggregation. S1 alone forms protein aggregates when incubated at 43°C (pink triangles). In the presence of dUNC–45, S1 aggregation is decreased (red diamonds). ATP enhances dUNC–45 conferred heat protection (green squares). dUNC–45 is stable by itself during the experiment (black circles).

to yield a total aggregation suppression of approximately 94%. dUNC–45 by itself or in the presence of ATP or AMP-PNP does not aggregate at elevated temperatures (Figures 10,11).

In addition to suppressing protein aggregation, dUNC–45 can refold CS that was denatured by urea (Figure 12), which is also enhanced by nucleotide. The results of refolding chemically denatured CS are similar to the chaperone activity displayed by GroEL and αB-crystallin [Muchowski and Clark, 1998]. Table 1 summarizes the *in vitro* chaperone function of dUNC–45 using various substrates, in the presence and absence of ATP or its analogue, AMP-PNP.

Even though nucleotide binding enhances dUNC–45 chaperone function, unlike Hsp90, dUNC–45 does not hydrolyze ATP in the conditions that we have tested (data not shown). If dUNC–45 does not hydrolyze ATP, then it probably elicits a conformational change in the dUNC–45 protein upon binding. To test this hypothesis, intrinsic tryptophan fluorescence [Vivian and Callis, 2001] was used to indicate protein conformational change. dUNC–45 contains five tryptophan residues and we employed its intrinsic fluorescence to help us measure dUNC–45 conformational change upon ATP binding. Figure 13 shows ATP dependent quenching of dUNC–45 tryptophan fluorescence over time, which indicates that ATP is binding to dUNC–45. ATP binding was further confirmed by using a fluorescent analogue of ATP (TNP-ATP, data not shown). We also tested the possibility that ATP binding might induce oligomerization of dUNC–45 by using native protein gel analysis. ATP bound

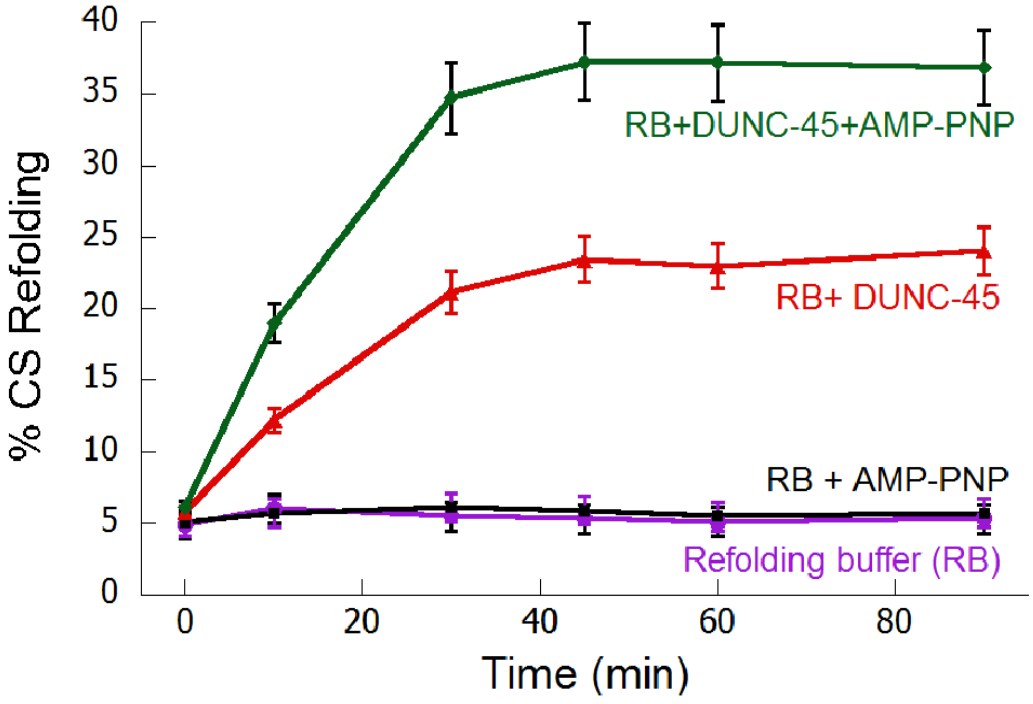

Figure 12. dUNC–45 refolds chemically denatured citrate synthase (CS). Urea denatured CS does not refold in the refolding buffer or in the presence of AMP-PNP (purple and black curve respectively). dUNC–45 facilitated the refolding of CS (red curve), which is enhanced in the presence of AMP-PNP (green curve).

Table 1. Chaperone function of recombinant dUNC–45 with various substrates in the presence or absence of ATP or its non-hydrolyzable analogue AMP-PNP.

	Refolding of CS (%)	**Suppression of CS Aggregation (%)**	**Suppression of α-lactalbumin Aggregation (%)**	**Suppression of Myosin Aggregation (%)**	**Suppression of Myosin S–1 Aggregation (%)**
dUNC–45 alone	22 ± 4.5	25 ± 10	49	39	56
dUNC–45 with ATP or AMP-PNP	31 ± 5.4	60 ± 8.5	79	70	94
ATP or AMP-PNP alone	6 ± 1.2	0	0	0	0

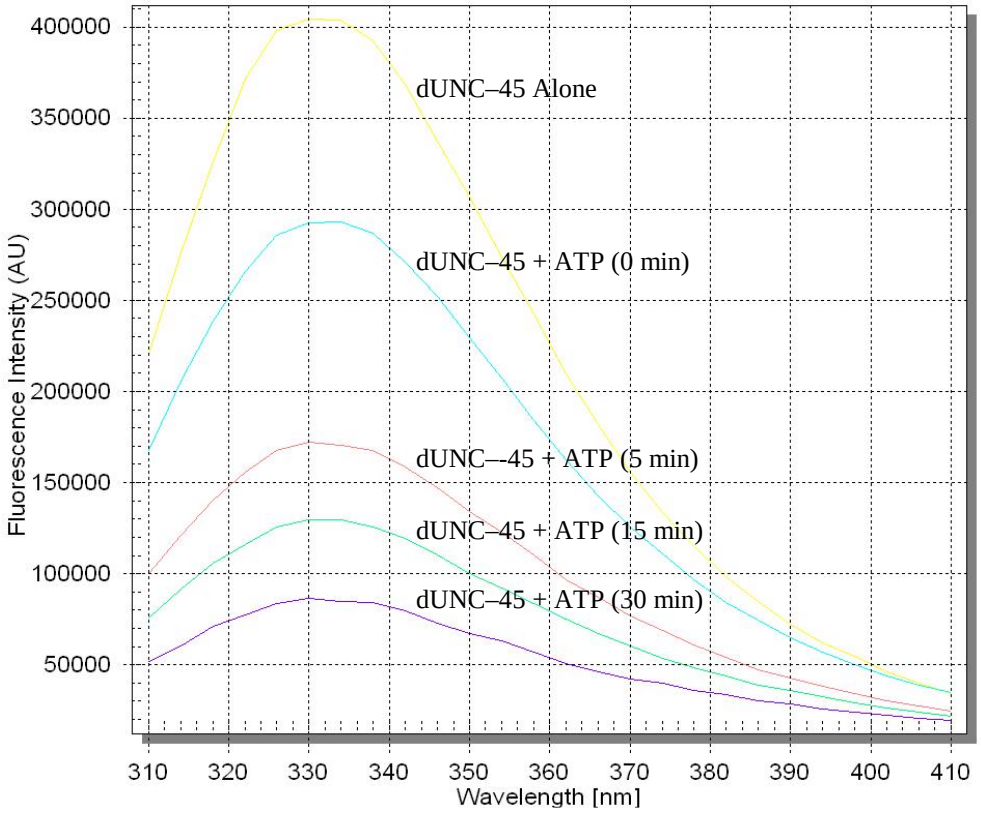

Figure 13. ATP binds dUNC–45. Intrinsic tryptophan fluorescence of dUNC–45 is quenched in the presence of ATP in a time dependent manner which suggests a direct interaction between dUNC–45 and ATP. This interaction is rapid and continuous over the course of the experiment.

dUNC–45 actually ran faster than dUNC–45 alone on the native gel. This suggests a more compact conformation of dUNC–45 upon ATP binding, therefore eliminating the possibility of oligomerization (not shown).

The results of the *in vitro* chaperone assays support the conclusion that dUNC–45 exhibits intrinsic chaperone function, yet the details of the physical interaction between dUNC–45 and myosin are unknown. Does UNC–45 bind only the motor domain near the actin biding region [Toi *et al.*, 2003] as previously thought, or are there multiple binding sites? To visualize the physical interaction between dUNC–45 and myosin and to get insight on how dUNC–45 prevents heat induced myosin aggregations, electron microscopy of rotary shadowed full-length myosin, in the absence and in the presence of dUNC–45 and at different temperatures, was performed by Dr. Anthony Cammarato (Figure 14), a structural biologist in the laboratory. At 25°C, myosin appeared as a double headed molecule jointed by the coiled-coil tail; dUNC–45 appeared globular with approximately the same size as the myosin head. When heated at 43°C for 30 minutes with AMP-PNP, the two heads of the myosin molecule fused to form one lollipop-like structure. Furthermore, the lollipop-like structures can also fuse with each other to form a spider-like structure with the coiled-coil tails radiating outward resembling the appendages. Only 2% of myosin appeared normal when heated alone. In the presence of dUNC–45 and AMP-PNP, however, 69% of the myosin molecules appeared as double-headed structure when heated at 43°C for 30 minutes. The protection benefit of dUNC–45 on

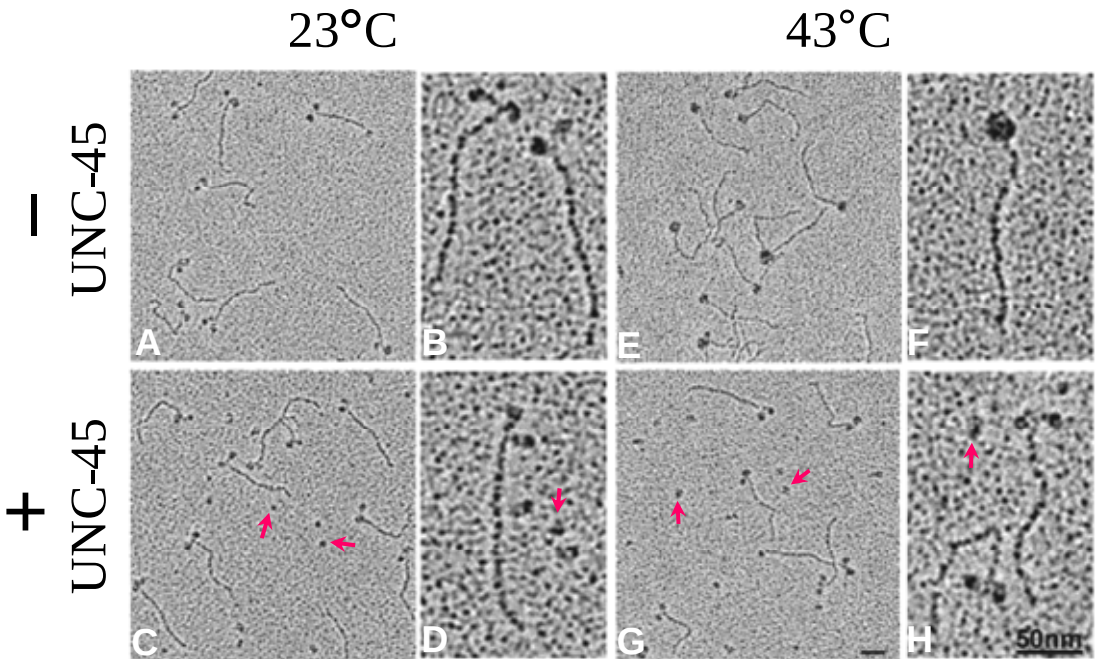

Figure 14. dUNC–45 helps maintain myosin structural integrity at elevated temperature. Electron micrographs showing rotary shadowed myosin exhibiting normal two-headed structure at 23°C (A, B, C, D). At elevated temperature for 30 minutes with 3.5 mM AMP-PNP, the myosin heads fuse to form a lollipop-like structure (E, F) with only 2% of the molecules appearing normal. In the presence of dUNC–45 and AMP-PNP, myosin is protected from heat induced aggregation of the two heads (G, H) with 69% of the myosin molecules appearing normal. The presence of dUNC–45 (arrows) does not perturb myosin structure (C, D) and its shape remains globular even at elevated temperature (G, H)

heated myosin is apparent in the electron micrographs, yet we were unable to visualize the direct interaction between myosin and dUNC–45 using this approach. The difficulty could be due to the rapid chaperone reaction rate of dUNC–45 for denatured myosin and the harsh EM conditions employed here.

As shown in chapter one, dUNC–45 is localized to the Z discs of sarcomeres. However, in order for dUNC–45 to protect myosin from stress induced denaturation, as it does in the *in vitro* assays described above, it needs to translocate to the A bands, where myosin is localized. To test whether such translocation takes place during stress, third instar wild-type (*yw*) larvae were heat shocked at 37°C for two hours and dUNC–45 localization was examined using immunofluorescence confocal microscopy. Figure 15 shows dUNC–45 localization in normal and heat shocked body-wall muscles relative to α-actinin (Z discs) and actin (I bands). Similar to what was seen in chapter one, dUNC–45 is localized to the Z disc when larvae were grown at 25°C. After heat shock, dUNC–45 localization became more diffused and extra bandings appeared that correlates with the A bands. In addition to moving from the Z disc to the A band, heat shock treatment also up-regulates dUNC–45 protein level as shown in Figure 16, at least in adults. Cold shock, CO_2 treatment, starvation, and hydrogen peroxide treatment all increased dUNC–45 levels, though to different extents.

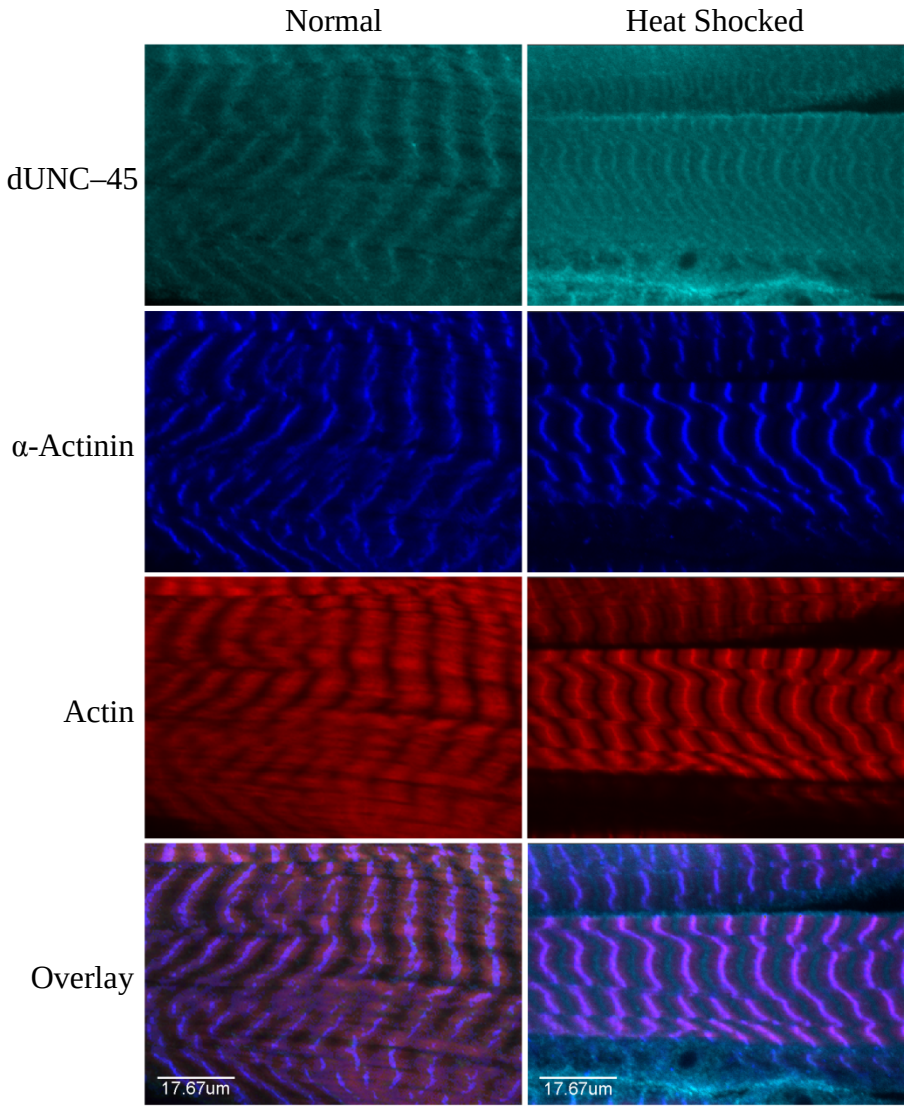

Figure 15. dUNC–45 translocates to the A band upon heat shock. Fluorescence confocal microscopy showing dUNC–45 localizes to the Z-disc in the body wall muscle of third instar *yw* larvae under normal growing conditions. dUNC–45 co-localizes with α-actinin (a Z disc protein) and bisects the actin staining (I band). After heat shock treatment, the localization of α-actinin and actin are not affected. The appearance of an extra banding pattern in the dUNC–45 staining panel (upper right) demonstrates that dUNC–45 translocates to a new location in the sarcomere upon heat shock. Comparison with α-actinin and actin localization after heat shock treatment (overlay lower right) suggest dUNC–45 localization in the A band in order to protect myosin from heat stress.

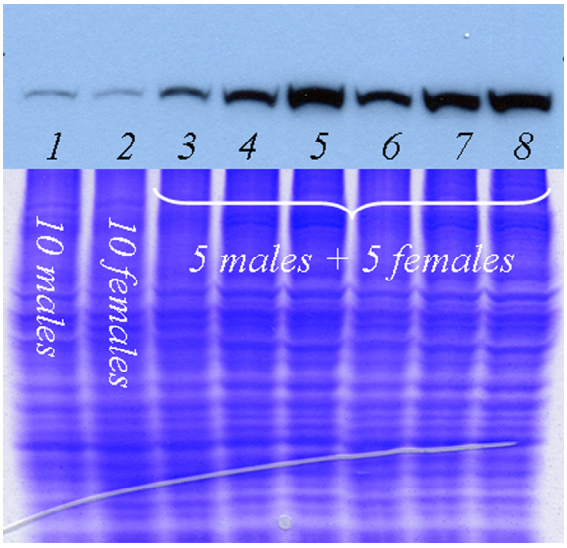

Lane	Treatment
1-3	Control at 25ºC
4	Starved
5	Heat shocked
6	Cold shocked
7	Carbon dioxide treated
8	Hydrogen peroxide treated

Figure 16. dUNC–45 is up regulated during stress. Western blot analysis showing dUNC–45 level is increased in response to various stress treatments (upper panel). Coomassie blue stained SDS polyacrylamide gel (lower panel) is used to show relative protein loaded in each land.

Discussion

In this study, we examined dUNC–45's ability to function as a chaperone using *in vitro* assays. dUNC–45 is able to protect citrate synthase (Figure 10), α-lactalbumin, and myosin (Figure 11) from heat induced aggregation. Furthermore, dUNC–45 also aids in refolding chemically-denatured CS (Figure 12). The fact that dUNC–45 can refold urea-denatured CS lends credibility to its chaperoning capability because chemically-denatured proteins are thought to be composed of random coils [McCarney *et al.*, 2005] and are, therefore, impossible to refold without the aid of a chaperone.

dUNC–45 chaperone function is enhanced by ATP (Figures 10, 11, 12, and Table 1), similar to other well known chaperones. Both Hsp90 and Hsp70 functions are dramatically enhanced by ATP. Upon ATP binding at its N-terminal domain, the Hsp90 dimer forms a closed circle encasing the substrate in the central cavity [Maruya *et al.*, 1999; Pearl and Prodromou, 2006], while ATP hydrolysis causes a conformational change and tight substrate binding in Hsp70 [Zhu *et al.*, 1996; Mayer and Bukau, 2005]. Unlike Hsp90 and Hsp70, dUNC–45 does not hydrolyze ATP, at least in the conditions that we have tested. ATP binding to dUNC–45 is therefore likely to elicit a conformational change as confirmed by the intrinsic fluorescence data of dUNC–45 in the presence of ATP (Figure 13). Chaperone binding of ATP without hydrolysis seems to be a futile act, yet is it not without precedent. αB-crystallin, belonging to the small heat shock protein family, also shows enhanced chaperone function upon ATP binding, yet ATP hydrolysis cannot be confirmed [Muchowski and Clark, 1998; Horwitz, 2003]. Table 1 summarizes the *in vitro* chaperone function of

dUNC–45 using various substrates, in the presence and absence of ATP or its analogue, AMP-PNP.

To visualize the physical interaction between dUNC–45 and myosin, and to illustrate evidence that dUNC–45 exhibits intrinsic chaperone function, electron microscopy of rotary shadowed full-length myosin, in the absence and in the presence of dUNC–45 and at different temperatures, was carried out. Visual examination of the electron micrographs revealed that 69% of myosin retained the normal, double-head structure when incubated with dUNC–45 at 43°C, which is drastically higher than the 2% seem when myosin was incubated at 43°C alone. The electron micrographs also suggest that dUNC–45 interacts only with the motor domain of myosin because the tail regions of myosin do not seem to be involved in aggregation formation.

To investigate the *in vivo* mechanism of dUNC–45 function, fluorescence confocal microscopy was performed. Translocation of dUNC–45 upon heat shock stress from the Z disc to the A band was evident in the micrographs (Figure 15) by comparing dUNC–45 localization with actin (I band) and α–actinin (Z disc). The dUNC–45 staining in the A band upon stress is not in a bi-partite pattern as expected of myosin heads, which could be due to the masking by the diffused dUNC–45 in the cytosol. It may also suggest that dUNC–45 binds in the M line of the sarcomere with either the rod of the myosin or other M line proteins. Western blot analysis of adult flies after heat shock or other stress treatments (Figure 16) also showed increased dUNC–45 levels, therefore, dUNC–45 functions *in vivo* during stress by translocating from the Z disc to the A band and by up-regulating its protein level. There are five

heat shock factor 1 (hsf1) binding sites in the dUNC–45 promoter [Birch-Machin *et al.*, 2005], which should be responsible for the increase in protein concentration seen here. It is important to note, however, that the Western blot analysis performed here did not control for efficiency in tissue homogenization nor for protein amount loading. As dUNC–45 appears to become more cytosolic during stress, it is possible the increased signal seen on the Western blot is due to greater solubility of the protein.

The translocation of dUNC–45 upon stress has also been documented in zebrafish [Etard *et al.*, 2008]. The authors tracked localization of a zebrafish UNC–45b-GFP construct through myofibrillogenesis and showed that UNC–45 first associates with myosin in the cytosol along with Hsp90. This association remained stable while thick filaments are incorporated into the sarcomere. Disruption of either UNC–45b or Hsp90 prevented myofibrillogenesis and muscle development. After sarcomere assembly is complete, UNC–45 and Hsp90 both move to the Z disc until needed, for example, during stress. Translocation of UNC–45 during stress is accompanied by an increase in protein level (Figure 16).

Whether UNC–45 is a chaperone or a co-chaperone *in vivo* is an issue that is yet to be resolved. Even thought UNC–45 exhibited intrinsic chaperone function *in vitro*, it probably functions as a co-chaperone during myosin production as supported by most *in vivo* data. Thus far, eukaryotic chaperonin TRiC/CCT (TCP1-ring complex/chaperonin containing TCP1) [Srikakulam and Winkelmann, 1999], Hsp70, Hsp90 [Srikakulam and Winkelmann, 2004], and UNC–45 have been identified to be important for myosin maturation. The inclusion of UNC–45 in this mix, either general

cell or striated muscle specific isoforms, was not able to completely compliment myosin folding *in vitro*, therefore, the list of players aiding myosin folding is likely to grow longer. However, if UNC–45 only functions as a co-chaperone, why does it display intrinsic chaperone activity? Is it possible that after myosin is folded and incorporated into the thick filament, UNC–45 alone is sufficient to refold/protect stressed myosin? If that is true, then it explains the observations that dUNC–45 is able to preserve myosin structural integrity during our *in vitro* myosin protection assays, and that Hsp90 function is indispensible for myofibrillogenesis *in vivo*.

References

Barral, J. M., Hutagalung, A. H., Brinker, A., Hartl, F. U. and Epstein, H. F. (2002). Role of the myosin assembly protein UNC-45 as a molecular chaperone for myosin. Science *295*, 669-671.

Birch-Machin, I., Gao, S., Huen, D., McGirr, R., White, R. A. and Russell, S. (2005). Genomic analysis of heat-shock factor targets in *Drosophila*. Genome Biol *6*, R63.

Bose, S., Weikl, T., Bugl, H. and Buchner, J. (1996). Chaperone function of Hsp90-associated proteins. Science *274*, 1715-1717.

Buchner, J., Schmidt, M., Fuchs, M., Jaenicke, R., Rudolph, R., Schmid, F. X. and Kiefhaber, T. (1991). GroE facilitates refolding of citrate synthase by suppressing aggregation. Biochemistry *30*, 1586-1591.

Craig, R., Smith, R. and Kendrick-Jones, J. (1983). Light-chain phosphorylation controls the conformation of vertebrate non-muscle and smooth muscle myosin molecules. Nature *302*, 436-439.

Elsevier. Copyright. http://www.elsevier.com/wps/find/ authorsview.authors/authorsrights May 06, 2010.

Etard, C., Behra, M., Fischer, N., Hutcheson, D., Geisler, R. and Strahle, U. (2007). The UCS factor Steif/Unc–45b interacts with the heat shock protein Hsp90a during myofibrillogenesis. Dev Biol *308*, 133-143.

Etard, C., Roostalu, U. and Strahle, U. (2008). Shuttling of the chaperones Unc45b and Hsp90a between the A band and the Z line of the myofibril. J Cell Biol *180*, 1163-1175.

Horwitz, J. (2003). Alpha-crystallin. Exp Eye Res *76*, 145-153.

Liu, L., Srikakulam, R. and Winkelmann, D. A. (2008). Unc45 activates Hsp90-dependent folding of the myosin motor domain. J Biol Chem *283*, 13185-13193.

Margossian, S. S. and Lowey, S. (1982). Preparation of myosin and its subfragments from rabbit skeletal muscle. Methods Enzymol *85 Pt B*, 55-71.

Maruya, M., Sameshima, M., Nemoto, T. and Yahara, I. (1999). Monomer arrangement in HSP90 dimer as determined by decoration with N and C-terminal region specific antibodies. J Mol Biol *285*, 903-907.

Mayer, M. P. and Bukau, B. (2005). Hsp70 chaperones: cellular functions and molecular mechanism. Cell Mol Life Sci *62*, 670-684.

McCarney, E. R., Kohn, J. E. and Plaxco, K. W. (2005). Is there or isn't there? The case for (and against) residual structure in chemically denatured proteins. Crit Rev Biochem Mol Biol *40*, 181-189.

Melkani, G. C., Cammarato, A. and Bernstein, S. I. (2006). alphaB-crystallin maintains skeletal muscle myosin enzymatic activity and prevents its aggregation under heat-shock stress. J Mol Biol *358*, 635-645.

Miller, B. M., Nyitrai, M., Bernstein, S. I. and Geeves, M. A. (2003). Kinetic analysis of *Drosophila* muscle myosin isoforms suggests a novel mode of mechanochemical coupling. J Biol Chem *278*, 50293-50300.

Muchowski, P. J. and Clark, J. I. (1998). ATP-enhanced molecular chaperone functions of the small heat shock protein human alphaB crystallin. Proc Natl Acad Sci U S A *95*, 1004-1009.

Pearl, L. H. and Prodromou, C. (2006). Structure and mechanism of the Hsp90 molecular chaperone machinery. Annu Rev Biochem *75*, 271-294.

Picard, D. (2002). Heat-shock protein 90, a chaperone for folding and regulation. Cell Mol Life Sci *59*, 1640-1648.

Reddy, G. B., Narayanan, S., Reddy, P. Y. and Surolia, I. (2002). Suppression of DTT-induced aggregation of abrin by alphaA- and alphaB-crystallins: a model aggregation assay for alpha-crystallin chaperone activity in vitro. FEBS Lett *522*, 59-64.

Srikakulam, R., Liu, L. and Winkelmann, D. A. (2008). Unc45b forms a cytosolic complex with Hsp90 and targets the unfolded myosin motor domain. PLoS One *3*, e2137.

Srikakulam, R. and Winkelmann, D. A. (1999). Myosin II folding is mediated by a molecular chaperonin. J Biol Chem *274*, 27265-27273.

Srikakulam, R. and Winkelmann, D. A. (2004). Chaperone-mediated folding and assembly of myosin in striated muscle. J Cell Sci *117*, 641-652.

Toi, H., Fujimura-Kamada, K., Irie, K., Takai, Y., Todo, S. and Tanaka, K. (2003). She4p/Dim1p interacts with the motor domain of unconventional myosins in the budding yeast, Saccharomyces cerevisiae. Mol Biol Cell *14*, 2237-2249.

Vivian, J. T. and Callis, P. R. (2001). Mechanisms of tryptophan fluorescence shifts in proteins. Biophys J *80*, 2093-2109.

Zhu, X., Zhao, X., Burkholder, W. F., Gragerov, A., Ogata, C. M., Gottesman, M. E. and Hendrickson, W. A. (1996). Structural analysis of substrate binding by the molecular chaperone DnaK. Science *272*, 1606-1614.

Acknowledgements

Portions of this chapter have been published in BBRC. [Melkani, G. C., Lee, C. F., Cammarato, A. and Bernstein, S. I. (2010). *Drosophila* UNC-45 prevents heat-induced aggregation of skeletal muscle myosin and facilitates refolding of citrate synthase. *Biochem Biophys Res Commun* 396, 317-322.] As an author on the journal article, rights were retained to "prepare other derivative works, to extend the journal article into book-length form, or to otherwise re-use portions or excerpts in other works, with full acknowledgement of its original publication in the journal. [Elsevier]." Data used in this chapter taken from the journal article include all *in vitro* chaperone assays performed in the absence of ATP.

The experiments performed by Chi Lee include: 1) Expressed and purified dUNC–45 from *E. coli.* 2) Confocal immunofluorescence microscopy. 3) Western blotting. Dr. Girish Melkani performed all the *in vitro* chaperone activity and binding assays. Dr. Anthony Cammarato performed the electron microscopy.

Chapter 3: Structure determination of *Drosophila* UNC–45

Introduction

Myosin is a superfamily of motor proteins whose function is required for muscle contraction, cell division, cell motility, intracellular transport, and signal transduction [Coluccio, 2008]. Classical genetic studies in the model organism *C. elegans* revealed a plethora of mutations that restrict worm movement [Brenner, 1974]. One such investigation identified a temperature sensitive mutant allele of a gene called *unc–45* that resulted in disruption of myofilament organization and an uncoordinated movement in worms at the restrictive temperature. This phenotype was reversible if the shift to a permissive temperature occurred during the embryonic or larval stages of development [Epstein and Thomson, 1974]. Analysis of adult worms of a mutant strain grown at the restrictive temperature revealed a 50% decrease in thick filaments and scrambling of myosin isoforms A and B [Barral *et al.*, 1998].

The *unc–45* gene was molecularly cloned [Ao and Pilgrim, 2000; Barral *et al.*, 2002] and shown to encode a protein of three domains. Homologs of the UNC–45 protein have since been identified in diverse eukaryotic species. Two genes encoding distinct UNC–45 isoforms are present within the genomes of fish and mammals [Price *et al.*, 2002; Wohlgemuth *et al.*, 2007]. UNC–45A, also known as the general cell isoform, is expressed in all tissues while the striated muscle isoform UNC–45B is expressed exclusively in tissues that contain striated muscle.

UNC–45 is part of a larger family of myosin-interacting proteins that include the Cro1p protein from *P. anserina*, She4p from the budding yeast *S. cerevisiae*, and the fission yeast *S. pombe* protein Rng3p [Jansen *et al.*, 1996; Wendland *et al.*, 1996; Berteaux-Lecellier *et al.*, 1998; Wong *et al.*, 2000]. Each of these shares sequence homology throughout a carboxy-terminal region of roughly 500 amino acids referred to as the UCS (UNC–45, Cro1p, She4p) domain [Hutagalung *et al.*, 2002]. All UCS proteins studied thus far influence myosin function, although with different consequences [Yu and Bernstein, 2003].

Structurally, UNC–45 is unique among UCS domain-containing proteins as it contains an amino-terminal tetratricopeptide repeat (TPR) domain [Barral *et al.*, 1998]. TPR repeats are a helical tandem repeat motif common to many proteins that participate in protein-protein interactions [Groves and Barford, 1999], especially with the acidic carboxy-terminus of the heat shock protein Hsp90. Bridging the TPR and UCS domains is a region of approximately 400 amino acids in length that does not display significant homology to any proteins of known structure. This region is referred to as the Central domain.

As part of an effort to improve understanding of the molecular mechanisms by which UCS domain-containing proteins interact with and influence the function of myosin motor proteins, we have begun structural and *in vitro* biochemical studies on purified recombinant UNC–45 from the fruit fly *Drosophila melanogaster* (dUNC–45) [Melkani *et al.*, 2010]. Here we report the x-ray crystal structure of dUNC–45 determined to a resolution of 3.0 Å. The crystallographic model reveals that both the

Central and UCS domains consist of a continuous stack of armadillo repeats. Analysis of sequence homology between functionally diverse UCS domain-containing proteins suggests that they share a conserved surface which may interact with myosin. A loop within armadillo repeat 14 is conserved between both general cell and skeletal muscle isoforms of UNC–45 from diverse species. Removal of this loop, which is sensitive to proteolysis in solution, appears to weaken the interaction of dUNC–45 with purified *Drosophila* indirect flight muscle (IFM) myosin (preliminary data not shown) suggesting that this mobile region might form part of an allosteric myosin-binding regulatory mechanism.

Materials & Methods

Plasmids. Preparation of the dUNC–45 expression plasmid has been reported previously [Melkani *et al.*, 2010]. Mutation of Leu63 to Met (L63M) was carried out by PCR-based mutagenesis of the native sequence template with the primer 5'-CGTGCTGCCGCTTATCTGAAGATGGGAAAGTATGAAAATGCGG-3' (mutations underlined) and its complement according to the QuickChange protocol (Stratagene). Similarly, the dUNC–45TPR expression plasmid was created by introducing a TAA stop codon by mutagenesis at amino acid position 122 with the primer 5'-GGCAACAAAACCGTACAGTAAATGCTCCAGAGGCTTCATG-3' and its complement. Construction of the dUNC–45ΔL plasmid, in which amino acids 587-613 are replaced by the pentapeptide linker Gly-Ser-Gly-Ser-Gly, relied on the primer 5'-GGTCACTACTTTTGTGAATCTGGGATCCGGTAGCGGTGAG CTGGACGACGT AGATTTC-3' (loop replacement underlined) and its complement.

The dUNC–45ΔTPR construct was prepared by subcloning amino acids 138-947 of native dUNC–45 into the NdeI and XhoI sites of pET–16b with the primers 5'-ACCGCTTTGCATATGAATGCCAAGACATCC-3' and 5'-ACGTTCTCGAGTTAATCATCGATAATCTCA-3' (restriction sites underlined). The original template and all mutations were confirmed by sequencing.

Protein expression, purification, and crystallization. Expression of dUNC–45 in *E. coli* has been described elsewhere [Melkani *et al.*, 2010]. Se-Met substituted proteins were expressed in a defined medium supplemented with Se-Met. All dUNC–45 proteins used in this study contain amino-terminal decahistidine tags. Affinity and size exclusion chromatography purification of dUNC–45 has been described previously [Melkani *et al.*, 2010]. Peak fractions from size exclusion were pooled and concentrated by centrifugation to a final concentration of roughly 20 mg/ml. The purified protein was divided into 50 µl aliquots, flash frozen in liquid nitrogen, and stored at -80 C. Indirect flight muscle myosin from *Drosophila melanogaster* was prepared from dissected whole flies as described previously [Swank *et al.*, 2001].

Crystals of dUNC–45 were grown by the hanging drop vapor diffusion technique. Protein aliquots were thawed, centrifuged at 13,500 rpm for 10 minutes and stored on ice. 2 µl of protein were mixed with 1 µl of mother liquor solution (0.1 M Na citrate pH 5.6, 0.2 M ammonium acetate, and 25% (w/v) polyethylene glycol 4000, 1% (v/v) ethylene glycol) on a siliconized glass cover slip and then sealed by

vacuum grease over 1 ml mother liquor. Single crystals of up to 0.4 x 0.4 x 0.4 mm grew at 18°C after 2~4 days.

Data collection and processing. Native and Se-Met crystal that were approximately 0.15 mm on each edge were transferred by nylon loop directly in to a mother liquor solution augmented with 18% glycerol for 1 minute before flash cooling and storage in liquid nitrogen. The 0.125 mm L63M Se-Met crystal was transferred stepwise into stabilizer solutions containing 15% or 30% dextrose and 200 µM MEEVD peptide for ten minutes each prior to flash cooling in liquid nitrogen. Synchrotron data were collected at 100 K on an ADSC 345 CCD detector and processed in HKL2000 [Otwinowski and Minor, 1997]. Data collection statistics are summarized in Table 2.

Structure solution, model building, and refinement. The processed Se-Met dUNC–45 data set was run under the single anomalous dispersion (SAD) routine within the AutoSol module of Phenix [Adams *et al.*, 2010]. Only one molecule was determined to occupy the asymmetric unit. The Phenix AutoBuild module was next run using all of the reflection intensities collected in the native 3.0 Å data set. The resulting initial model contained 524 amino acids with an R-factor of 0.446 and R-free of 0.469. Although the initial model was almost entirely extended polypeptides, maps calculated from this model indicated an extremely high degree of alpha-helical electron density. Consequently, manual model building commenced by maximizing alpha-helical polypeptide structure and proceeded by building and fitting connecting loops into 2Fo-Fc electron density maps in Coot [Emsley *et al.*, 2010]. The positions

Table 2. Data collection and refinement statistics

	Native	Se-Met	L63M
Data collection			
X-ray source	ALS 8.2.2	ALS 8.2.1	ALS 8.2.2
Wavelength (Å)	1.00000	0.97950	0.97940
Space group	P23	P23	P23
Unit cell (Å)			
a,b,c	184.079	184.577	188.016
Monomers/asymmetric unit	1	1	1
Resolution range[a]	50.00-3.00 (3.11-3.00)	50.00-3.30 (3.42-3.30)	50.00-3.20 (3.31-3.20)
R_{sym} (%)	11.5 (81.9)	13.7 (53.6)	11.8 (78.5)
Observations	400,191	291,598	406,585
Unique reflections	42,099	31,539	36,692
Completeness (%)	99.8 (97.8)	99.7 (99.1)	100 (100)
Redundancy	9.5 (6.5)	9.2 (7.3)	11.1 (10.1)
Average intensity ($<I/\sigma>$)	19.2 (2.0)	15.2 (3.1)	15.7 (2.1)
Structure solution by SAD			
Figure of merit[b]			
Centric		0.422	0.432
Acentric		0.128	0.138
Overall		0.374	0.387
Refinement			
Resolution range (Å)	50.0-3.0		50.0-3.2
Reflections used	39,354		30,656
Protein atoms	6,077		6,087
R_{cryst} (%)/R_{free} (%)[c]	20.1/23.6		26.0/30.9
Geometry			
R.m.s. bond lengths (Å)	0.013		0.019
R.m.s. bond angles (°)	1.293		2.316
Mean B (Å^2)	58.7		38.3
Ramachandran plot[d]			
Most Favorable (%)	93.8		
Allowed (%)	5.8		
Disallowed (%)	0.4		

[a] Data in parentheses are for the highest resolution shell
[b] Phenix Autosol [Davis *et al.*]
[c] Calculated against a cross-validation set of 5.0% of the data selected at random prior to refinement
[d] Molprobity [Landau *et al.*, 2005]

of the 19 Se sites determined in the original SAD solution were used as a guide throughout the course of model building and refinement. The final model contains dUNC–45 amino acids 138-923. The R-factor is 0.201, the R-free is 0.236, and 99.6% of the peptide bonds exhibit allowable combinations of Ramachandran angles as judged by Molprobity [Davis *et al.*, 2007]. The L64M structure was determined independently by SAD in Phenix, built using the native dUNC–45 structure as a guide, and refined in Phenix. Structure solution and refinement statistics are summarized in Table 2.

Structural analysis. The five most divergent five UCS-domain containing proteins were selected for amino acid conservation analysis using the web-based application ConSurf [Landau *et al.*, 2005]. Figures were made in PyMol [DeLano, 2002].

Proteolysis assay. Chymotrypsin (2 µg) was added to 100 µg native full length dUNC–45 and dUNC–45ΔL in 100 µl. Reactions were incubated at room temperature and 10 µl samples were taken at 5, 20, 60, 180 minutes, quenched with 1 µl 250 µM PMSF and 4 µl of 4X Laemmli buffer, heated to 96°C for 2 minutes, centrifuged, and stored at -20°C. The collected samples were separated by SDS PAGE and analyzed by Coomassie blue stain.

Results

Structure determination. The x-ray crystal structure of dUNC–45 was solved by single anomalous dispersion (SAD) using seleno-methionine-substituted protein crystals and refined against native data collected to a limit of 3.0 Å resolution

(Table 2). During the process of phasing, it was discovered that the relatively large unit cell (~184 Å on each edge) contained close to 80% solvent by volume. Despite the high degree of solvent, continuous electron density could be observed throughout the crystal in three dimensions (Figure 17).

Initial experimental electron density maps clearly revealed stacks of alpha helices. Upon model building, however, we were surprised to find that the helical density corresponded entirely to the Central and UCS domains, while electron density corresponding to the anticipated three amino-terminal helical TPR motifs remained unaccounted for throughout the course of refinement. We concluded that the TPR domain exhibits significant flexibility relative to the Central and UCS domains. This flexibility might result from disorder of the entire TPR domain or it could be afforded by the stretch of nearly twenty amino acids that link the end of the TPR consensus and the first amino acid that could be refined within electron density (Asn138).

Model building was initiated by building into the clearly helical portions in the experimental electron density map and followed by construction of connecting loops. Refinement statistics and the correct placement of 19 refined Se sites at methionine side chains in the refined model indicated that our crystallographic model was correct. However, it remained worrisome that the only portion of the dUNC–45 molecule suspected of containing a known structure, the presumably alpha-helical TPR domain, remained unaccounted for while the entire 786 amino acids present in the model exhibited a structure composed entirely of alpha-helical stacks. Therefore, in an effort both to confirm the disorder of the suspected TPR motif and correctness of the refined

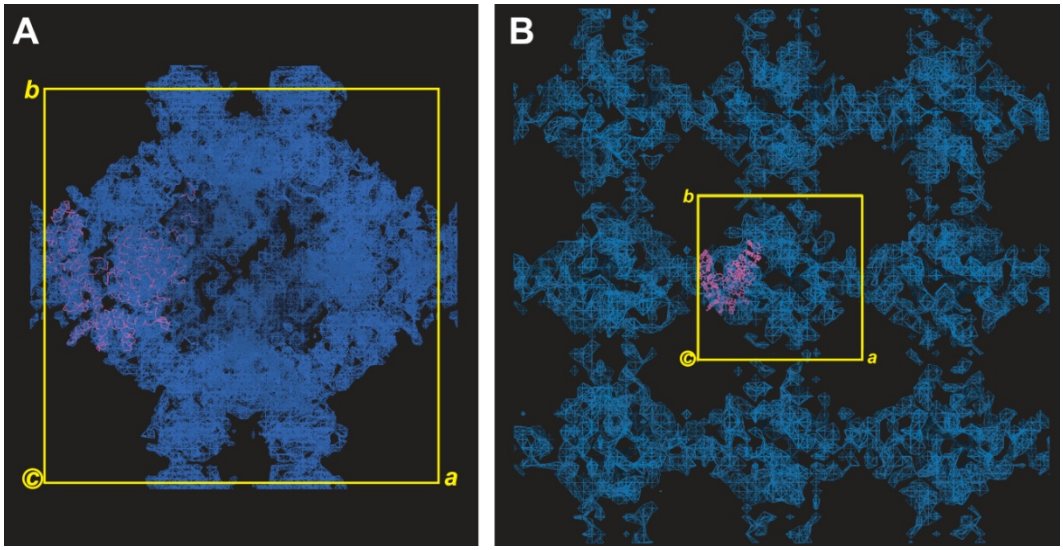

Figure 17. Packing in the dUNC–45 crystal. A) A 2Fo-Fc electron density map generated with phases estimated experimentally by SAD is contoured in blue at 1.5 σ. The C_α-trace of one dUNC–45 monomer is depicted in pink. The cubic unit cell is shown in yellow and axes are labeled. Clipping of the front one third of the unit cell electron density uncovers an extensive solvent-filled cavity. B) Panning back from the view in A) reveals a network of large channels between neighboring unit cells. As the unit cell symmetry is cubic, the image would be the same after 90° rotation about the a-, b-, or c-axis. Note that the radius of the solvent channel is observed at its smallest diameter and that it opens to a solvent-filled sphere of roughly 160 Å in diameter in all three dimensions. Also note that the electron density is continuous throughout the crystal in all three dimensions.

dUNC–45 crystallographic model, we prepared crystals of a seleno-methionine-substituted dUNC–45 protein in which amino acid Leu63 was replaced by a methionine residue. This amino acid position was chosen because it occupies a stable position in known TPR domain structures and is not involved in core packing of the TPR stacked alpha helices. Furthermore, several TPR domain-containing proteins contain methionine at an analogous position [Das *et al.*, 1998]. X-ray diffraction data were collected on the dUNC–45 Leu63Met mutant crystal and the structure was solved by SAD and refined to 3.20 Å resolution (Table 2). With the exception of some differences in the conformations of loops and a slight change in the angle between the Central and UCS domains (discussed later) the dUNC–45 Leu63Met mutant structure is practically identical to our original 3.0 Å model. Most notably, no additional Se site was detected nor was additional TPR domain electron density observed in the Leu63Met model. This experiment supports our conclusion that the amino-terminal TPR domain, which is projected toward the vast solvent channel by each of the dUNC–45 monomers in our crystal, exhibits disorder and/or flexibility relative to the Central and UCS domains. Studies are currently being carried out to determine whether the dUNC–45 TPR domain possesses an ordered structure in solution.

dUNC–45 crystal structure. The dUNC–45 x-ray crystal structure includes the Central and UCS domains (amino acids 138-923). The structure is composed entirely of stacked repeating alpha helical motifs reminiscent of armadillo (ARM) repeats. ARM repeats are alpha helical tandem repeat motifs that are approximately

40 amino acids in length. They were first described structurally in the β-catenin and importin-α proteins [Huber *et al.*, 1997; Conti *et al.*, 1998]. The fundamental repeating motif of an individual ARM repeat is a short helix followed by two longer helices (Figure 18). The two longer helices run nearly antiparallel to one another. Successive ARM repeats stack upon one another and exhibit a slightly left-handed superhelical twist such that the third helix from each layer stacks to generate a concave corkscrew face.

The stack of ARM repeats present in the entire dUNC–45 x-ray crystal structure is roughly 180 Å in length. It is, however, folded back upon itself so that the longest dimension in the structure is approximately 100 Å. This corresponds roughly to the UCS domain (Figure 19A). The Central domain is approximately the same length. However, due to bends in the structure, its longest dimension is roughly 60 Å. Overall, the dUNC–45 structure is roughly horseshoe shaped with one arm, containing the UCS domain, longer than the other.

The Central and UCS domains are practically continuous (Figure 19A). There is no break and the same ARM-like repeat structure that begins in the Central domain continues to the end of the UCS domain. Designation in the past based on sequence alignment have suggested between 524-539 as a border between the two domains. On the basis of the x-ray structure, we suggest that the UCS domain of dUNC–45 begins between ARM repeats 12 and 13 at around amino acid 511 (524 in *C. elegans*). In the other non-UNC–45 UCS domain-containing proteins, it remains to be seen whether the UCS domain functions as an independent domain.

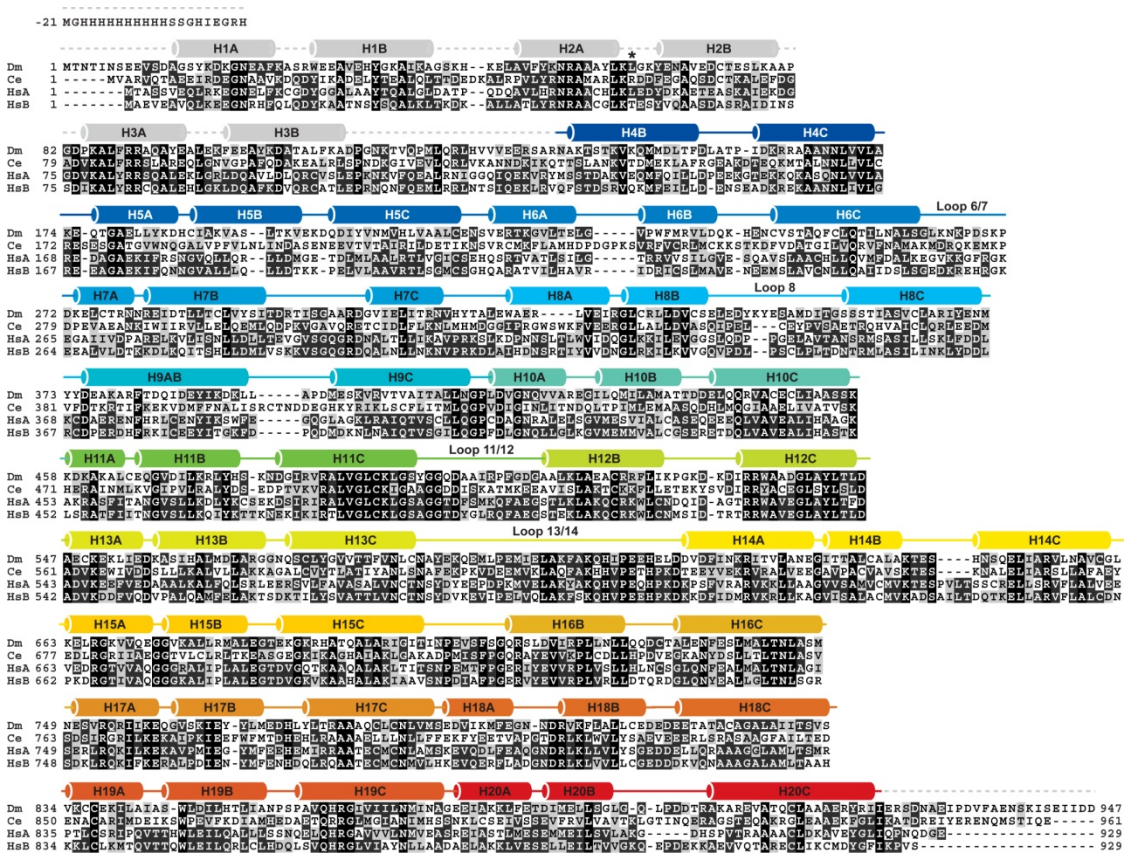

Figure 18. Primary amino acid sequence and secondary structure of dUNC–45. dUNC–45 (accession no. AAK93568) was aligned with the UNC–45 proteins from *C. elegans* (Ce; accession no. AAD01976) and both *H. sapiens* striated muscle (Hs-SM; accession no. AAI01064) and general cell (Hs-GC; accession no. AAH45635) isoforms. Black boxes highlight identical positions while dark grey boxes indicate conserved positions and light grey boxes signify substitution of a homologous amino acid. dUNC–45 secondary structure is indicated with helices represented as cylinders above their corresponding amino acids. Each stacked helical layer is assigned a number and individual helices within each stack are distinguished by a letter. Secondary structure of the amino-terminal TPR domain, which is present but disordered in the crystal, is depicted in light grey and assigned by homology to other TPR domain-containing proteins. Leu63, marked with an asterisk, was mutated to Met for SAD data collection and structure solution of the Leu63Met mutant.

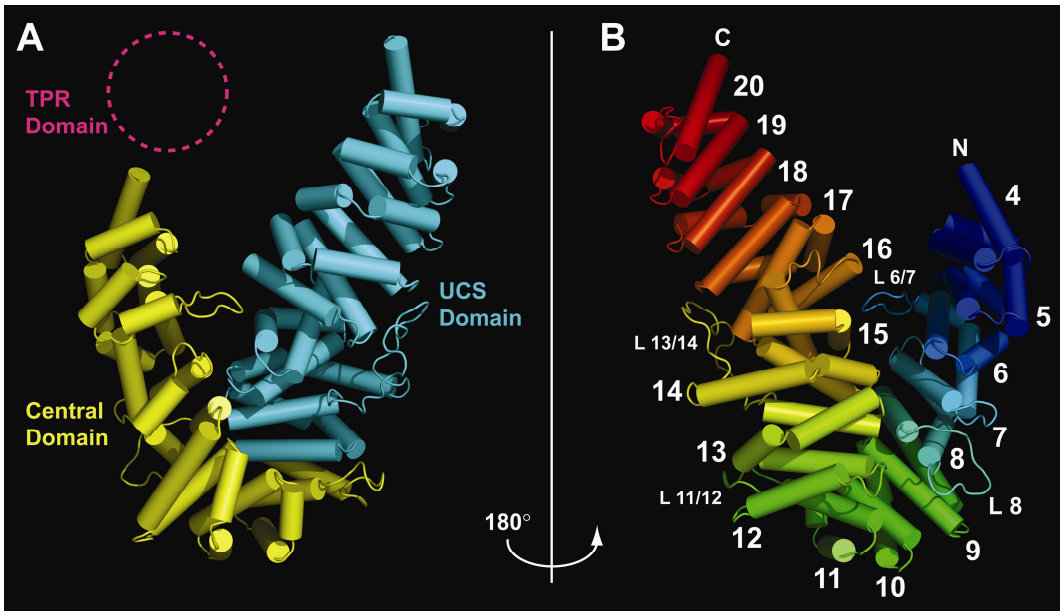

Figure 19. Ribbon diagram representation of the dUNC–45 x-ray crystal structure. A) The dUNC–45 x-ray crystal structure is depicted with cylindrical representation of helices. The domains are colored separately with the disordered TPR domain represented by a dashed circle in pink, the Central domain in yellow, and the UCS domain in cyan. B) Rotation of dUNC–45 about the y-axis. The protein is colored and numbered by helical layer consistent with Figure 18. The amino- and carboxy-termini of the protein are noted along with the position of Loop 14 in the UCS domains.

Surface features of dUNC–45. In an effort to gain insight into the surface characteristics of the dUNC–45 protein, examination of the electrostatic surface potential and surface polarity were implemented (Figure 20). Using the program APBS [Baker *et al.*, 2001], we performed a calculation of the electrostatic surface potential on a solvated dUNC–45 and plotted the results as a color gradient where blue represents positive potential (up to +30kT/e), red represents negative potential (to -30kT/e), and white represents a surface potential that is electrically neutral. The results of this analysis revealed that the surface of the dUNC–45 molecule is fairly randomly charged with two notable exceptions (Figure 20A, B). First, the face of UCS domain that corresponds to the ARM repeat A helices is extremely acidic. Second, the groove on the inner surface of the dUNC–45 UCS domain created by the stack of C helices displays markedly less electrostatic potential. Rather, this region appears as a mottled grey with faint red and blue hues.

The unique surface properties of the UCS domain groove are even more pronounced when surfaces are colored to represent the identity of the amino acids. We used a qualitative routine to color the dUNC–45 surface according to amino acid polarity (hydrophobic, semipolar, polar, positive, negative, aromatic). When colored thus, it is clear that the UCS domain groove presents a strong hydrophobic surface. The white surface stands out when compared against the rest of the molecular surface, which is more or less randomly colored (Figure 20C,D).

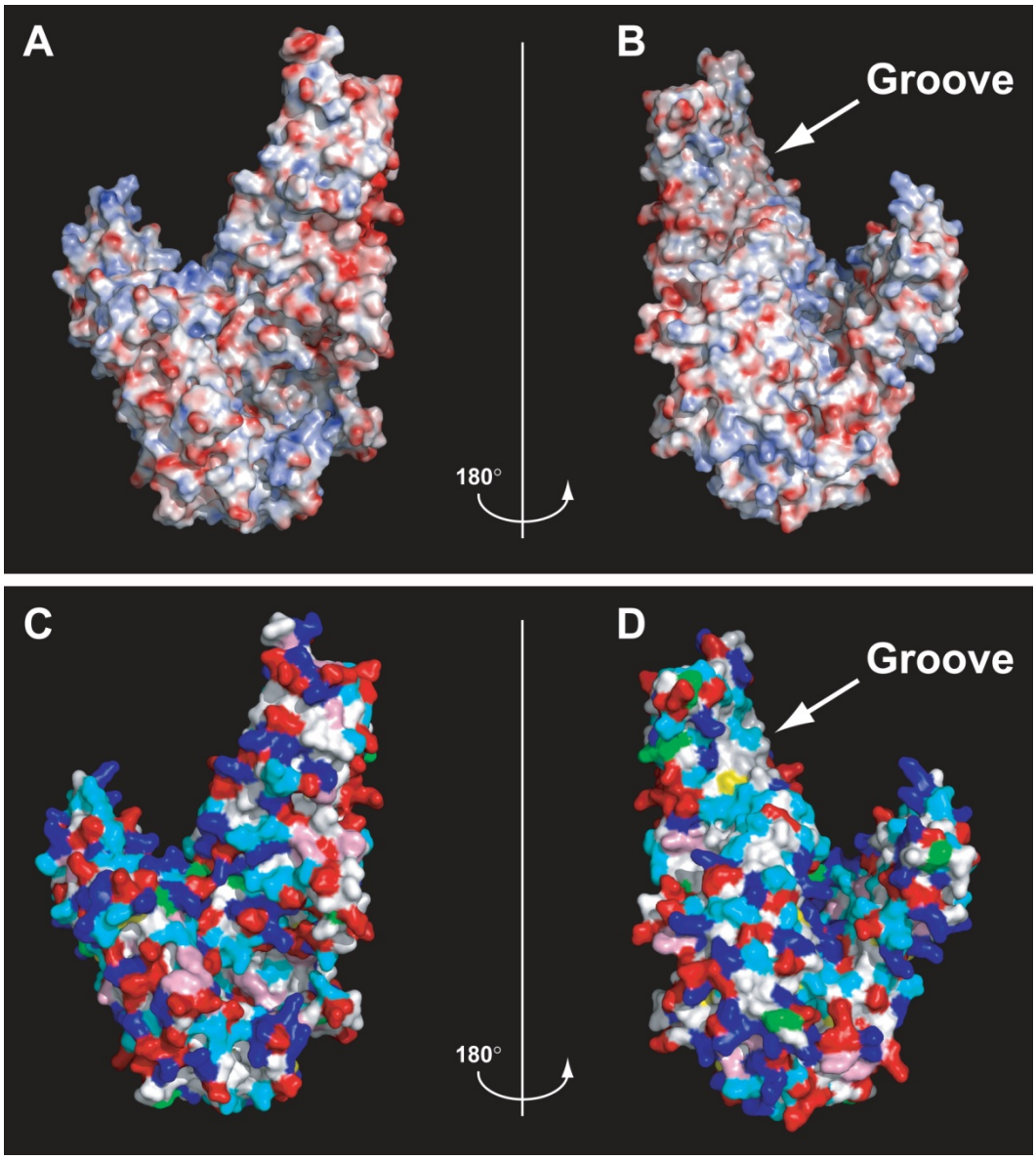

Figure 20. Surface representations of the dUNC–45 x-ray crystal structure. A) Electrostatic surface potential was calculated by the program APBS and displayed using PyMol. Negative potential is depicted in red while positive potential is represented in blue. B) The same model rotated 180° about the y-axis. C) Surface polarity is represented by the following color scheme: white-hydrophobic; yellow-semipolar (cysteine); polar-cyan; positive-blue; negative-red; aromatic-pink. Note that in both electrostatic surface and surface polarity models, the UCS domain "groove" is labeled and exhibits a distinctively less charged surface than the rest of the molecule. The two views of the dUNC–45 molecule are oriented identically as in Figure 19.

Armadillo repeats. As revealed by the dUNC–45 x-ray crystal structure, a total of 17 ARM repeat layers (numbered 4 through 20) can be clearly defined (Figure 19B). Each ARM repeat layer is numbered and each of the three helices in any repeat is designated as A, B, or C, respectively (Figure 18). Not every layer possesses a perfect ARM repeat, as several contain insertions or other modifications from the consensus. In particular, the first ARM repeat (numbered 4 so as to reserve layers 1, 2, and 3 for the suspected TPR repeat motifs) contains only the second (B) and third (C) helices. This is most likely a consequence of disorder at the amino-terminal end of the dUNC–45 protein in the crystal. ARM repeat 8 contains a loop between helices B and C that is not conserved among related UNC–45 proteins. ARM repeat 9 contains a helix that is longer than usual. We designate this helix H9AB as it takes the place of both the first two helices in this layer. This modification, which is more similar in structure to a HEAT repeat [Andrade *et al.*, 2001], could be responsible for the introduction of a sharp bend at this part of the structure. Layer 12 contains an ARM repeat wherein the helix A is unwound. Electron density for the region of the protein that would correspond to helix H12A is present and this region of the protein is involved in crystal packing interactions with one of its close-packed neighbors. It is not clear whether this structure is a consequence of crystal packing, whether this region is never a helix, whether this layer contributes to bending of the structure, or whether it is simply a consequence of the crystal-packing environment. A loop of more than thirty amino acids in length links the ARM repeats of layers 13 and 14. The amino acids in this loop are highly conserved among UNC–45 proteins from diverse

species and the electron density corresponding to this region is excellent. As is the case with the loop in layer 12, the Loop 13/14 is involved in mediating contact with one of the neighboring molecules in the crystal. Finally, Layer 16 possesses only HB and HC helices. Unlike in the case of Layer 12, this does not appear to influence the global fold or change the trajectory of the UCS domain ARM repeat stack.

Identification of a conserved surface in the UCS domain. Other than their sequence homology, a physical and/or functional interaction with myosin is the defining feature shared by UCS domain-containing proteins (Figure 21). In an effort to identify conserved surface amino acids that might be involved in mediating interaction with myosin, we carried out an alignment of the UCS domains from five divergent proteins: dUNC–45 (DmUNC–45), the human striated muscle UNC–45 protein (HsUNC–45B), *P. anserina* Cro1p, *S. cerevisiae* She4p, and *S. pombe* Rng3p. The results of pairwise homology are summarized in Table 3. Using the freely available ConSurf server, we assigned values of homology to each position within the conserved UCS domain and then mapped those values to the surface of the dUNC–45 model [Landau *et al*., 2005]. The result is a strikingly high degree of conservation at amino acid positions that line the hydrophobic groove near the UCS domain carboxy-terminus (Figure 22). As a consequence of this observation, we hypothesize that conserved hydrophobic amino acids that line the surface of the UCS domain concave face formed by ARM repeat C helices are involved in the interaction of these proteins with myosin.

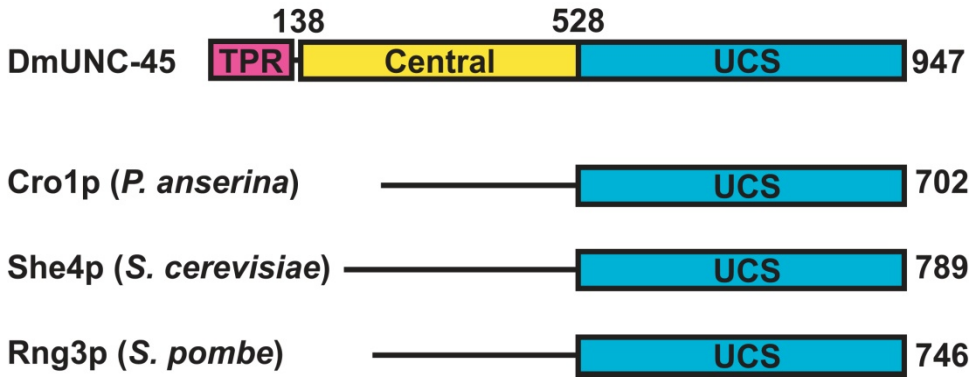

Figure 21. The domain organization of UNC–45 illustrated by the lone isoform encoded in the genome of *Drosophila melanogaster* (DmUNC–45). An amino-terminal tetratricopeptide repeat (TPR) domain (magenta) is followed in sequence by a Central domain (yellow) and UCS domain (cyan). Amino acid numbering is indicated. UCS domains are shared by additional myosin-interacting proteins in other species such as Cro1p from the *Podospora anserina*, the budding yeast *Saccharomyces cerevisiae* She4p protein, and Rng3p in the fission yeast *Schizosaccharomyces pombe*.

Table 3. Sequence homology among UCS domain-containing proteins

	HsUNC–45B	Cro1p	She4p	Rng3p
dUNC–45	39 (62)	28 (48)	19 (37)	24 (42)
HsUNC–45B		28 (48)	21 (38)	22 (40)
Cro1p			20 (41)	26 (48)
She4p				21 (39)

Analysis was carried out using EMBOSS pairwise alignment [Rice *et al.*, 2000]. Sequence identity and similarity (in parentheses) are expressed as percentages. Amino acid numbers: dUNC–45 (528-923); HsUNC–45B (523-929); Cro1p (287-702); She4p (359-791); Rng3p (340-746).

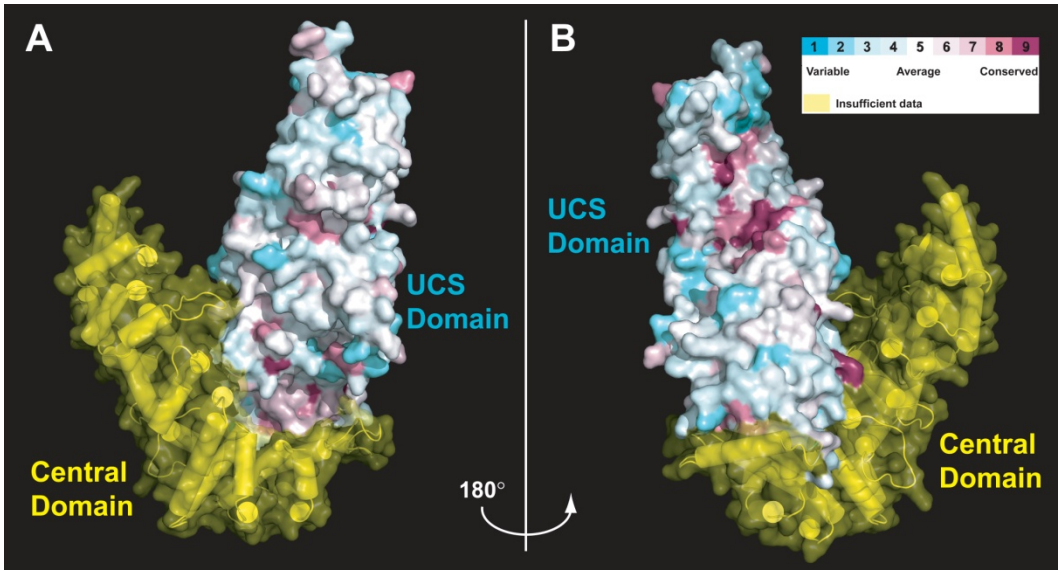

Figure 22. Conservation of UCS-domain amino acid positions mapped onto the surface of dUNC–45. A) In this molecular surface representation of the dUNC–45 x-ray crystal structure the Central domain is depicted in semitransparent yellow. The amino acid sequences of the five UCS domain-containing proteins listed in Table 3 have been aligned and a numeric value of homology (1-9) has been assigned to each position. This value has then been mapped onto the surface. B) The back face of dUNC–45 is displayed with the color scheme used to identify surface residues conserved across diverse UCS domain-containing proteins. Note the higher than normal degree of conservation within the groove of the UCS domain. This correlates with the less charged areas illustrated in Figure 20.

Limited proteolysis with chymotrypsin. One of the most striking features of the dUNC–45 x-ray crystal structure is an ordered loop that exists between ARM repeats 13 and 14. This loop, which we designate as L13/14, is nearly thirty amino acids in length and, due most likely to crystal packing forces, exhibits a remarkably ordered conformation in our structural model (Figure 23). Furthermore, the consensus stacking of ARM repeats 13 and 14, the placement of the L13/14 near the proposed myosin interacting site, and sequence conservation among UNC–45 proteins of amino acids in this region suggest a possible functional consequence for this loop.

Among several hydrophobic amino acids that are present on L13/14 are the aromatic amino acids Tyr497 and Phe512, which are susceptible to chymotryptic cleavage. In order to test whether this loop is flexible in solution and, therefore, available to function in regulating binding and as an independent confirmation of the correctness of our crystallographic model to predict behavior in solution, we performed a proteolysis experiment [Srikakulam *et al.*, 2008] with limiting amounts of chymotrypsin on the recombinant dUNC–45 protein of native sequence and a modified version in which amino acids 587-613, which correspond to L13/14, were replaced by the pentapeptide linker Gly-Ser-Gly-Ser-Gly (Figure 24). The modified protein, which we refer to as dUNC–45ΔL, expressed and purified similarly to the native protein. However, it proved significantly resistant to proteolysis by chymotrypsin (Figure 25). The native recombinant dUNC–45 protein was rapidly cleaved into roughly 66 and 34 kDa fragments as illustrated by SDS-PAGE. Similar

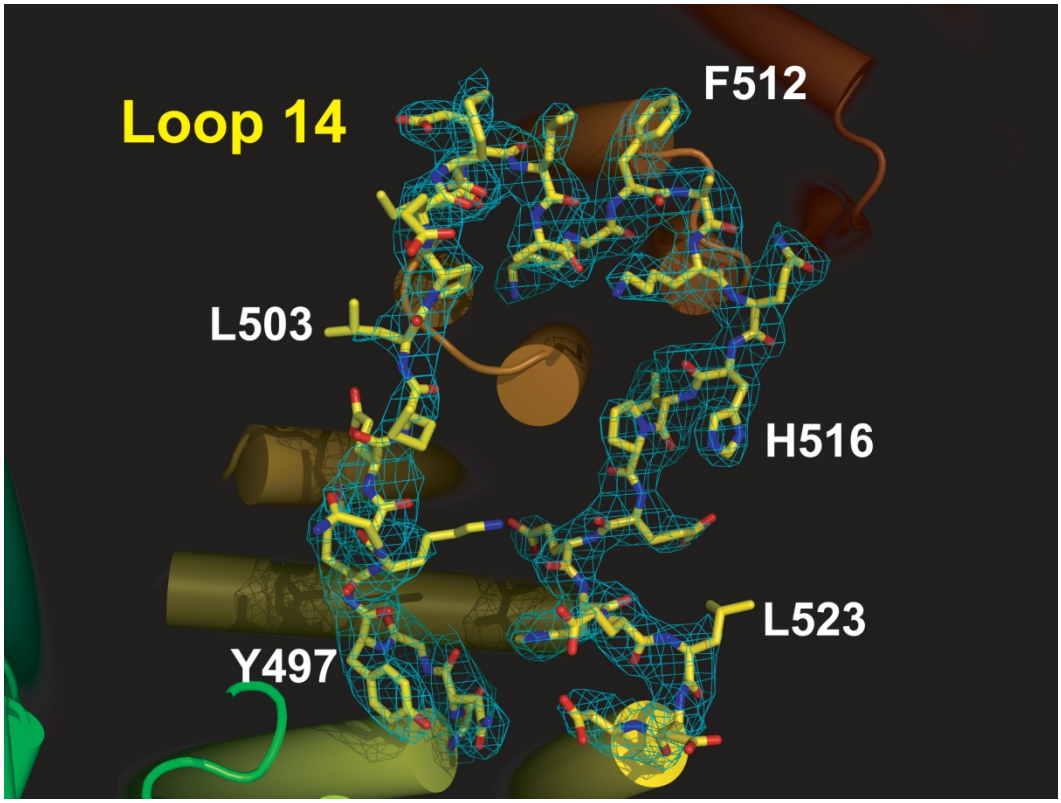

Figure 23. Electron density about the Loop 14 region of dUNC–45. The coloring scheme is the same as in Figure 19B. Loop 14 is shown in a stick representation with electron density from a refined 2Fo-Fc map contoured at 1.1 σ depicted as a cyan colored mesh. Several individual amino acids are labeled. This electron density is representative of the quality throughout the final refined map.

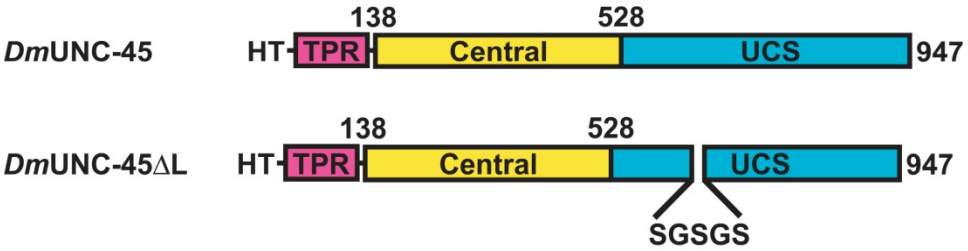

Figure 24. Purified protein constructs used in proteolysis assays. The full length dUNC–45 (*Dm*UNC–45) used in all the studies contains an amino-terminal histidine tag (HT). An additional construct dUNC–45ΔL (*Dm*UNC–45ΔL) was made with UCS domain Loop 14 replaced by a Ser-Gly-Ser-Gly-Ser linker. Each of these proteins was expressed in *E. coli* and purified to homogeneity. The color scheme is consistent with that of previous figures.

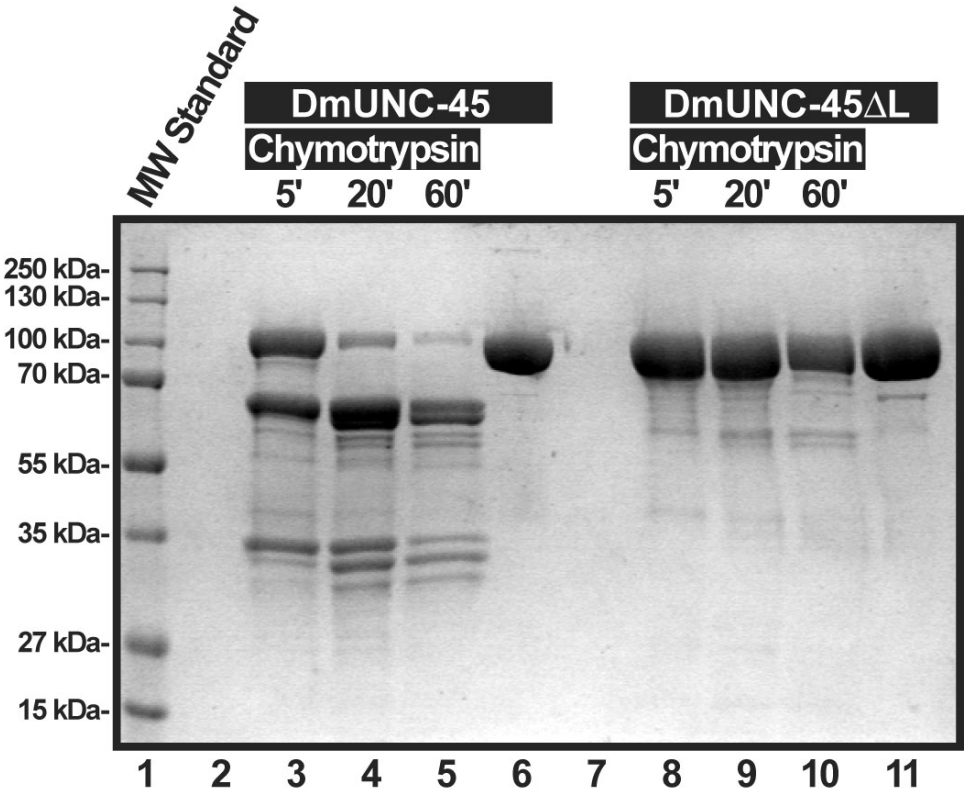

Figure 25. Limited proteolysis of dUNC–45 (DmUNC–45) with chymotrypsin. Coomassie-stained 10% SDS-PAGE gel reveals that the full length dUNC–45 protein is readily cleaved into 66 and 34 kDa fragments (lanes 3-5) while the construct lacking Loop 14 (ΔL) is resistant to proteolytic cleavage by chymotrypsin (lanes 8-10).

analysis of a construct that lacks its TPR domain (amino acids 1-137; dUNC–45ΔTPR) yielded a similar pattern of proteolysis as the full length protein, except that the 66 kDa band ran as a smaller fragment, as would be expected for cleavage of an amino-terminally shortened protein cleaved at the L13/14 loop (data not shown). Finally, it is interesting to note that the TPR domain from the larger amino-terminal proteolytic fragment remains intact over the course of the limited proteolysis experiment. This might indicate that the TPR domain is, in fact, well-ordered and that the lack of structural data derives from flexibility of the entire domain afforded by the amino acids that link it to the rest of the of the dUNC–45 molecule. Notably, there are no aromatic amino acids present within the TPR linker region (122-138) for chymotrypsin cleavage.

Discussion

All UCS domain-containing proteins that have been studied share the ability to influence myosin-mediated processes in cells [Yu and Bernstein, 2003]. Despite this clear functional correlation, it has been difficult to ascribe a specific mechanism to UCS-domain containing proteins. Previous studies have relied primarily on genetics and characterization of mutant phenotypes. In order to understand the mechanisms by which UCS domain-containing protein such as UNC–45 function, it is necessary that high quality structural models be available to direct the framing of hypotheses and design of constructs. Our success in determining the x-ray crystal structure of the UNC–45 protein from the fruit fly *Drosophila melanogaster* provides the first such structure.

The dUNC–45 crystal structure reveals that the Central and UCS domains form a contiguous stack of armadillo repeats. In the crystal the structure exhibits a highly bent conformation. However, we suspect that in solution this molecule is capable of assuming a more extended conformation. Furthermore, the amino-terminal TPR domain exhibits too much flexibility relative to the rest of the molecule in the crystal to be observed in electron density maps. These observations suggest that dynamic movement between the extremes of linear and bent conformations might be a hallmark of UNC–45 function.

The structure reveals that the groove that runs along the concave face of the UCS ARM repeat stack C helices exhibits a surface chemistry that is unique when compared with the rest of the molecule. Both electrostatic calculations as well as surface polarity analysis indicate that this surface if more hydrophobic than any other portion of the dUNC–45 surface. The most intriguing observation, however, is the high degree of amino acid sequence identity of amino acids within this groove. This strongly suggests that the diverse myosin interaction activities observed experimentally in diverse UCS-domain containing proteins rely on this conserved hydrophobic surface.

We show that the several ARM repeats break from the consensus giving rise to the observed bend in the dUNC–45 structure and the presence of loops. The largest of these, loop L13/14, is solvent exposed and highly sensitive to cleavage by the protease chymotrypsin. Recombinant expression of a version of dUNC–45 in which L13/14 is replaced by a polar linker capable of spanning the distance between the ends of ARM

repeats 13 and 14 leads to a soluble protein that resists proteolysis by limiting quantities of chymotrypsin.

The dUNC–45 x-ray crystal structure raises our understanding of this enigmatic and compelling molecule to a new level. In the future, we expect to join researchers in using this structural information to aid in discovering the mechanisms by which UCS-domain containing proteins influence myosin activity and, consequently, basic cellular physiology.

References

Adams, P. D., Afonine, P. V., Bunkoczi, G., Chen, V. B., Davis, I. W., Echols, N., Headd, J. J., Hung, L. W., Kapral, G. J., Grosse-Kunstleve, R. W. *et al.* (2010). PHENIX: a comprehensive Python-based system for macromolecular structure solution. Acta Crystallogr D Biol Crystallogr *66*, 213-221.

Andrade, M. A., Petosa, C., O'Donoghue, S. I., Muller, C. W. and Bork, P. (2001). Comparison of ARM and HEAT protein repeats. J Mol Biol *309*, 1-18.

Ao, W. and Pilgrim, D. (2000). *Caenorhabditis elegans* UNC–45 is a component of muscle thick filaments and colocalizes with myosin heavy chain B, but not myosin heavy chain A. J Cell Biol *148*, 375-384.

Baker, N. A., Sept, D., Joseph, S., Holst, M. J. and McCammon, J. A. (2001). Electrostatics of nanosystems: application to microtubules and the ribosome. Proc Natl Acad Sci U S A *98*, 10037-10041.

Barral, J. M., Bauer, C. C., Ortiz, I. and Epstein, H. F. (1998). Unc–45 mutations in *Caenorhabditis elegans* implicate a CRO1/She4p-like domain in myosin assembly. J Cell Biol *143*, 1215-1225.

Barral, J. M., Hutagalung, A. H., Brinker, A., Hartl, F. U. and Epstein, H. F. (2002). Role of the myosin assembly protein UNC–45 as a molecular chaperone for myosin. Science *295*, 669-671.

Berteaux-Lecellier, V., Zickler, D., Debuchy, R., Panvier-Adoutte, A., Thompson-Coffe, C. and Picard, M. (1998). A homologue of the yeast SHE4 gene is essential for the transition between the syncytial and cellular stages during sexual reproduction of the fungus Podospora anserina. EMBO J *17*, 1248-1258.

Brenner, S. (1974). The genetics of *Caenorhabditis elegans*. Genetics *77*, 71-94.

Coluccio, L. M., ed. (2008). Myosins. A Superfamily of Molecular Motors (Springer).

Conti, E., Uy, M., Leighton, L., Blobel, G. and Kuriyan, J. (1998). Crystallographic analysis of the recognition of a nuclear localization signal by the nuclear import factor karyopherin alpha. Cell *94*, 193-204.

Das, A. K., Cohen, P. W. and Barford, D. (1998). The structure of the tetratricopeptide repeats of protein phosphatase 5: implications for TPR-mediated protein-protein interactions. EMBO J *17*, 1192-1199.

Davis, I. W., Leaver-Fay, A., Chen, V. B., Block, J. N., Kapral, G. J., Wang, X., Murray, L. W., Arendall, W. B., 3rd, Snoeyink, J., Richardson, J. S. *et al.* (2007). MolProbity: all-atom contacts and structure validation for proteins and nucleic acids. Nucleic Acids Res *35*, W375-383.

DeLano, W. L. (2002). The PyMOL Molecular Graphics System (Palo Alto, CA USA, DeLano Scientific LLC).

Emsley, P., Lohkamp, B., Scott, W. G. and Cowtan, K. (2010). Features and development of Coot. Acta Crystallogr D Biol Crystallogr *66*, 486-501.

Epstein, H. F. and Thomson, J. N. (1974). Temperature-sensitive mutation affecting myofilament assembly in Caenorhabditis elegans. Nature *250*, 579-580.

Groves, M. R. and Barford, D. (1999). Topological characteristics of helical repeat proteins. Curr Opin Struct Biol *9*, 383-389.

Huber, A. H., Nelson, W. J. and Weis, W. I. (1997). Three-dimensional structure of the armadillo repeat region of beta-catenin. Cell *90*, 871-882.

Hutagalung, A. H., Landsverk, M. L., Price, M. G. and Epstein, H. F. (2002). The UCS family of myosin chaperones. J Cell Sci *115*, 3983-3990.

Jansen, R. P., Dowzer, C., Michaelis, C., Galova, M. and Nasmyth, K. (1996). Mother cell-specific HO expression in budding yeast depends on the unconventional myosin myo4p and other cytoplasmic proteins. Cell *84*, 687-697.

Landau, M., Mayrose, I., Rosenberg, Y., Glaser, F., Martz, E., Pupko, T. and Ben-Tal, N. (2005). ConSurf 2005: the projection of evolutionary conservation scores of residues on protein structures. Nucleic Acids Res *33*, W299-302.

Melkani, G. C., Lee, C. F., Cammarato, A. and Bernstein, S. I. (2010). *Drosophila* UNC–45 prevents heat-induced aggregation of skeletal muscle myosin and facilitates refolding of citrate synthase. Biochem Biophys Res Commun *396*, 317-322.

Otwinowski, Z. and Minor, W. (1997). Processing of X-ray Diffraction Data Collected in Oscillation Mode. In: Macromolecular Crystallography, Part A., Vol 276 (New York, Academic Press).

Price, M. G., Landsverk, M. L., Barral, J. M. and Epstein, H. F. (2002). Two mammalian UNC–45 isoforms are related to distinct cytoskeletal and muscle-specific functions. J Cell Sci *115*, 4013-4023.

Rice, P., Longden, I. and Bleasby, A. (2000). EMBOSS: the European Molecular Biology Open Software Suite. Trends Genet *16*, 276-277.

Srikakulam, R., Liu, L. and Winkelmann, D. A. (2008). Unc45b forms a cytosolic complex with Hsp90 and targets the unfolded myosin motor domain. PLoS One *3*, e2137.

Swank, D. M., Bartoo, M. L., Knowles, A. F., Iliffe, C., Bernstein, S. I., Molloy, J. E. and Sparrow, J. C. (2001). Alternative exon-encoded regions of *Drosophila* myosin heavy chain modulate ATPase rates and actin sliding velocity. J Biol Chem *276*, 15117-15124.

Wendland, B., McCaffery, J. M., Xiao, Q. and Emr, S. D. (1996). A novel fluorescence-activated cell sorter-based screen for yeast endocytosis mutants identifies a yeast homologue of mammalian eps15. J Cell Biol *135*, 1485-1500.

Wohlgemuth, S. L., Crawford, B. D. and Pilgrim, D. B. (2007). The myosin co-chaperone UNC–45 is required for skeletal and cardiac muscle function in zebrafish. Dev Biol *303*, 483-492.

Wong, K. C., Naqvi, N. I., Iino, Y., Yamamoto, M. and Balasubramanian, M. K. (2000). Fission yeast Rng3p: an UCS-domain protein that mediates myosin II assembly during cytokinesis. J Cell Sci *113 (Pt 13)*, 2421-2432.

Yu, Q. and Bernstein, S. I. (2003). UCS proteins: managing the myosin motor. Curr Biol *13*, R525-527.

Acknowledgements

This chapter is a manuscript draft. The experiments and tasks performed by Chi Lee include: 1) Cloned the dUNC–45 cDNA and constructed the pChi7 plasmid for bacterial expression and purification of dUNC–45. 2) Preparated the dUNC–45 native and Se-Met proteins. 3) Optimized crystal growing and cryo-protectant conditions. 4) Data collection processing using HKL2000. 5) dUNC–45 structure solution, building, and refinement using CCP4, PHENIX, COOT, Refmac5, and MolProbity. The derivation of the native and the L63M crystal structures were both first modeled by Chi Lee.

Subsequently, Arthur Hauenstein has participated in all stages of crystal cultivation process and performed further optimization for the L63M crystal. Clarke Gasper and Valerie Engelke were responsible for constructing the dUNC–45TPR, dUNC–45ΔL, and dUNC–45ΔTPR plasmids, followed by protein expression, purification, and crystal cultivation and preservation. Furthermore, Clarke Gasper carried out the limited proteolysis analysis of the native and dUNC–45ΔL proteins. Jonathan Fleming performed the final validation of the dUNC–45 x-ray crystal structure and completed the data analysis of the structure.

Conclusion

UNC–45 is a part of the UCS protein family whose members are all important for myosin folding, stability, and maintenance. Due to the importance of myosin function in a variety of essential cellular processes, mutations in UCS proteins manifest into defects in cytokinesis, sarcomere disorganization, and developmental arrest [Yu and Bernstein, 2003]. Investigation of *C. elegans* UNC–45 mutants reveal movement defects caused by depressed myosin accumulation and a loss of thick filaments in muscle [Epstein and Thomson, 1974]. Since myosin is an important protein for the cell, by virtue of its association, UNC–45 has garnered the attentions of scientists. Model systems such as yeast, *C. elegans* and cultured myogenic cell lines contributed insights concerning the protein domains [Barral *et al.*, 1998; Venolia *et al.*, 1999], interacting partners [Barral *et al.*, 2002; Wesche *et al.*, 2003], and phenotypic effects associated with mutations in the UNC–45 protein [Epstein and Thomson, 1974; Wong *et al.*, 2000; Price *et al.*, 2002]. The discovery that UNC–45 could be a myosin specific chaperone [Barral *et al.*, 2002] fueled a new found interest in this protein which spurred on further research. Since 2002, more than 20 research papers were published, each reaffirming the importance of UNC–45 and other UCS proteins in myosin folding and function. Furthermore, an infusion of data from the zebrafish model assisted the understanding of UNC–45 function tremendously. As *Drosophila* is a model system for muscle research, our work should result in deeper understanding of UNC–45 function and its mechanism of action. The focus of this dissertation project was on investigating *Drosophila* UNC–45 (dUNC–45) protein function *in vivo*

and *in vitro*. Moreover, by solving the X-ray crystal structure of *Drosophila* UNC–45, it sets the stage for a detailed understanding of its interaction with myosin and will aid in possible future therapeutic use of this protein/gene in muscle related diseases and beyond.

Chapter one characterized dUNC–45 *in vivo* function by comparing expression and localization of dUNC–45 and myosin between wild-type flies and a d*unc–45* knock mutant line. Western blot analysis shows that dUNC–45 is expressed at all developmental stages in wild-type flies. Immunofluorescence confocal microscopy shows dUNC–45 co-localizes with non-muscle myosin during the initial stages of embryogenesis in the embryonic blastoderm, but later it co-localizes most strongly with skeletal muscle myosin in the body-wall muscle and the pharyngeal muscle. Furthermore, examination of the body-wall muscle under high magnification revealed that dUNC–45 localizes to the Z-discs of sarcomeres under normal growth conditions.

To use the power of *Drosophila* genetics as a basis of analyzing UNC–45 function, a d*unc–45* mutant $Tom34^{EY03034–33}$ (*T–33*) was created. *T–33* contains a 1.3 kb deletion that removes a majority of the first and second exons of *unc–45*, including the translation start site. Zygotic expression of dUNC–45 is disrupted in *T–33*, resulting in nearly non-detectable dUNC–45 levels in maturing embryos as well as embryonic lethality. Confocal microscopy evidence confirms that skeletal muscle myosin accumulation is not disrupted in 14 hour old homozygous *T–33* embryos. However, myosin is dramatically decreased in embryonic body wall muscles of 22 hour old embryos as confirmed with immunoblotting. Furthermore, electron

microscopy of these muscles showed few thick filaments and a lack of regular thick/thin filament lattice spacing. The lethality, protein accumulation, and muscle defect phenotype can be rescued with a wild-type d*unc–45* transgene, indicating that the mutant phenotypes are due to the dUNC–45 deficiency. Our results suggest that UNC–45 function *in vivo* involves a post-translational interaction with myosin. Such interaction is necessary for the stability of myosin and subsequent thick filament formation.

Chapter two characterized dUNC–45 chaperone function using *in vitro* assays to assess its ability to prevent protein aggregation and to allow refolding of chemically denatured protein. Furthermore, dUNC–45 chaperone function *in vivo* was explored by looking at its localization and expression in heat stressed third instar larvae. Bacterially expressed recombinant dUNC–45 was purified and tested in the chaperone assays using citrate synthase, α-lactalbumin, and dUNC–45's native substrate myosin. Light scattering experiments show that dUNC–45 alone can suppress heat-induced CS aggregation ~25% and heat-induced chicken skeletal myosin S1 aggregation ~56%. In the presence of ATP or its non-hydrolyzable analogue, AMP-PNP, dUNC–45 chaperone function is enhanced. Heat-induced aggregation of CS is suppressed ~60% in the presence of dUNC–45 and ATP, while heat-induced aggregation of myosin S1 is suppressed more than 95%. The ability of dUNC–45 to protect myosin from heat is also visually represented by electron micrographs of rotary shadowed myosin with AMP-PNP at elevated temperature in the presence or absence of dUNC–45. In the absence of dUNC–45, myosin forms a lollipop-like structure as a result of fusion

between the two motor domains of a myosin dimer. dUNC–45 can prevent the heat-induced fusion of the two motor domains as well as eliminate the aggregation of the lollipop-like structures. In addition to suppressing heat-induced protein aggregation, dUNC–45 can refold chemically-denatured CS. In the presence of dUNC–45, ~23% of urea-denatured CS regained its enzymatic activity which is further increased to ~36% with the inclusion of AMP-PNP. ATP binding to dUNC–45 is confirmed by monitoring the intrinsic tryptophan fluorescence of dUNC–45 which quenched in a time dependant manner, suggesting a conformational change in dUNC–45 upon ATP binding. Even though dUNC–45 binds ATP, hydrolysis of ATP was not detected. *In vivo*, dUNC–45 translocates from the Z disc to the A band where myosin resides during stress as evident by immunofluorescence confocal microscopy of body-wall muscle from heat shocked wild-type third instar larvae. This translocation may allow it to exercise its protective effect and could be accompanied by an increase in dUNC–45 expression as shown on Western blots of wild-type flies under various stress conditions.

Chapter 3 detailed the process and outcome of solving the x-ray crystal structure of dUNC–45. Bacterially expressed recombinant dUNC–45 used for *in vitro* chaperone assays was crystallized using the hanging-drop vapor diffusion technique. The dUNC–45 crystals were suitable for x-ray diffraction studies. Complete diffraction data were collected using a synchrotron x-ray source to a resolution limit of 3.0 Å and the phase was solved using the single anomalous dispersion method of selenium-labeled methionine derivative crystals. The final dUNC–45 structure

revealed that the TPR domain is flexible relative to the rest of the protein in the crystal. The Central and UCS domains form 17 stacked tandem helical motifs similar to those of armadillo repeats. The continuous armadillo repeats from the central to the UCS domain suggest the two domains could function as a single entity, but two sharp turns in the protein superstructure results in a bent horseshoe-shaped conformation, separating the two domains in the crystal structure. Solution and electron microscopy data suggest that dUNC–45 exhibits a more elongated conformation in solution. Sequence alignment of five divergent UCS proteins assisted in identifying conserved surface amino acids that might be involved in its interaction with myosin. Within the UCS domain, helices H16C, H17C, H18C, H19C, and H20C form a flat hydrophobic groove containing a patch of conserved surface amino acids. There is also a proteolytically sensitive solvent exposed loop between H13C and H14A in the UCS domain that hides a smaller patch of conserved surface amino acids at its base. Preliminary data suggest that removal of this loop reduces the affinity of myosin for dUNC–45 in fluorescence-based immunoassays. Our structural and biochemical data suggest that together, these two adjacent locations on the dUNC–45 UCS domain might provide a surface for myosin folding and/or protection. The position of amino acids residues shown previously to affect UNC–45 function when mutated [Price *et al.*, 2002] support our hypothesis that one surface of the rigid UCS domain constitutes the myosin-interaction surface. The x-ray crystal structure of dUNC–45 provides a structural template for future biochemical investigations into the function of this intriguing protein.

Many of the data presented here indicate that *Drosophila* deploys and uses UNC–45 in a similar fashion to other organisms. The *in vivo* Z disc localization of dUNC–45 in sarcomeres under normal growing conditions is also seen in the zebrafish [Etard *et al.*, 2008]. The decreased myosin expression and the absence of thick filaments in the d*unc–45* mutant are reminiscent of the defects in the *unc–45* *C. elegans* mutant grown at the restrictive temperature [Epstein and Thomson, 1974] and RNAi knock down of *unc–45b* in zebrafish embryos [Wohlgemuth *et al.*, 2007]. The *in vitro* chaperone function of dUNC–45 is similar to that shown in *C. elegans* UNC–45 [Barral *et al.*, 2002]. Further, the heat shock induced translocation of dUNC–45 from the Z disc to the A band was demonstrated to occur in the zebrafish as well [Etard *et al.*, 2008].

The results of dUNC–45 studies are useful in resolving conflicts in the literature. The conclusion that dUNC–45 and myosin interact post-translationally echos the results derived from *in vitro* myosin translation experiments [Liu *et al.*, 2008], but it is in contrast to the findings on the yeast UCS protein Rng3 [Amorim and Mata, 2009] where the authors suggest a co-translational association with myosin. Previously, Rng3 was found to be required for purified yeast myosin II (Myo2p) to function in the *in vitro* motility assay even though the myosin molecules retained their actin-activated ATPase function and were thought to be in their native conformation. This suggest that Rng3 performs an additional function in stablizing myosin [Lord and Pollard, 2004; Lord *et al.*, 2008]. Our data showing that myosin is synthesized *in vivo* in the absence of UNC–45 weakens the proposition that UCS proteins associate with

myosin co-translationally and the data from dUNC–45 strengthen the argument for a post-translational interaction between myosin and the UCS protein.

Another discrepancy in the literature concerns whether UNC–45 is a cytosolic protein. Findings in *Drosophila* using immunofluorescence confocal microscopy and results of monitoring GFP labeled zebrafish UNC–45B through development both show the Z disc localization of UNC–45 in mature muscle. However, over-expression of flag-tagged mouse UNC–45B in the C2C12 mouse myogenic cell line led the authors to conclude that mouse UNC–45B is a cytosolic protein because the UNC–45B-Flag protein fractionated to the cytosolic fraction of the cell lysate [Srikakulam *et al.*, 2008]. Our results suggest that the Z disc is the storage site for UNC–45, which agrees with results from the zebrafish model [Etard *et al.*, 2008]. It is possible that the 0.5% triton-x used during the extraction process is strong enough to disassociate UNC–45B-Flag from the Z disc resulting in the distribution in the cytosolic fraction. Furthermore, during development, dUNC–45 is distributed cytosolically in the muscle bundles of 12-14 hour embryos (Figure 4G, chapter 1) before the completion of myofibrillogenesis. Similarly, UNC–45-GFP is ubiquitously distributed in the cytoplasm in 24 hour post fertilization zebrafish embryos [Etard *et al.*, 2008]. Therefore, it is plausible that over-expression of flag-tagged mouse UNC–45B delayed myofibrillogenesis in the C2C12 cells resulting in the cytosolic localization in the cell fractionate. The most novel aspect of this dissertation project lies in the crystal structure of dUNC–45. This is the first x-ray crystal structure solved for a UCS protein. As protein function is based on its structure, detailed information

on the structure of a protein can yield insight into the mechanism of its function. Myosin, the native substrate for UNC–45, can be used to illustrate the benefit of knowing the structure of a protein. Published in 1993, the first x-ray crystal structure of the myosin motor domain was the culmination of more than 40 years of efforts [Rayment *et al.*, 1993]. Since then, mutagenesis of various regions in the molecule has contributed to a greater insight of how it functions as a cellular motor protein. From the importance of the converter domain [Littlefield *et al.*, 2003] to understanding how the energy from ATP hydrolysis is transformed into mechanical work [Holmes and Geeves, 2000; Huxley, 2000], it is the myosin structure that allowed for the testing of structure based hypotheses. Furthermore, the myosin crystal structure explained how small molecules such as blebbistatin inhibit myosin function [Kovacs *et al.*, 2004].

Even though the mechanism of dUNC–45 function is not readily apparent by analysis of its structure, initial evaluation suggests a possible hydrophobic groove for myosin binding in the UCS domain. Disruption of this hydrophobic groove using site directed mutagenesis can verify such hypothesis. The solvent exposed loop (loop 14) in the UCS domain presents another interesting site for mutagenesis. Preliminary data suggest that this mobile region might form part of an allosteric myosin-binding regulatory mechanism (not shown). In depth investigation of the dUNC–45ΔL protein *in vitro* is underway to discern the involvement of this loop in the interaction between dUNC–45 and myosin. A dUNC–45ΔL transgenic fly line can also be created to

examine its effect on the organismal level to fully utilize the benefit offered by the fly model system.

The current crystal structure of dUNC–45 is roughly horseshoe shaped yet rotary shadowed mouse UNC–45B combined with class averaging of single molecule analysis suggest an extended conformation [Srikakulam *et al.*, 2008]. Our preliminary small angle x-ray scattering data (not shown) are in agreement with the extended conformation of dUNC–45. Figure 26 shows a possible extended dUNC–45 configuration with the interacting partners indicated.

The results of the *in vitro* chaperone assay showed an enhancement of dUNC–45 chaperone function in the presence of ATP. It is unclear where ATP binds on the dUNC–45 molecule. Attempts have been made in solving the dUNC–45 crystal structure in the ATP bound form by growing co-crystals of dUNC–45 and ATP. dUNC–45 crystals formed successfully in the presence of 6.6 mM ATP using similar conditions as for the native crystal. Two data sets of dUNC–45/ATP were obtained using a synchrotron x-ray source but data analyses were unsuccessful due to possible crystal cracking and damage during handling. Once solved, the ATP bound dUNC–45 structure can help grasp the knowledge needed to understand the molecular mechanism of ATP-conferred enhancement on dUNC–45 chaperone function.

Thus far, research efforts in the field have largely focused on UNC–45B, the striated muscle isoform, in demonstrating its importance on myosin folding, stability, and maintenance. Figure 27 is a schematic representation of *in vivo* UNC–45 function during myogenesis and stress. Diseases that affect myosin accumulation such as

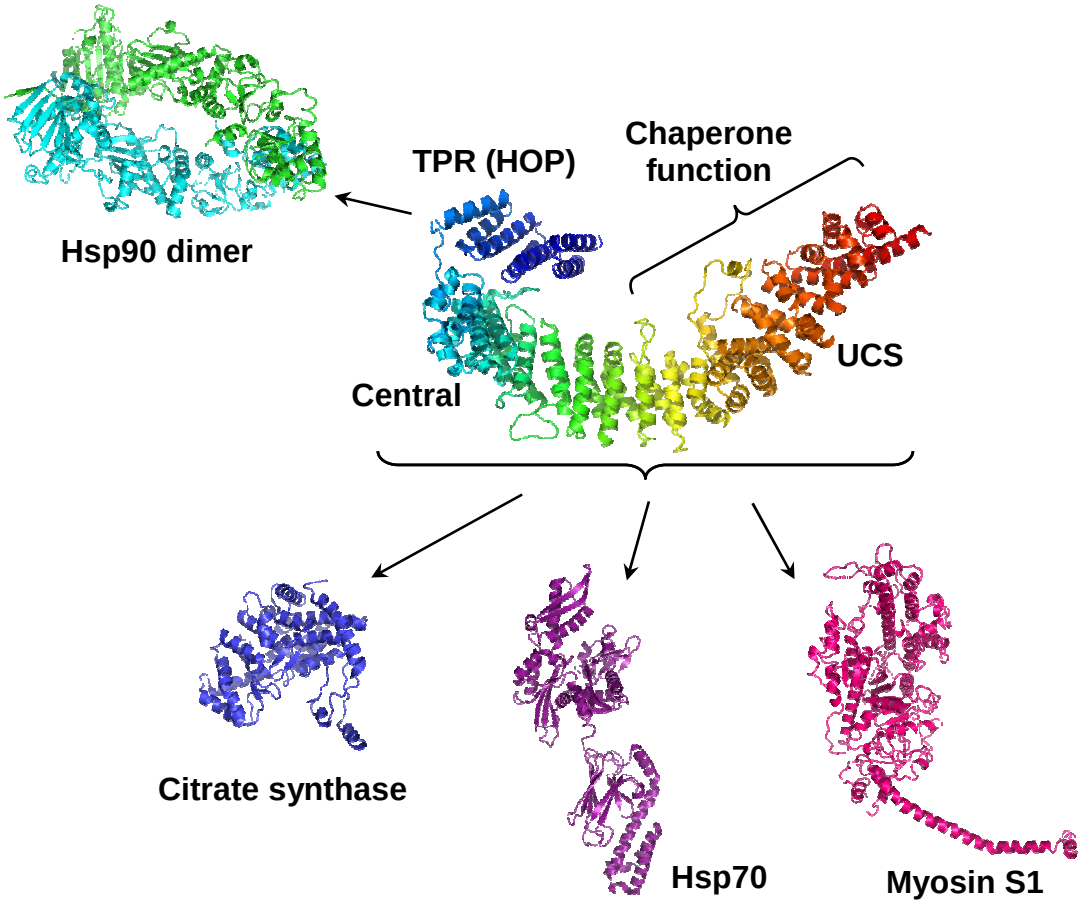

Figure 26. Model showing a theoretical extended dUNC–45 structure domains and their interacting proteins. A canonical TPR motif was modeled to provide a more complete picture of the dUNC–45 structure in solution. TPR (Human heat shock organizing protein, PDBID 1ELR). Myosin S1(chicken skeletal muscle myosin, PDBID 2MYS with light chains excluded). Hsp70 (*E. coli* DnaK, PDBID 2KHO). Citrate synthase (porcine heart CS, PDBID 3ENJ). Hsp90 (*S. cerevisiae* Hsp90 dimer in the ATP bound closed conformation, PDBID 2CG9).

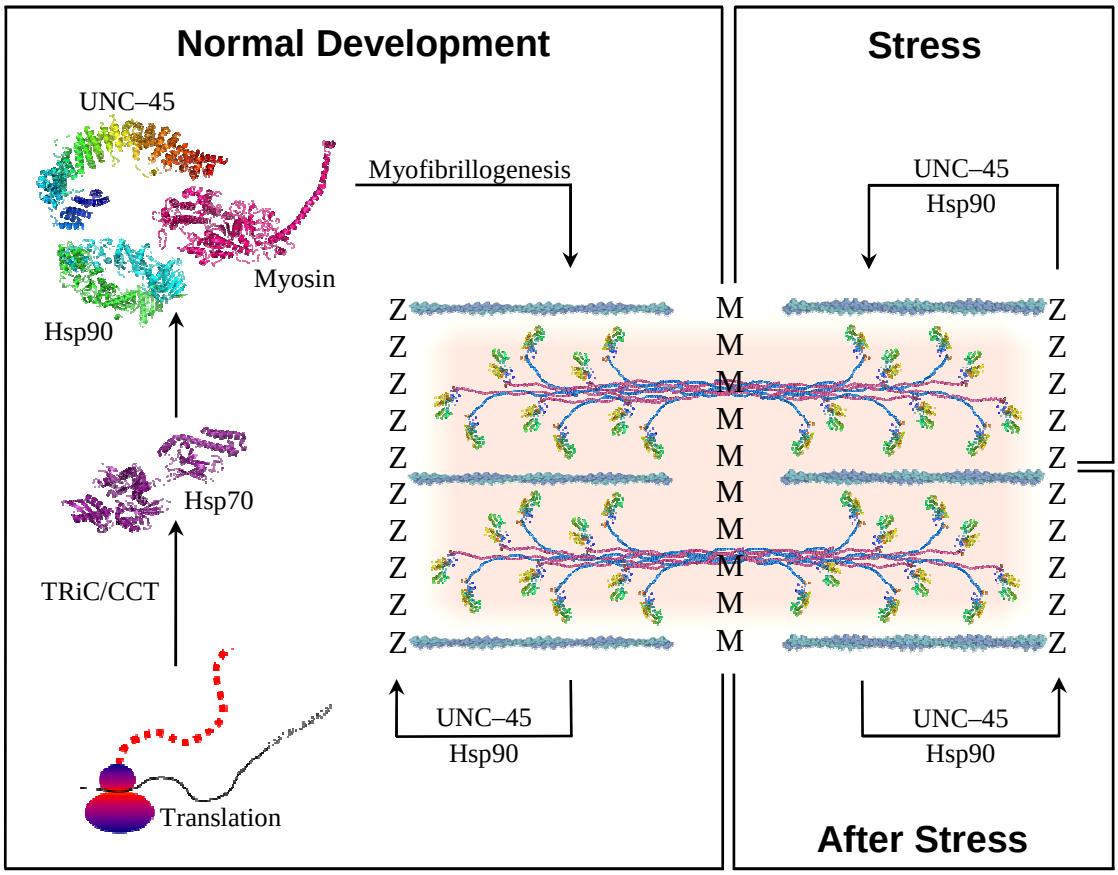

Figure 27. Model of UNC–45 function *in vivo*. During normal development, myosin maturation involves chaperones such as TriC/CCT, Hsp70 [Srikakulam and Winkelmann, 1999, 2004]. Data from zebrafish studies suggest myosin forms a complex with UNC–45 and Hsp90 in the cytosol [Etard *et al*., 2008]. The complex remains stable until the end of myofibrillogenesis. Once myosin successfully incorporates into thick filaments, UNC–45 and Hsp90 dissociate from myosin and move over to the Z disc. Upon stress, UNC–45 and Hsp90 translocate from the Z disc to the A band and protect myosin from denaturation. Since both *Drosophila* and *C. elegans* UNC–45 display chaperone function *in vitro* [Barral *et al*., 2002], it is possible that UNC–45 could function to protect myosin independently of Hsp90. In situations where UNC–45 alone is not enough to protect myosin, Hsp90 could then partake in preserving myosin structural integrity. After the stress is over, UNC–45 and Hsp90 may return to the Z disc until needed. Pink area represents a single sarcomere. Z = Z disc. M = M line. Blue/green actin thin filaments project out from the Z discs, and two myosin thick filaments are pictured across the M line.

cachexia [Acharyya *et al.*, 2004; Chamberlain, 2004] and critical illness myopathy [Deconinck *et al.*, 1998; Lacomis and Campellone, 2002] present themselves as being possible targets for UNC–45B mediated therapies. Relatively little is published on UNC–45A. Sequence comparison between the two human or mouse isoforms reveal only 55-56% identity with 74% similarity [Price *et al.*, 2002]. Of the studies published, one has demonstrated that over-expression of UNC–45A leads to enhanced breast cancer cell proliferation and increased motility [Bazzaro *et al.*, 2007] while another showed increased UNC–45A levels in a variety of cancer cell lines [Epping and Bernards, 2009] including melanomas and carcinomas. If a causative relationship can be proven between UNC–45A and the cancer cells, then the UNC–45 structure presented here will be of great value in formulating strategies for potential treatments.

References

Amorim, M. J. and Mata, J. (2009). Rng3, a member of the UCS family of myosin co-chaperones, associates with myosin heavy chains cotranslationally. EMBO Rep *10*, 186-191.

Barral, J. M., Bauer, C. C., Ortiz, I. and Epstein, H. F. (1998). Unc–45 mutations in *Caenorhabditis elegans* implicate a CRO1/She4p-like domain in myosin assembly. J Cell Biol *143*, 1215-1225.

Barral, J. M., Hutagalung, A. H., Brinker, A., Hartl, F. U. and Epstein, H. F. (2002). Role of the myosin assembly protein UNC–45 as a molecular chaperone for myosin. Science *295*, 669-671.

Bazzaro, M., Santillan, A., Lin, Z., Tang, T., Lee, M. K., Bristow, R. E., Shih Ie, M. and Roden, R. B. (2007). Myosin II co-chaperone general cell UNC–45 overexpression is associated with ovarian cancer, rapid proliferation, and motility. Am J Pathol *171*, 1640-1649.

Deconinck, N., Van Parijs, V., Beckers-Bleukx, G. and Van den Bergh, P. (1998). Critical illness myopathy unrelated to corticosteroids or neuromuscular blocking agents. Neuromuscul Disord *8*, 186-192.

Epping, M. T. and Bernards, R. (2009). Molecular basis of the anti-cancer effects of histone deacetylase inhibitors. Int J Biochem Cell Biol *41*, 16-20.

Epstein, H. F. and Thomson, J. N. (1974). Temperature-sensitive mutation affecting myofilament assembly in *Caenorhabditis elegans*. Nature *250*, 579-580.

Etard, C., Roostalu, U. and Strahle, U. (2008). Shuttling of the chaperones Unc45b and Hsp90a between the A band and the Z line of the myofibril. J Cell Biol *180*, 1163-1175.

Holmes, K. C. and Geeves, M. A. (2000). The structural basis of muscle contraction. Philos Trans R Soc Lond B Biol Sci *355*, 419-431.

Huxley, A. F. (2000). Mechanics and models of the myosin motor. Philos Trans R Soc Lond B Biol Sci *355*, 433-440.

Kovacs, M., Toth, J., Hetenyi, C., Malnasi-Csizmadia, A. and Sellers, J. R. (2004). Mechanism of blebbistatin inhibition of myosin II. J Biol Chem *279*, 35557-35563.

Lacomis, D. and Campellone, J. V. (2002). Critical illness neuromyopathies. Adv Neurol *88*, 325-335.

Littlefield, K. P., Swank, D. M., Sanchez, B. M., Knowles, A. F., Warshaw, D. M. and Bernstein, S. I. (2003). The converter domain modulates kinetic properties of *Drosophila* myosin. Am J Physiol Cell Physiol *284*, C1031-1038.

Liu, L., Srikakulam, R. and Winkelmann, D. A. (2008). Unc45 activates Hsp90-dependent folding of the myosin motor domain. J Biol Chem *283*, 13185-13193.

Lord, M. and Pollard, T. D. (2004). UCS protein Rng3p activates actin filament gliding by fission yeast myosin-II. J Cell Biol *167*, 315-325.

Lord, M., Sladewski, T. E. and Pollard, T. D. (2008). Yeast UCS proteins promote actomyosin interactions and limit myosin turnover in cells. Proc Natl Acad Sci U S A *105*, 8014-8019.

Price, M. G., Landsverk, M. L., Barral, J. M. and Epstein, H. F. (2002). Two mammalian UNC–45 isoforms are related to distinct cytoskeletal and muscle-specific functions. J Cell Sci *115*, 4013-4023.

Rayment, I., Rypniewski, W. R., Schmidt-Base, K., Smith, R., Tomchick, D. R., Benning, M. M., Winkelmann, D. A., Wesenberg, G. and Holden, H. M. (1993). Three-dimensional structure of myosin subfragment–1: a molecular motor. Science *261*, 50-58.

Srikakulam, R., Liu, L. and Winkelmann, D. A. (2008). Unc45b forms a cytosolic complex with Hsp90 and targets the unfolded myosin motor domain. PLoS One *3*, e2137.

Srikakulam, R. and Winkelmann, D. A. (1999). Myosin II folding is mediated by a molecular chaperonin. J Biol Chem *274*, 27265-27273.

Srikakulam, R. and Winkelmann, D. A. (2004). Chaperone-mediated folding and assembly of myosin in striated muscle. J Cell Sci *117*, 641-652.

Venolia, L., Ao, W., Kim, S., Kim, C. and Pilgrim, D. (1999). unc–45 gene of *Caenorhabditis elegans* encodes a muscle-specific tetratricopeptide repeat-containing protein. Cell Motil Cytoskeleton *42*, 163-177.

Wesche, S., Arnold, M. and Jansen, R. P. (2003). The UCS domain protein She4p binds to myosin motor domains and is essential for class I and class V myosin function. Curr Biol *13*, 715-724.

Wohlgemuth, S. L., Crawford, B. D. and Pilgrim, D. B. (2007). The myosin co-chaperone UNC–45 is required for skeletal and cardiac muscle function in zebrafish. Dev Biol *303*, 483-492.

Wong, K. C., Naqvi, N. I., Iino, Y., Yamamoto, M. and Balasubramanian, M. K. (2000). Fission yeast Rng3p: an UCS-domain protein that mediates myosin II assembly during cytokinesis. J Cell Sci *113 (Pt 13)*, 2421-2432.

Yu, Q. and Bernstein, S. I. (2003). UCS proteins: managing the myosin motor. Curr Biol *13*, R525-527.